Present earth-surface processes and historical hydro-environmental fluctuations inferred from lake-catchment systems

糸野　妙子

2014 年 4 月

博　士　論　文

Present earth-surface processes and historical hydro-environmental fluctuations inferred from lake-catchment systems

金沢大学大学院自然科学研究科

環境科学専攻

環境動態講座

学　籍　番　号　1123142403

氏　名　　糸野　妙子

主任指導教員名　長谷部　徳子

Present earth-surface processes and historical hydro-environmental fluctuations inferred from lake-catchment systems

Contents

1. Introduction

Lacustrine sediments contain both high-resolution regional environmental records and global information in lake-catchment systems. Therefore, they have been widely used for reconstructing not only regional environmental changes from the paleo-limnological point of view, but also long-term global environmental changes from the paleo-climatical point of view. In addition, they are also of great use for reconstructing short-term environmental changes (precipitation, water discharge, etc.) and understanding earth-surface processes (erosion, transportation, sedimentation) in the lake-catchment system.

Considering above views, this thesis consists of three parts:

1. Disastrous flood events found in Lake Biwa sediments (Chapter 2); this chapter aims to clarify rapid hydrological changes in the instrumental period using a large lake-catchment system (Lake Biwa) with long environmental records because short-term changes should be finally discussed in the context of long-term and global ones. Long-term hydro-climatological changes found in Lake Biwa sediments are closely linked to long-term and global environmental changes (e.g., Kashiwaya et al., 1991; Meyers et al., 1993).

2. Reconstructing hydro-environmental fluctuation in snowfall area (Chapter 3); hydrological fluctuations in winter are often distorted with snow cover area in Japan, where different processes from summer season should be also considered for establishing general expressions on erosion and sedimentation. To make clear the difference in processes and influences on physical properties, Onuma lake-catchment system in southern Hokkaido is discussed.

3. Present earth surface processes and pond sediment information (Chapter 4); process understanding is essential for clarifying causal relations in earth surface phenomena and proper interpretation of sediment information. Instrumental observation (monitoring) is of great use for the process understanding. Chapter 4 deals with the instrumental observation for a small pond-catchment system (Takidani-ike) near Kanazawa University.

2. Disastrous flood events found in lacustrine sediments from Lake Biwa

This chapter is mainly based on the paper (Itono, T., Kashiwaya, K. and Sakaguchi, A. (2012) Disastrous flood events found in lacustrine sediments from Lake Biwa: Transactions, Japanese Geomorphological Union, **33**, 453-468).

2.1. Introduction

Lacustrine sediments contain high-resolution regional environmental records in lakes and their surrounding catchments in addition to global information. Therefore, they have been widely used for reconstructing not only regional environmental changes from the paleo-limnological point of view, but also long-term global environmental changes from the paleo-climatical point of view.

Generally, comparatively small lake-catchment systems have been used for reconstructing short-term environmental changes (precipitation, water discharge, etc.) and understanding environmental processes (erosion, transportation and sedimentation in the lake-catchment). For example, detailed records of Holocene river-flood activity (including instrumental and historical data) inferred from sediments in Lake Meringsdalsvatnet, Norway, reveal that river-flood frequency is related to regional climatic trends (Støren et al., 2010). Analytical results for varved sediments in Cheakamus Lake, Canada, indicate that there are several floods in a year, depending on some decadal intervals (Menounos and Clague, 2008). Analyses of lacustrine sediments in Lake Piaseczno, Poland, show that changes in sediment discharge have been influenced mainly by human activity (land-use, deforestation, etc.) during the last 100 years (Tylmann et al., 2009). Chikita (1986) reported that the lake sediment processes

are controlled mainly by the transportation and deposition of the fine suspended grains due to river-induced turbidity currents and sediment dispersion in Lake Okotanpe, Hokkaido.

On the other hand, large and deep lake-catchment systems have been used not only as a record of short-term changes but also of long-term changes. In Lake Baikal, various time-scale sediment cores have been discussed (e.g. Kashiwaya, 2003).

Lake Biwa has been a subject of study in the field of limnology in Japan. It has also been used to study both short-term and long-term environmental changes and processes. Most short-term studies deal mainly with recent environmental changes related to human activity and natural external forces (e.g., Itoh et al., 2010; Taishi, 1995; Taishi and Kashiwaya, 1993). Lake drilling for the purpose of clarifying long-term environmental changes was initiated at Lake Biwa by Horie (1984) in 1970. The results have been published in various reports (Horie, 1984; Yamamoto, 1984; Yamamoto et al., 1985; Takemura, 1990; Kashiwaya et al., 1991, etc.).

Most core sediment studies published previously deal mainly with short- and long-term temporal changes in various environments. However, studies involving environmental reconstruction using core sediments on the basis of process-understanding are limited. Therefore, we here discuss the lake-catchment processes and hydro-environmental changes in the instrumental observation period in the Lake Biwa system mainly on the basis of the physical properties of lacustrine sediments. In particular, we focus on two disastrous flood events in the instrumental observation period for discussion.

2.2. Area studied and material

(1) *Lake Biwa*

Lake Biwa, located in Shiga prefecture, is the largest and oldest fresh water lake in Japan (Fig. 2.1). Lake Biwa has a tectonic origin, its water area is 674 km^2, and the area of the drainage basin excluding the lake surface area is 3174 km^2. Lake Biwa consists of two basins, the northern basin and the southern basin. Their average water depths are 43 m and 4 m, respectively. The maximum water depth is 104 m (in the northern basin), and the average depth for the total lake is 41 m. There are several lacustrine terraces (numbered one to three) in the basin, indicating some water level changes related to crustal movement, etc. (Uemura, 1987). There are 121 inflow rivers, one outflow river (the Seta), and one artificial outflow river (Biwako Sosui) in the drainage basin. Thus, Lake Biwa may be called a semi-closed lake (Somiya, 2000).

The Lake Biwa district is influenced by both the climate of the Japan Sea side and that of the Pacific Ocean side. There is a clear difference in annual precipitation between the northern and southern parts of the drainage basin. The average precipitation from 1981 to 2010 was 2691 mm in the north catchment (Yanagase) influenced by the Japan Sea climate and 1530 mm in the south catchment (Otsu) influenced by the Pacific Ocean climate. Winter precipitation in the north catchment is mainly snowfall.

The lake water level has been observed at the Torii-gawa observatory since 1874. However, since 1992 the level has been defined as the average of observations at 5 sites. In order to control the water level, the Seta was dragged from 1896 to 1910. The Nangou barrier in the Seta for (manual) water level control was constructed in 1905, and a new one was constructed to control the water level artificially (electrically) in 1969.

According to Horie (1984), the origin of Lake Biwa is thought to be very old. Since

the birth of the lake, its basin has subducted continuously during the late Cenozoic, and has not been filled in spite of a thick sediment accumulation on the lake floor. Its development has been controlled by tectonic movements throughout the late Cenozoic. Parts of the sediments deposited on the bottom of this old lake area are distributed on hills and terraces in the area around Lake Biwa and the Iga Basin. They are called the Kobiwako Group, and make up strata from the Pliocene to the earlier Pleistocene with a depth of 1,000 to 1,500 m.

(2) *Samples*

To obtain environmental information, several sediment core samples were taken at points T1, T5 and T13 in the northern basin (Fig. 2.1) by a research vessel (“Hakken”) from the Lake Biwa Environmental Research Institute. The sampling points in the northern basin (probably under climatic conditions similar to those of Lake Yogo), T1 and T13, were considered suitable for comparison with data from a previous study in Lake Yogo (Shimada et al., 2002). One sampling point, T5, in the central basin, was chosen so that the average hydro-environmental fluctuations in Lake Biwa could be inferred. Information on the obtained cores is given in Table. 2.1. Short core samples, BW05T1-11, BW06T5 and BW07T13, at the three points, respectively, were obtained with a gravity core sampler (1-m) using an acrylic tube with a diameter of 5.2 cm. A long core sample, BW05T1-4, was obtained at point T1 using a piston core sampler (4-m) with a polyvinyl chloride pipe of 7.6 cm in diameter.

2.3. Analytical items and method

Core sediments were sliced for various analyses at appropriate intervals as shown in Table. 2.1. The analytical items discussed here include the following: mineral content,

grain density, mineral grain size and radioactive concentrations of Cs-137, Pb-210ex and C-14. Here mineral materials are defined as what remains after the removal of organic matter, HCl-solvable matter and biogenic silica.

The mineral content was determined by the method of Mortolock and Froelich (1989). The mineral grain size was determined using a laser diffraction particle size analyzer (SHIMADZU SALD-2000J). The density was measured with an auto-pycnometer with helium gas (Micrometerics Accypic 1330).

The radioactive concentrations of Cs-137 and Pb-210ex in BW05T1-11 and BW07T13 were measured with high-performance Germanium semiconductor detectors (GTM-100220, GEM-25-P4; ORTEC) and low-energy Germanium detectors (LO-AX-51370, GLP-36360; ORTEC) at the Radioisotope Laboratory for Natural Science and Technology, Kanazawa University. The analytical program used here was PKview, developed by the Radiochemistry Laboratory, Kanazawa University. The radioactive concentration of BW06T5 was measured at the Low Level Radioactivity Laboratory, Kanazawa University (Sakaguchi, personal com.). The C-14 dating for the wood material was determined by the accelerator mass spectrometry method at the Institute of Accelerator Analysis Limited.

We selected 10 main stations in the drainage basin among 13 sites in order to determine the typical precipitation in the catchment. Hikone Local Meteorological Observatory, located in the central part of the drainage basin, possesses data covering the longest period among the 10 main local stations in Shiga. To check the representativeness of the data in Hikone, we compared the monthly fluctuation of precipitation in Hikone with the average precipitation at the 10 stations. The result, shown in Fig. 2.2a, indicates that there is a similar trend between the two levels of

precipitation, although there is a small difference between their values. Hence we used the data collected in Hikone.

Results and discussion

2.4. Precipitation and water level

Water discharge from the catchment and precipitation are the main means of transporting materials in the system. First, the hydrological conditions will be discussed.

The annual rainfall in Hikone is shown in Fig. 2.2b. As shown, there is little clear correlation between annual precipitation and large mass transport for the Meiji heavy rainfall of 1896 (MH) and the Isewan Typhoon of 1959 (IT). It is reported that annual rainfall is not always related to large mass transport in lake-catchment systems, and annual excess rainfall is often more convenient for mass transport in the systems (Kashiwaya et al., 1986). Here we introduce a 70-mm excess rainfall (annual summation of excess quantity over 70 mm/day). A daily rainfall of 70 mm was a criterion for heavy rainfall advisory in this district (Hikone Local Meteorological Observatory, 1993). The excess rainfall is shown in Fig. 2.2c.

There have been two disastrous floods around Lake Biwa during the instrumental observation period beginning in 1874 (Shiga Prefecture, 1966). One resulted from the Meiji heavy rainfall in Sep., 1896. The total rainfall for the period from Sep 3-12 was 1008 mm in Hikone. The rainfall on Sep 7 was 597 mm. The number of killed and missing was 34, and more than 58,000 houses and more than 29,000 ha rice fields were flooded in Shiga Prefecture (Shiga Prefecture, 1966). The other flood was caused by the Isewan Typhoon of Sep 26-27, 1959. The rainfall on Sep 26 was 195.8 mm in Hikone.

Sixteen people were killed and more than 20,000 houses were flooded in Shiga Prefecture (Shiga Prefecture, 1966). There is a difference in total rainfall between the MH period and the IT period, but there was a greater difference in the water level of Lake Biwa between the two periods (Fig. 2.3, Ministry of Land, Infrastructure, Transport and Tourism, personal communication). The lake water level during the MH was 3.76 m above the standard level (0 m) as measured at Torii-gawa Observatory. Since the Nango barrier was constructed in 1905, the fluctuation in water level has been comparatively stable. The lake water level during the IT was 0.87 m, not as high as that during the MH.

2.5. Physical properties of sediments obtained

Fig. 2.4 shows the physical properties of the core samples (mineral content, density and mineral grain size). Most of the physical properties show nearly the same trends in the three cores (arrows in the figure). Two positive peaks can be detected in the density and mineral content in the upper parts (0-20 cm) of the three cores. On the other hand, one coarser peak (upper) and one finer peak (lower) are found in mineral grain size in the upper part, at nearly the same depth as the two peaks of the density and mineral content. The upper peak is located at 6-10 cm of BW05T1-11, 8-10 cm of BW06T5 and 5-8 cm of BW07T13. The lower peak is located at 12-15 cm of BW05T1-11, 13-19 cm of BW06T5, and 14-18 cm of BW07T13. These two peaks in the three cores seem to reflect the same events that occurred in the lake-catchment system according to the dating data discussed in the next section.

2.6. Radioactive concentration and sedimentation rate

Fig. 2.5 shows the fluctuations in radioactive concentration. Table 2.2 shows the results of C-14 dating. The layers of the largest Cs-137 concentration are at 6 cm (1.37 g/cm^2; mass depth), 7 cm (1.83 g/cm^2; mass depth) and 4 cm (0.74 g/cm^2; mass depth) for BW05T1-11, BW06T5 and BW07T13, respectively (arrows in the figure). The Cs-137 peak corresponds to the layer for 1963 (Shimada et al., 2002; Katsuragi, 1983).

The sedimentation rate between 1963 and the sampling year can be calculated assuming that none of the surface layer was missing. The sedimentation rates for the three cores are 0.032 g/cm^2/yr for BW05T1-11, 0.042 g/cm^2/yr for BW06T5 and 0.017 g/cm^2/yr for BW07T13. The average sedimentation rate is 0.030 g/cm^2/yr, which is not very different from the average sedimentation rate of 0.038 g/cm^2/yr over the past 6300 years determined by the acoustic estimation method of the sedimentation layer (Inouchi, 1987).

2.7. The relationship between rainfall and the physical properties of sediment

Here we discuss the hydro-environmental fluctuations mainly in the instrumental observation period (during the past 100-150 years). Considering the sedimentation rate discussed above, the upper part of the cores above 10 g/cm^2 is the focus of this discussion (Fig. 2.6).

To make clear the trend of the fluctuations in physical properties and hydrological factors, a numerical filter (Ormsby, 1961) is used for the density, mineral content, mineral grain size, 70-mm excess rainfall and maximum water level. The results are shown in Fig. 2.6.

The upper peaks of the mineral content, density and mineral grain size may correspond to the year of the IT (1959), considering the Cs-137 concentration and

filtered excess rainfall. At point T1, an increase in grain size was also found in the IT period, but it was not so large, compared with the recent fluctuation. Point T1 may be influenced by the artificial flumes constructed between Lake Yogo and Lake Biwa since 1960. Additionally, point T1 may have been influenced by snowmelt in the spring because the catchments of the inflow rivers (the Oh and the Yogo) near point T1 are part of a large snowfall area. This possibility will be discussed elsewhere.

The sedimentation rates thus inferred from the IT period and the sampling year are 0.047~0.052 g/cm^2/yr, 0.044~0.048 g/cm^2/yr and 0.039~0.041 g/cm^2/yr for BW05T1-11, BW06T5 and BW07T13, respectively, considering the peaks in mineral content and density. Assuming these sedimentation rates, the year of the MH (1896) corresponds to the depths of 5.12~5.64 g/cm^2 for BW05T1-11, 4.81~5.31 g/cm^2 for BW06T5, and 4.26~4.51 g/cm^2 for BW07T13.

The second peaks in mineral content and grain density are within these intervals, suggesting that the peaks may be assigned to the MH period. In addition, the second peak in excess rainfall also corresponds to the year 1896, because the excess annual rainfall is strongly related to sediment discharge in the catchment (Kashiwaya et al., 1995). In the filtered rainfall, the first (latest) peak represents the IT (1959) and the second large peak represents the MH (1896). These findings support the possibility that the second peak in the physical properties can be assigned to the year 1896.

The two peaks in mineral content and density may also be closely related to the high sediment discharge. It is reported that high density is related to sedimentary anomalies such as flood events (Taishi and Kashiwaya, 1993). An increase in mineral content suggests a large input of mineral matter with a large sediment discharge in the catchment. Large sediment discharges due to heavy rainfall transport high-density

materials (including more mineral content than usual).

Now we discuss Pb-210ex activity (Fig. 2.5), which is defined as the Pb-210 activity minus the Pb-214 activity. Pb-210ex activity exponentially decreases with time if the sedimentation rate is constant. If the rate is not constant, such as in flood intervals, the exponential decrease will be disturbed. The IT period and the MH period can be identified based on disturbances in the sediment from Lake Biwa (Taishi, 1995). The disturbances seem to be recorded in the Pb-210ex concentration at nearly the same depths as the two peaks in mineral content and grain density, although this is not entirely clear (Fig. 2.5; shaded region). This also suggests that the deeper peaks in mineral content and grain density should be assigned to the MH (Fig. 2.6).

We can conclude that the IT period and the MH period are recorded in the physical properties of lacustrine sediment. The mineral content and grain density may also be good proxies for rainfall intensity.

2.8. Grain size fluctuation

Here we discuss the sedimentary processes that occurred in flood events (the IT period and the MH period) on the basis of the physical properties of sediments (Fig. 2.6, Table. 2.3).

In general, grain size distribution is correlated to the magnitude of the sediment discharge and/or the rainfall intensity in the catchment (erosion and transportation by water discharge). In particular, rainfall intensity and/or excess rainfall are closely related to grain size (Kashiwaya et al., 1995, Shimada et al., 2002). However, the results obtained for the Lake Biwa sediments show that the mineral grain size in the IT period was large, while that in the MH period was small (Fig. 2.6). This anomaly requires

explanation. Fig. 2.7 shows the mineral grain size distribution in the layers inferred as deposition in the IT and MH periods. The grain size distribution in a normal period, between the IT period and the MH period, is also shown in Fig. 2.7 (dashed lines). Both are bimodal distributions. It is reported that quartz grains coarser than 20 μm in Lake Biwa sediments are thought to be fluvial on the basis of the grain size distribution, oxygen isotope composition and micromorphologic features (Xiao et al., 1997). The coarser grains, i.e. larger than 30 μm, may be fluvial in Fig. 2.7. These findings suggest that the direct input from rivers at the sampling point in the MH period was much smaller than that in the IT period.

Next, we checked the sedimentary conditions in the MH and IT periods. Fig. 2.8 shows a map of the flood area in the MH period (Biwako Chisuikai, 1968). In this period, the water level was higher than in any of the other heavy rainfall periods, and high water disasters occurred in the catchment. It is important to mention that in the MH period, the distance from the river mouth to the sampling points was longer than usual due to the severely high water level. For example, at point T13, the distance from the Ane to the sampling point (ca. 6.3 km) was 2.0 times longer than at present (3.2 km). The distance from the Ado to the sampling point (T5; located in the central basin, ca. 7.0 km) was 1.3 times longer than at present (5.4 km). At T1, located in Shiozu Bay of northern Lake Biwa, the distances from the Yogo and the Oh to the sampling point were also longer than today. This increase in distance (water level increase) may be closely related to a decrease in the large fraction of the grain size distribution, although the distance alone does not always control the distribution.

It is probable that some of the coarse grains were deposited near the mouths of the rivers when the water level was high, and limited grains reached the sampling points. A

two-dimensional advective diffusion model (Ochiai and Kashiwaya, 2003) indicates that the grain size becomes smaller when the distance is longer, which is consistent with the present findings. This may explain the comparatively small mineral grain size at the sampling points in the MH period.

It may be said that the grain size distribution in lakes is a function of the rainfall intensity in the catchment and the distance transported from the river mouth. It is important to consider water level changes to gain a proper understanding of grain size parameters.

3. Reconstructing hydro-environmental fluctuation in snowfall area

3.1. Introduction

In this chapter, we'll discuss hydro-environmental fluctuation in Onuma lake-catchment system (northern Japan) during the past 100 years, the instrumental observation period. Some short core sediments were obtained from Lake Onuma in Sep. 2011 (Fig. 3.1).

There are some instrumental observation data for meteorological and hydrological conditions around the system, which is an advantage of this area for considering hydro-environmental changes and earth surface processes.

3.2. Area studied and material

Lake Onuma is located in the south of Hokkaido-Komagatake Volcano (hereafter HKV) (Fig.3.1). It was formed by debris-avalanche deposits by the eruption of HKV in AD 1640 (Kurumisaka debris-avalanche: Yoshimoto et al., 2007). The beginning of HKV eruption was at least ca. 110,000 years ago (Ganzawa et al., 2005). Since the HKV eruption started, there were two sector collapses and four plinian eruptions: Ko-i, Ko-h, Ko-g and Ko-f were in ca. 32,000, 17,000, 6,000 and 5,500 years ago, respectively. HKV erupted again in AD1640 (Ko-d). In historical period, four plinian eruptions (Ko-d, Ko-c2, Ko-c1 and Ko-a) occurred: they were in AD1640, 1694, 1856 and 1929, respectively (Table. 3.1) (Yoshimoto et al., 2007). The geological map is shown in Fig. 3.2 (Yoshimoto et al., 2007).

Lake Onuma consists of two basins, the eastern basin (Onuma basin) and the western basin (Konuma basin) (Fig.3.1). The water area for the two basins is 5.12 km^2

and 3.80 km^2, respectively. The average water depth for the two basins is 6.4 m and 2.3 m, respectively, the average for the two basins is 4.7 m. The maximum water depth is 13.6 m located in Onuma basin. The average residence time is 2.9 months. The catchment area of Lake Onuma is 173 km^2 (Tanaka, 2005), which increased by the result of constructing an artificial water supply from the Himekawa district (Fig., 3.1a, dashed line). There are 3 inflow rivers: the Shukunobe, the Ikusa, and the Karima while one outflow river, the Orito. An artificial channel was constructed at the south of Konuma basin in 1961 for electric power plant and irrigation. After that, the outflow to the Orito was blocked by the sluice gate.

To obtain environmental information, several sediment core samples were taken in Lake Onuma (Fig. 3.1) with boats of the Fisheries Cooperative Association of Lake Onuma in 2011 and 2012. Information on the obtained cores is given in Table. 3.2.

Some short core samples were also obtained in 2011. Sampling point 2, the deepest point of the lake. Some sampling points (1, 5 and 6) are useful to discuss hydro-environmental changes in the lake-catchment system. Short core samples, ON11-2-1, ON11-2-2, ON11-1, ON11-5 and ON11-6, were obtained with a gravity core sampler (1-m) using a polyvinyl chloride tube with a diameter of 5.2 cm.

In 2012, three 4-m cores (ON12B, ON12C and ON12D) were obtained from Onuma basin and one 4-m core (ON12A) was from the Konuma basin (Fig. 3.1). ON12C was obtained at deepest point of Onuma basin. These core samples were obtained with a piston core sampler (maximum 4-m in length) with a polyvinyl chloride pipe of 8.3 cm in diameter. Short core samples were also obtained at the same sampling points of the long cores using the gravity core sampler (1-m) to obtain information on top part of surface sediments which are often lost when using the piston core sampler.

3.3. Analytical items and method

Core sediments were sliced for various analyses at appropriate intervals. The analytical items discussed here include the following: mineral content, biogenic silica content, grain density, mineral grain size and radioactive concentrations of Cs-137, Pb-210ex and C-14. Mineral matter is defined as what remains after the removal of organic matter, HCl-solvable matter and biogenic silica.

The mineral content and biogenic silica content was determined by the method of Mortolock and Froelich (1989). The mineral grain size was determined using a laser diffraction particle size analyzer (SHIMADZU SALD-2000J). The density was measured with an auto-pycnometer with helium gas (Micrometerics Accypic 1330).

The radioactive concentrations of Cs-137 and Pb-210ex in BW05T1-11, BW07T13, ON11-1, ON11-5 and ON12C were measured with high-performance Germanium semiconductor detectors (GTM-100220, GEM-25-P4; ORTEC) and low-energy Germanium detectors (LO-AX-51370, GLP-36360; ORTEC) at the Radioisotope Laboratory for Natural Science and Technology, Kanazawa University. The analytical program used here was PKview, developed by the Radiochemistry Laboratory, Kanazawa University. The radioactive concentration of ON11-2-2 and ON11-6 were measured at the Low Level Radioactivity Laboratory, Kanazawa University (Ochiai, personal com.).

Result and discussion

3.4. Precipitation and river discharge

Physical properties of lacustrine sediments reflect hydrological conditions in the lake-catchment system (e.g. precipitation in the catchment, river discharge, water level change, etc).

Firstly, precipitation around the system will be discussed, using data observed by three meteorological observatories not so far from the system (Fig. 3.1b). Mori observatory is located near the Onuma catchment (Fig. 3.1b). Hakodate Marine Observatory is located in ca. 20 km south of Lake Onuma (Fig. 3.1b), but the instrumental observation period is much longer (ca. 140 years) than Mori Observatory (ca. 70 years). Therefore, data from Mori are mainly used and estimated data (compared to Hakodate data) are additionally used in this discussion (average monthly precipitations for Mori, Hakodate and Onuma are shown Fig. 3.3a). Data from Onuma Observatory are not used because its observation interval is limited). Here two precipitations (annual precipitation and excess annual precipitation) are discussed. The annual precipitation and 5-year running average of annual precipitation in Mori and Hakodate are shown in Fig. 3.3b and 3.3c. There are good relationships between annual precipitations in Mori and in Hakodate: the correlation coefficient for annual precipitation (R=0.72) and for the 5-year running average (R=0.81, Fig. 3.3e). Therefore this relationship in 5-year running average is used for estimating the average annual precipitation in Mori since 1875 (Fig. 3.3d).

It is reported that the annual excess rainfall is more related to mass transport than annual rainfall (Kashiwaya et al., 1986). After several trial calculations, a 30 mm excess daily rainfall is employed here. It is an annual summation of excess amount of 30 mm daily rainfall. Results for Mori and Hakodate are shown in Fig. 3.4b. The relationship

between Mori and Hakodate is not so good (Fig. 3.4d). To make clear the trend of fluctuation, a numerical filter (Ormsby, 1961) is used for the 30 mm excess daily rainfall for Mori and Hakodate (Fig. 3.4c). Fig. 3.4e shows the relationship between filtered excess rainfall in Mori and in Hakodate. The correlation coefficient (R) is 0.50, indicating a weak one.

These suggest that estimated annual rainfall in Mori is available for further discussion, but filtered excess one is only used as a first order approximation in the present stage. Further discussion is required for the precipitation.

Secondly, precipitation and river discharge around Lake Onuma are discussed. Let us check Fig. 3.3a and Fig. 3.5a. These show fluctuations of the average monthly precipitation in Mori and the river discharge in Lake Onuma (Hokkaido Electric Power Company, personal communication). The largest monthly average precipitation and river discharge during the interval of 1981 to 2010 are in August (Fig. 3.3a) and in April (Fig. 3.5a), respectively. This may be reflected in large rainfall intensity event (flood, typhoon, heavy rainfall, etc.) in summer and snowmelt inflow in spring. It is reported that surface water discharge due to snow and/or ice melting as well as rainfall is a dominant external force for sedimentation rate in lake-catchment systems (Kashiwaya et al., 2012). The catchment of Lake Onuma was enlarged for water inflow in 1978. Both of total discharge (additional discharge and original discharge) and original discharge show nearby the same fluctuation (Fig. 3.5a, b). Original river discharge is used here for discussion.

Annual precipitation in Mori and river discharge in Lake Onuma is shown in Fig. 3.5c. The relationship between them is shown in Fig. 3.5d, and the correlation coefficient (R) is 0.88. The relationship between monthly precipitation and river

discharge are also checked (Fig. 3.6). The correlations are roughly good. However, they are not so good in winter-spring time (especially April and May, Fig. 3.6). This may be related to snowmelt season. About 68 % of average monthly temperature in December show below zero in Mori during 1938 to 2012. The precipitation is assumed to be snow when the temperature is below zero. It seems that December is the start of snowfall in Mori district. A part of the precipitation in winter is stored in the catchment as snow accumulation. Earth surface processes related to snowfall are a little different from those related to rainfall. It seems that erosional force is weaker in periods with snow cover than without snow cover. It is reported that the relationship between seasonal sedimentation rate and seasonal rainfall without snow cover period shows comparatively good correlation than that with snow cover period (Kashiwaya et al., 2012). In addition, the river discharge in snowmelt season is largest of the year (Fig. 3.5a). It may be related to large mass transport from the catchment in snowmelt period. As a convenient classification for process discussion, a year is divided into two periods (seasons); summer period (June to November) and winter period (December to May). There are good relationships between seasonal precipitation and river discharge (both in summer and winter period, Fig. 3.7), indicating lake-catchment processes are not the same in winter and summer. The correlation coefficients in summer and winter period are 0.85 and 0.86, respectively.

3.5. Physical properties of sediments

Fig. 3.8 shows physical properties of short core sediments (water content, mineral content, density and mineral grain size). Most of physical properties of the cores show two common patterns (broad convex; shaded region, and clear concave; arrow-A) in the

figure). Mineral content and density increased in the shaded region. However, it is not clear that all mineral grain size (hereafter grain size) in the cores increased. The increasing part is located at 5-15 cm of ON11-6, 26-44 cm of ON11-2-1 and 14-26 cm of ON11-1. Some clear peaks are found in the same depth of each core; a positive peak is found in mineral content, density and grain size (arrow-A in Fig. 3.8), and a negative peak is found in water content (ON11-2-1 is not clear). The peaks are located at 29cm of ON11-6, 70 cm of ON11-2-1 and, at 31 cm of ON11-1. These properties may reflect same abrupt hydro-environmental changes in the lake-catchment system. In addition, a positive peak is shown in grain size and negative peaks in water content, mineral content and density at 23 cm of ON11-2-1 (arrow-B in Fig. 3.8), which will be discussed with age model in the Section 3.6.

3.6. Age model

Fluctuations in radioactive concentration are shown in Fig. 3.9. The layers of largest Cs-137 radioactive concentration are at 27 cm (3.55 g/cm^2; mass depth), 16 cm (2.70 g/cm^2; mass depth) and 32 cm (5.46 g/cm^2; mass depth) for ON11-2-2, ON11-1 and ON11-5 from west to east in the lake, respectively. The largest peak value in Cs-137 concentration indicates that the layer deposited around 1963 at the peak time of fallout (Shimada et al., 2002; Katsuragi, 1983). The sedimentation rates during 1963 and 2011 (sampling year) for the core samples are 0.073 g/cm^2/yr, 0.055 g/cm^2/yr and 0.112 g/cm^2/yr for ON11-2-2, ON11-1 and ON11-5, respectively. The average sedimentation rate of whole core is obtained on the basis of regression curves of excess Pb-210. Regression curves are as follows;

$$Y = 410.3e^{-0.3976X} \quad \text{for ON11-6} \quad (3.1),$$

$$Y = 572.8e^{-0.3452X} \quad \text{for ON11-2-2} \quad (3.2),$$

$$Y = 711.4e^{-0.4881X} \quad \text{for ON11-1} \quad (3.3),$$

$$Y = 596.2e^{-0.2620X} \quad \text{for ON11-5} \quad (3.4),$$

where X is mass depth (g/cm^2). Y is radioactive concentration of excess Pb-210. The average sedimentation rates are 0.078 g/cm^2/yr, 0.090 g/cm^2/yr, 0.064 g/cm^2/yr and 0.119 g/cm^2/yr for ON11-6, ON11-2-2, ON11-1 and ON11-5, respectively.

ON11-2-1 and ON11-2-2 were obtained from nearly the same sampling point. Cs-137 peak of ON11-2-1 at 33 cm (4.14 g/cm^2) is estimated, comparing fluctuation in ON11-2-2 whole grain size with ON11-2-1 one (Fig. 3.10). Sedimentation rate of the ON11-2-1 for the upper part from the peak layer of Cs-137 concentration is given with this depth. Average sedimentation rate of the ON11-2-1 for the whole core is estimated, multiplying excess Pb-210-based sedimentation rate for the ON11-2-2 core by ratio of Cs-137-based rate for the ON11-2-1 to the ON11-2-2. These sedimentation rates of short cores are shown in Table. 3.3.

Next, let us discussion the changes in some physical properties with the age models.

Firstly, significant changes are found at 29 cm (6.14 g/cm^2), 70 cm (9.20g/cm^2) and 31 cm (6.00 g/cm^2) in the cores of ON11-6, ON11-2-1 and ON11-1, respectively (arrow (A) in Fig. 3.8). Positive peaks can be detected in mineral content and density, concave parts in water content. On the other hand, an isolated peak~~s~~ and complex peaks are found in grain size.

The date of the layer with arrow (A) is expressed as follows;

$$T(A) = 1963 - \{D(A) - D(1963)\}/SR(Pb) \quad (3.5),$$

where *T(A)* is the estimated date (year) of the layer with arrow (A). *D(A)* and *D(1963)* are mass depth of A-layer and 1963-layer, respectively. *SR(Pb)* is the sedimentation rate estimated by Pb-210 dating. Here average sedimentation rates with excess Pb-210 are used for the age estimation of the lower part below the 1963-layer. Using the eq. (3.5), the date of the layer with arrow-A for the ON11-2-1 and ON11-1 are 1915 and 1911, respectively. The date for the layer with arrow-A of ON11-6 is given by using only the excess Pb-210-based sedimentation rate, not using eq. (3.5), ca. 1933, because Cs-137 peak is not detected.

A piece of pumice was found in 48 cm (8.97 g/cm^2) depth of the core although all physical properties of sediment are not measured for the ON11-5 core yet. The major axis of the pumice is about 3 cm. Using eq. (3.5), the date at the depth of the pumice is given ca. 1933. The pumice is assumed to be the 1929 HKV eruption. Therefore the A-layer may be assigned to the 1929 eruption of HKV.

Next, let us discuss the ON11-2-1 core further, introducing a more detailed age model. The positive peak in grain size is also found at 23 cm (2.7 g/cm^2, arrow B in Fig. 3.8). The age of the peak is estimated 1980, using the average sedimentation rate for the upper part above 1963. The positive peak of 30 mm excess rainfall in Mori is also found in 1975 (Fig. 3.4b), which is corresponded to the year of the sixth typhoon attacking Mori Town on August 23, 1975. The daily rainfall on Aug. 23 is 210 mm. Two peoples were killed, 660 houses and 128 ha rice field were flooded in Mori Town (Mori Town, 1980). Suspended sediment in Lake Onuma measured by Hokkaido Government (2012) shows the largest value, 22 mg/l, in 1975 (Fig. 3.11). These support that the large mass

movement may have occurred in 1975. It is known that large excess rainfall is closely related to large grain size (e.g., Kashiwaya et al., 1986). Therefore the layer (arrow-B in Fig. 3.8) may be assigned to the year of sixth typhoon in 1975.

Figure 3.12 shows fluctuations in 30 mm excess rainfall, annual precipitation and some physical properties of ON11-2-1. A numerical filter (Ormsby, 1961) is used for the 30 mm excess daily rainfall in Mori and Hakodate to clarify the trends (Fig. 3.12a). Comparing the mineral grain size fluctuation with the original and filtered fluctuations in the 30 mm excess rainfall, we see that four positive peaks (1, 2, 4, 5; 5.0 g/cm^2 (39 cm), 2.7 g/cm^2 (23 cm), 1.1 g/cm^2 (11 cm) and 0.39 g/cm^2 (5 cm), respectively) and one negative peak (3; 2.1 g/cm^2 (19 cm)) in the grain size fluctuation are corresponded to the peaks in the 30 mm excess rainfall in Mori. Mineral grain size reflects rainfall intensity as mentioned before. Therefore the peaks in the grain size fluctuation are assumed to be the peaks of 30 mm excess rainfall in 1956, 1975, 1998, 2010 and 1988 (Fig. 3.12a, c). As mentioned above, the volcanic material related to the 1929 eruption is located at around the depth of 70 cm (Fig. 3.8).

Figure 3.13 shows the age model on ON11-2-1 using some dates including above ones, which will be used next.

3.7. The relationship between hydrological data and physical properties of sediments

Here I discuss about relationship between observational hydrological data and physical properties of sediments during the past 100 years. Some physical properties of the ON11-2-1 core are used for discussion, because it was obtained from deepest part of Lake Onuma, possibly having much information on hydro-environmental fluctuation in

the catchment. Figure 3.14 shows precipitation data (30 mm excess rainfall and 5-year running average of annual precipitation) and physical properties (grain size, mineral content and density) of ON11-2-1. Age of the physical properties is based on the age model given in Fig. 3.13. The fluctuations in 30 mm excess rainfall, annual precipitation and grain size seems to be harmonic especially since 1963 (arrows in Fig, 3.14). It is reported that rainfall intensity and/or excess rainfall are closely related to grain size (Kashiwaya et al., 1995; Shimada et al., 2002). It is also shown that the mineral grain size distribution may respond positively to the rainfall intensity in the catchment and negatively to the distance transported from the river mouth (Itono et al., 2012). An artificial channel was constructed at the south end of Lake Konuma for water inflow to the power station in 1965. Since then water level is controlled artificially. Therefore it seems that mineral grain size fluctuation mainly responds positively to rainfall intensity. On the other hand, there are unclear relationship among precipitation, mineral content and density.

Here, the relationship between physical properties of the ON11-2-1 sediment and hydrological data (precipitation and discharge) will be discussed. Hereafter 5-year running average of annual data is used for discussion. Grain size has a clear trend of gradual fining (Fig. 3.15a). Then detrended grain size is also picked up for discussion on external force (precipitation), canceling topographical effect (Fig. 3.15b).

Firstly, relationships between precipitation and physical properties (grain size, mineral content and density) after 1963 (in the interval of 1963-2009) are calculated. The results are shown in Fig. 3.16. Grain size has a good correlation with annual precipitation and summer precipitation, but it does not have a good correlation with winter precipitation. However, mineral content and density have little correlation with

both of annual and seasonal precipitation.

Annual precipitation is roughly controlled with summer one because summer precipitation is as twice as winter one. These indicate that grain size a good proxy for precipitation (rainfall), especially summer precipitation (rainfall). However, winter precipitation does not have a good correlation not only with grain size, but with mineral content and density as shown in Fig. 3.16. Two artificial changes in the lake-catchment system are included in the interval of present discussion; an artificial channel was constructed for power plant (1965) and catchment area was enlarged (1978). Then, let us discuss the relationships between precipitation and physical properties in comparatively stable interval (1966-1977). Calculated results are shown in Fig. 3.17. It seems that winter precipitation is more correlative with mineral content than summer precipitation and it is negatively correlative with grain size in spite of limited data, suggesting that catchment-lake processes in winter are different from those in summer. For example, large discharge is not always related to large precipitation in winter; it may increase mineral content, but it may not be always related directly to grain size because of limited surface erosion and transportation. The reason why density has not clear relationship with precipitation may be similar to the case of the mineral content. It needs further detailed discussion.

Next, let us discuss the estimation of precipitations using the grain size proxy. Estimated summer and annual precipitation using the regression equations in Fig. 3.16a are shown in Fig. 3.18a, b. As shown in these figures, estimated precipitations fairly agree with observed precipitations, especially summer precipitation. These indicate that grain size is a good proxy for precipitation (especially summer precipitation).

Next, winter precipitation and discharge are discussed. Ratio of summer

precipitation to winter precipitation is given by observational data in Mori during the past ca. 70 years (Fig. 3.19a). Using the ratio, winter precipitation is calculated. Discharges in summer and winter can be also calculated using the relationships between precipitations and discharge as shown in Fig. 3.7.

The relation mentioned above is expressed in the following;

$$SP_O(t)/WP_O(t) = fp(t) \quad (3.6),$$

$SP_O(t)$, observed summer precipitation at year t, $WP_O(t)$, observed winter precipitation at year t, and $fp(t)$ is ratio of summer precipitation to winter precipitation.

Assuming this relation is valid for estimated summer precipitation, $SP_e(t)$, and winter precipitation, $WPe(t)$, we have

$$SP_e(t)/WP_e(t) = fp(t) \quad (3.7).$$

As $fp(t)$ is given with observational data (cf. Fig. 3.19a), estimated winter precipitation is given by

$$WP_e(t) = SP_e(t)/fp(t) \quad (3.8).$$

Fig. 3.20b shows estimated precipitation in winter period. It fairly agrees with observed one. In addition, summation of $WP_e(t)$ and $SP_e(t)$ is corresponded to also similar with observed annual precipitation in Mori (Fig. 3.20c).

Now, let us estimate discharge using proxy precipitation. The relationships between

precipitation and discharge (Fig. 3.7) are given by

$$SP_O(t) = aSD_O(t) + b \quad (3.9),$$

and

$$WP_O(t) = a'WD_O(t) + b' \quad (3.10),$$

where $SP_O(t)$ and $SD_O(t)$ are observed summer precipitation and discharge at year t respectively. $WP_O(t)$ and $WD_O(t)$ are observed winter precipitation and discharge, a, b, a' and b' are coefficients, which are given in Fig. 3.7.

These equations are assumed to be valid for estimated precipitation and discharge, then estimated summer discharge, $SD_e(t)$, and winter discharge, $WD_e(t)$, are given with estimated summer precipitation and winter precipitation

$$SD_e(t) = (SP_e(t)-b)/a \quad (3.11),$$

$$WD_e(t) = (WP_e(t)-b')/a' \quad (3.12).$$

The ratio of estimated summer discharge to winter discharge, $fd_e(t)$, can be calculated using the equation:

$$fd_e(t) = SD_e(t)/WD_e(t) \quad (3.13).$$

The results are shown in Fig. 3.19b. As is shown, the estimated ratio is closely

related to observed one, indicating that mineral grain size is also available for estimating discharge in the lake.

4. Present earth-surface processes

4.1. Introduction

In this chapter, we'll discuss present earth-surface processes (erosion, transportation and sedimentation) in a small lake-catchment system. Observation in a small lake-catchment system is of great use for understanding of earth-surface processes; climatic conditions, geomorphological conditions and hydrological conditions are linked for proper interpretation to clarify physical processes related to sedimentation rate, physical properties of sediment, etc. Takidani-ike pond-catchment system (Kanazawa) has been used for the instrumental observation. The observation consists of sediment sampling with trap, water level measurement, temperature measurement, and precipitation measurement.

Observation in Takidani-ike system using sediment traps has continued since June 2000 (Fig. 4.1). The system has been used for several purposes, e.g. understanding of erosional process in the catchment, detection of heavy rainfall events in pond sediments, estimating the radioactive Cs input from the Fukushima Dai-ichi Nuclear Power Plant, etc. (Kashiwaya, 2012; Ochiai et al., 2013). Here we focus on sediment information, external conditions related to sedimentation, etc.

4.2. Area studied and material

Takidani-ike, located in Kanazawa (Ishikawa Prefecture), is a storage reservoir. The water area is 2370 m^2, and the area of drainage basin including the lake surface is 65000 m^2 (Fig. 4.1) (Ochiai et al., 2013). The maximum depth is about 5 m. Takidani-ike has been used for irrigation since the Edo period (more than 120 years ago), but has not

been dredged for the past several decades (Kashiwaya et al., 2012). The water level highly changes due to agricultural irrigation, especially summer period. There are two inflow channels, and two artificial outflow channels. The inflow channels are sometimes dried up when the water level is low and low precipitation in summer. The geological condition around the pond and catchment area is Miocene tuff (Kashiwaya et al., 2012).

Sediment trap were put in the pond bottom; center (TK-F) and near inflow channel (TK-B) (Fig. 4.1). The samples in the traps have been collected monthly in Takidani-ike since June 2000.

4.3. Analytical items and method

Sediment Traps used are made of steel and stainless-steel; former were used until March 2013 and the latter have been used since April 2013, respectively. Plane figure of sediment trap (cover and trap) is shown in Fig. 4.2.

Firstly samples are dried at 110 ℃ for more than 24 hours in the oven. Dried samples are used for various analyses: mineral content, grain density, and mineral grain size. Here mineral materials are defined as ones left after the removal of organic matter, HCl-solvable matter and biogenic silica from samples to be analyzed. The mineral content was determined by the method of Mortolock and Froelich (1989). The mineral grain size was measured using a laser diffraction particle size analyzer (SHIMADZU SALD-2000J). The density was measured with an auto-pycnometer using helium gas (Micrometerics Accypic 1330). Sedimentation rate with sediment trap is expressed as follows (Nishiji et al., 2004);

$$SR(t) = M(t)/S/T(t) \quad (4.1),$$

where *SR(t)* is the sedimentation rate of sediment trap ($g/m^2/day$), *M(t)*, the dried weight of sample (g), *S*, the area of sediment trap base (m^2), *T(t)*, the days of the sediment trap put in the pond at *t*-th observation.

Data obtained by the Kanazawa Local Meteorological Observatory are used for discussion. Precipitation around Takidani-ike is also measured with an optical infrared rain gauge (SE-PM525; SENECOM) with data logger (OPUS 200; G LUFFT Mess-u Regeltechnik GmbH). However, the data are not used here because data calibration is not established yet.

Water level is observed with two absolute pressure loggers (HOBO Water Level Logger, SE-U20-001-04, Onset Computer Corporation; hereafter Hobo), one of which is used in the pond bottom (W-HOBO) and another on shore of the pond (A-HOBO) (Fig. 4.1). Measuring interval with Hobos is almost every 10 minutes. The analytical program used here was HOBOware Pro, developed by Onset Computer Corporation. The average of the average atmospheric pressure at (*t*-1)-th observation and one at (*t*+1)-th observation is used for calibration when the atmospheric pressure is not measured at *t*-th observation or no data as HOBOware Pro type. In addition, capacitance water level gauges (WT-HR 64K water height data logger, Trutrack; hereafter Trutrack) were used in Takidani-ike since 2004. The Trutrack has been changed four times since then. The present Trutrack has been set in the pond since April 2011.

Results and discussion

4.4. Precipitation and water level

The monthly average precipitation and snowfall in 1981-2010 in Kanazawa are shown in Fig. 4.3a, b. Snowfall period starts in November, but main snowfall period is December to March. Figure 4.3c shows annual precipitation.

As mentioned before, water level in Takidani-ike is observed with two methods. Water level observed with HOBO (hereafter wl-HOBO) is shown in Fig.4.4a. There is some difference in the water level before and after data collecting with the wl-HOBO because its setting position is not always same. To cancel the difference, wl-HOBO was calibrated as follows,

$$D(1) = 2.9 - WL_f(1) = 0 \quad (4.2),$$

$$D(t) = \sum_1^t (WL_l(t-1) - WL_f(t)) \quad (t \geq 2) \quad (4.3),$$

$$WL_c(t) = WL_O(t) + D(t) \quad (4.4),$$

where $D(t)$ is difference between observed water level and the standard value. The standard value, $WL_f(1)$, is 2.9 m, which is the water level observed on May, 25, 2011. $WL_l(t\text{-}1)$ is the water level on the last time at (t-1)-th observation and $WL_f(t)$ is water level at the first time at t-th observation (water level just after the next setting). $WL_c(t)$ and $WL_O(t)$ are calibrated and observed water level at t-th observation, respectively. WL_c is shown in Fig 4.4b.

Next, water level observed with the present Trutrack (hereafter wl-Trutrack) is shown in Fig. 4.5. The water level sometimes shows negative value in summer and winter periods. Then, water level was lower than the bottom part of water logger, or Takidani-ike covered with ice. The wl-Trutrack shows constant minus values from

February, 5, 2012 to February, 12, 2012, indicating that Takidani-ike was covered with ice during the period. However, Trutrack logger is suitable for evaluating the absolute water level except the interval of low water level and ice cover because the wl-Trutrack is set in fixed-point. Then we tried to estimate missing values in wl-HOBO by using the wl-Trutrack data. The daily minimum water level is used for discussion. The wl-HOBO data are compared with wl-Trutrack data to interpolate missing part of wl-HOBO (April, 19-25, 2012) in the interval of May, 25, 2011 to October, 2, 2013. The relationship is shown in Fig. 4.6a. The regression curve is expressed in the following;

$$WL_C = 0.90WL_T+1.6 \quad (4.5),$$

where WL_C is wl-HOBO and WL_T is wl-Trutrack. Using eq. (4.5), missing period (April, 19-25, 2012) is interpolated. Finally, original data and interpolated data for missing period of wl-HOBO are used for further discussion (Fig. 4.6b).

4.5. Physical properties of sediments

Sedimentation rate with sediment trap is calculated using eq. (4.1). Figure 4.7 shows sedimentation rates for TK-F and TK-B since 2000. In general, sedimentation rate for TK-B trap is larger than sedimentation rate for TK-F trap. TK-B is set in near the coastal line of Takidani-ike. Sedimentation rate and physical properties (mineral grain size, mineral content and density) of TK-F and TK-B since 2009 are shown in Fig. 4.8 and Fig. 4.9, respectively. Most physical properties show similar trend in fluctuations (Fig. 4.8 and Fig. 4.9). Changes in sedimentation rate for both sites are roughly corresponded to those in physical properties for both sites (TK-F and TK-B). Mineral

grain size (hereafter grain size) of TK-B is coarser than that of TK-F. In addition, amplitude of grain size fluctuation for TK-B is larger than that for TK-F.

The relationship between sedimentation rate and physical properties for both sediment traps (TK-F and TK-B) are shown in Fig. 4.10. Here monthly sedimentation rate and physical properties are given with weighted average corresponding to observed period. The relationships between grain size and sedimentation rate is different for the two sites (Fig. 4.10a); grain size of TK-F is finer than grain size of TK-B although there is little difference in fundamental trend. On the other hand, the mineral content and density are not so different for the two sites (Fig. 4.10b, c). It seems that the relationships between sedimentation rate and physical properties in Takidani-ike sediments are consistent with the conclusion of analyses for Lake Biwa core sediments (Itono et al., 2012); grain size responds positively to the distance between inflow river mouth and sampling point, and mineral content and density mainly depend on sediment discharge of the lake-catchment system, not depending on the sampling point.

Difference in fundamental trend is limited, the average of sedimentation rate for TK-F and TK-B will be used for discussion as a representative value.

4.6. Factors related sedimentation rate

It is reported that sedimentation in ponds is mainly related to three factors; field conditions under which sediment material is produced (conditions of the catchment area; slope, valley density, snow cover, vegetation cover, etc.), external (erosional) conditions (rainfall intensity, etc.), and internal pond conditions (water level, bed morphology, ice cover, etc.) (Kashiwaya et al., 1997). Combination of catchment condition and pond condition may be expressed as system condition. The relationships

are expressed as follows;

$$SR(t) = P_f(t) \times C_f(t) \times E_f(t) \quad (4.6),$$

or simply

$$SR(t) = S_f(t) \times E_f(t) \quad (4.7),$$

where $SR(t)$ is the sedimentation rate, $P_f(t)$, the pond factor, $C_f(t)$, the catchment factor, $E_f(t)$, the external factor, and $S_f(t)$, the system factor. Snow cover and ice cover effect in winter are significant in Takidani-ike system (Kashiwaya et al., 2012). Possibly, different processes for the system should be considered additionally in winter period. However, days of full ice cover in the pond and complete snow cover in the catchment are limited. Then, let us continue present discussion, assuming that winter conditions are not so different from other seasons. Change in water level is related not only to pond factor but also to catchment factor because water level change is directly linked to change in catchment area. Hence, eq. (4.7) is used for data discussion. Assuming that water level and precipitation are independent variables and other factors are dependent on them, eq. (4.7) becomes

$$SR(t) \propto S_{WL}(t) \times E_p(t) \quad (4.8),$$

where $S_{WL}(t)$, function of water level, and $E_p(t)$, function of precipitation.

Firstly, let us check the relationship between $SR(t)$ (sedimentation rate) and $E_p(t)$

(rainfall intensity). Secondly, the relationship between *SR(t)* (sedimentation rate) and $S_{WL}(t)$ (water level) will be discussed.

Observational results for monthly and seasonal changes in sedimentation rate and precipitation are shown in Fig. 4.11 (a,b) and Fig. 4.12 (a,b), respectively. They roughly show a similar trend. The monthly sedimentation rate has a fair correlation with monthly precipitation in the interval of December, 2008 – August, 2013 (Fig. 4.13a). However, the relationship between the seasonal sedimentation rate and precipitation is more correlative than the monthly relationship in the same interval (Fig. 4.13b), suggesting the reservoir effect in the catchment (Kashiwaya et al., 2012). The relationships between the sedimentation rates (Y; g/m^2/day) and the precipitations (X_1; mm/day) are expressed as follows,

$$Y = 12X_1^{0.54} \quad \text{(for monthly relation)} \quad (4.9),$$

$$Y = 5.3X_1^{0.99} \quad \text{(for seasonally relation)} \quad (4.10).$$

The seasonal average sedimentation rate is calculated for three months; December-February, March-May, June-August and September-November. The seasonal precipitation is average of precipitation intensity during the period.

Next, let us discuss about system factor including pond factor and catchment factor (geomorphological conditions), which is expressed as water level fluctuation. The fluctuation is closely related to change in pond bottom emergence (change in erosible area); erosional and sedimentary conditions. In Takidani-ike system, water level is controlled artificially from spring to summer for irrigation (Fig. 4.6b). Decrease in water level (WL_D; m) at time t is expressed as follows,

$$WL_D(t) = 5.0\text{-}WL_C(t) \quad (4.11),$$

because the maximum depth of Takidani-ike is 5.0 m.

Observational results for monthly and seasonal sedimentation rate and decrease in water level (WL_D) are shown in Fig. 4.14 (a,b), indicating that not only seasonal relationship between sedimentation rate (Y) and $WL_D(X_2)$ but also monthly relationship shows a fair correlation. The regression equations for them are;

$$Y = 6.1X_2^{1.9} \quad \text{(for monthly relation)} \quad (4.12),$$

$$Y = 4.9X_2^{2.1} \quad \text{(for seasonally relation)} \quad (4.13).$$

These results suggest that sedimentation rate is related to both water level and precipitation, especially seasonal precipitation.

4.7. Estimation of sedimentation function

As discussed above, sedimentation rate is related not only to rainfall intensity, but also to water level in the lake-catchment system. Therefore, let us discuss the sedimentation rate as a function with two independent valuables (precipitation intensity and water level change) with multiple regression analysis.

Calculated result of monthly sedimentation rate for the interval of Jun. 2011 – Sep. 2013 is shown with a multiple regression expression;

$$SR_M(t) = 2.8P_M(t)^{0.41} \times WL_{DM}(t)^{1.9} \quad (4.14),$$

where $SR_M(t)$ is monthly average sedimentation rate (g/m^2/day), $P_M(t)$ is monthly precipitation intensity (mm/day) and $WL_{DM}(t)$ is monthly average decrease in water level (m) at month *t*. Temporal sedimentation rate given by the multiple regression equation is shown in Fig. 4.15 with rates by two simple regression equations. The summary of statistics is shown in Table. 4.1.

Next, seasonal sedimentation rate is calculated for the interval of summer period in 2011 to summer period in 2013 (Fig. 4.16). The regression equation is expressed as follows,

$$SR_S(t) = 0.75P_S(t)^{1.0} \times WL_{DS}(t)^{2.1} \quad (4.15),$$

where $SR_S(t)$ is seasonal average sedimentation rate (g/m^2/day), $P_S(t)$ is seasonal average precipitation intensity (mm/day) and $WL_{DS}(t)$ is seasonal average decrease in water level (m) at season *t*. Temporal seasonal sedimentation rate given by the multiple regression equation is shown in Fig. 4.16 with rates by two simple regression equations. The summary of statistics is shown in Table. 4.1.

Results discussed above support that the sedimentation rate (both monthly and seasonal sedimentation) is expressed as a function of two factors; precipitation intensity and water level change. The results also show that the correlation for the seasonal relationship (R=0.77) is better than one for the monthly relationship (R=0.58). This is partially related to the weak relationship between monthly sedimentation rate and precipitation, which suggests that reservoir effect in the catchment, as mentioned before, should be considered.

On the basis of above consideration, we may say that eq. (4.7) is fundamentally appropriate for a lake-catchment system and the sedimentation rate discussed here is a function of rainfall intensity and decrease in water level (increase in erodible area).

5. Conclusions

The analytical results for lacustrine sediments obtained from Lake Biwa and for hydrological data suggest that: i) disastrous flood events, namely the Isewan Typhoon (IT; 1959) and the Meiji heavy rainfall (MH; 1896), are recorded in the physical properties of the lacustrine sediments (mineral content, density, grain size); ii) the density and mineral content respond positively to rainfall intensity (70-mm excess rainfall); and iii) the mineral grain size distribution may respond positively to the rainfall intensity in the catchment and negatively to the distance transported from the river mouth. These lead to that physical parameters of sediments are closely related to hydrological conditions, which is indicated also in long-term hydro-climatological studies. This suggests that interpretation of physical properties supported with modern observation is of great help for considering the properties in the long-term fluctuation if the relationship between signal and noise is properly recognized in short-term and long-term fluctuations.

Analytical results for the physical properties of Lake Onuma sediments and hydrological data around the Lake Onuma system (snowfall area) indicate that: i) earth-surface processes are different between summer and winter periods; ii) the mineral grain size correlates highly with summer precipitation, and fairly with annual precipitation, suggesting that it may be a proxy for precipitation; and iii) the mineral grain size is also available for estimating discharge in the lake.

Observational and analytical results for a small pond-catchment system called Takidani-ike show (the system is used for clarifying erosion and sedimentation processes in a lake-catchment system in order to establish suitable proxy data from

sedimentary records) that; the sedimentation rate (both monthly and seasonal sedimentation) is expressed as a function of two factors; precipitation intensity (external factor) and water level change (system factor, closely related to size of erosible area). The correlation for the seasonal relationship is better than one for the monthly relationship, suggesting that reservoir effect in the catchment should be considered. The results also show that some physical properties (mineral grain size, etc.) may be used as proxies for sedimentation rate.

These provide precious information for proper interpretation of data without observation and a significant clue for establishing mathematical expressions of past proxy data.

Acknowledgements

I thank Dr. Kumagai, M., Lake Biwa Environmental Research Institute, for making it possible for us to obtain the Lake Biwa sediment core samples, and the Ministry of Land, Infrastructure, Transport and Tourism, Kinki Regional Development Bureau, Biwako Office, for providing us with the data on the water level in Lake Biwa. I thank Dr. Sakaguchi, A., Hiroshima University, for experiment of radioactivity of Lake Biwa sediment core (BW06T5) and valuable discussion, I also thank Prof. Yamamoto, M. and Dr. Aota, Y., Kanazawa University, for cooperation to obtain the Lake Biwa sediment core samples.

I thank Prof. Ganzawa, Y. and Prof. Tanaka, K., Hokkaido University of Education, for cooperating to obtain Lake Onuma sediment and valuable discussion, and the Hakodate Marine Observatory for providing us with the data on precipitation in Mori Observatory, Hakodate Marine Observatory and Onuma Observatory, Hokkaido Electric Power Company for providing us with the data on discharge in Lake Onuma, and Mori Town and Mori Library given us the history book and information of Mori Town. I also thank Dr. Ochiai, S., Kanazawa University, for experiment of radioactivity of Lake Onuma sediments cores (ON11-2-2 and ON11-6) and valuable discussion, and Mr. Enkbayar, B., Mongolian Academy of Sciences, for an assistance in experiment about density of Lake Onuma sediment. Thanks are due to Dr. Katsuki, K., Korea Institute of Geoscience and Mineral Resources, for given columnar sections, Dr. Katsuta, N., Gifu University, for obtaining scanned XRF data, Prof. Hyodo, M., Kobe University, for obtaining magnetic susceptibility, and Dr. Wang, Y., Chinese Academy of Sciences, for taking photographs of sediment cores, about 4-m core sediments obtained from Lake

Onuma in 2012. I wish to acknowledge obtaining 4-m core sediments from Lake Onuma with Prof. Mitamura, M., Osaka City University, Dr. Kim, J. Y., Korea Institute of Geoscience and Mineral Resources, Prof. Shen, J., Chinese Academy of Sciences, and Prof. Nagao, S., Kanazawa University.

I thank Dr. Nagamura, Y., Kanazawa University, for laboratory management of experiment at the Radioisotope Laboratory for Natural Science and Technology, Kanazawa University, and Prof. Yokoyama, A., Dr. Uesugi, M. and Dr. Murakami, T., Kanazawa University, for variable discussion about analyses of Cs-137 and excess Pb-210. I thank Mr. Yoshida, E. and Ms. Yoshida, M. for kindness supports in observation of rain gauge near Takidani-ike. I am grateful to Dr. Fukushi, K., our colleagues belong to the Hydrogeomorphological Laboratory and Isotope-geochemical Laboratory, Kanazawa University, and member of study abroad program from National Taiwan University and Kyung Hee University for cooperation to obtain sediment from Takidani-ike and Dojyo-ike. I also thank Dr. Fukui, K., Tateyama Caldera Sabo Museum, for cooperation to obtain Dojyo-ike sediment.

I appreciate the valuable discussion and encouragement from Prof. Kashiwaya, K. and Dr. Hasebe, N., Kanazawa University, as a supervisor. I would like to thank Dr. Matsuki, A. Dr. Endo, N. and Dr. Aoki, T., our colleagues in the Hydrogeomorphological Laboratory and Isotope-geochemical Laboratory at Kanazawa University, for valuable discussion, and staffs in Earth Science Course, Kanazawa University, for their support of this thesis.

I thank Japan Society for the Promotion of Science for Young Scientists for support of my study. I wish to acknowledge encouragement with my parents, Mr. Itono, T. and Ms. Itono, Y.

References

Biwako Chisuikai ed. (1968) *Biwako Chisui Enkakushi (A History of Water Control in Lake Biwa)*, Biwako Chisuikai, Otsu, 1179p. (in Japanese).

Chikita, K. (1986) Sedimentation in an intermountain lake, Lake Okotanpe, Hokkaido. I. Sedimentary processes derived from the grain size distribution of surficial sediments: Japanese Journal of Limnology, **47**, 53-61.

Fujie, T. (2005) An analysis on changes of erosional environment in catchment-pond systems based on pond sediments and surrounding physical information: MSc thesis, Kanazawa University (in Japanese with English abstract).

Ganzawa, Y., Kito, N., Yanai, S. and Sadakata, N. (2005) Discovery of primary tephra layers and research of the early stage of the volcanic history of Hokkaido-Komagatake volcano, Japan: The Journal of the Geological Society of Japan, **111**, 581-589 (in Japanese with English abstract).

Hikone Local Meteorological Observatory ed. (1993) *Shigaken no Kisyou (Meteorology in Shiga Prefecture) -Centenary Edition for Hikone Local Meteorological Observatory-*. Ministry of Finance, Tokyo, 92 (in Japanese).

Hokkaido Government (2012) Hokkaido no Mizukankyou (Hydro-environment in Hokkaido): < http://envgis.hokkaido-ies.go.jp/mizu_index.html> (accessed 13.06.2013)

Horie, S. ed. (1984) *Lake Biwa*, Dr W. Junk Publishers, Dordrecht, 654 p.

Inouchi, Y. (1987) Acoustic estimation method of sedimentation rate -Case study in Lake Biwa-: Earth Science (Chikyu Kagaku), **41**, 231-241 (in Japanese with English abstract).

Itoh, N., Tamamura, S. and Kumagai, M. (2010) Distributions of polycyclic aromatic hydrocarbons in a sediment core from the north basin of Lake Biwa, Japan: Organic Geochemistry, **41**, 845-852.

Itono, T., Kashiwaya, K. and Sakaguchi, A. (2012) Disastrous flood events found in lacustrine sediments from Lake Biwa: Transactions, Japanese Geomorphological Union, **33**, 453-468.

Kashiwaya, K. (2012) Earth surface processes and environmental changes in lake–catchment systems: Transactions, Japanese Geomorphological Union, **33**, 121-136.

Kashiwaya, K. ed. (2003) *Long Continental Records from Lake Baikal*, Springer-Verlag, Tokyo, 370p.

Kashiwaya, K., Fukuyama, K. and Yamamoto, A. (1991) Time variation in coarse materials from lake bottom sediments and secular paleoclimatic change: Geophysical Research Letters, **18**, 1245-1248.

Kashiwaya, K., Ochiai, S., Okimura, T., Nahm, Wook-Hyun., Yang, Dong-Yoon. and Kim, Ju-Yong. (2012) Erosion and sedimentation in Lake-catchment systems in Japan and Korea on the basis of an elementary process model: Transactions, Japanese Geomorphological Union, **33**, 219-236.

Kashiwaya, K., Okimura, T. and Harada, T. (1997) Land transformation and pond sediment information: Earth Surface Processes and Landforms, **22**, 913-922.

Kashiwaya, K., Okimura, T. and Kawatani, T. (1986) Dendrochronological information and hydrological conditions for landslides in Mt. Futatabisan Area of Rokko Mountains: Transactions, Japanese Geomorphological Union, **7**, 281-290 (in Japanese with English abstract).

Kashiwaya, K., Okimura, T., Kawatani, T., Aoki, T. and Isozumi, Y. (1995) Surface erosional environment and pond sediment information: *In* Slaymarker, O. ed. *Steepland Geomorphology*. John Wiley & Sons Ltd, Chichester, 219-231.

Katsuragi, Y. (1983) A study of ^{90}Sr fallout in Japan: Papers in Meteorology and Geophysics, **33**, 277-291.

Menounos, B. and Clague, J. J. (2008) Reconstructing hydro-climatic events and glacier fluctuations over the past millennium from annually laminated sediments of Cheakamus Lake, southern Coast Mountains, British Columbia, Canada: Quaternary Science Reviews, **27**, 701-713.

Meyers, P. A., Takemura, K. and Horie, S. (1993) Reinterpretation of late Quaternary sediment chronology of Lake Biwa, Japan, from correlation with marine glacial-interglacial cycles: Quaternary Research, **39**, 154-162.

Mori Town ed. (1980) *Mori Choushi (History of Mori Town)*, Mori Town, Sapporo, 1279p. (in Japanese).

Mortlock, R. A. and Froelich, P. N. (1989) A simple method for the rapid determination of biogenic opal in pelagic marine sediments: Deep-Sea Research, **36**, 1415-1426.

Nishiji, K., Kashiwaya, K., Muroi, K. and Kunika, K. (2004) Analytical results of Dojo-ike sediment in Tateyama Caldera: Ann. Rep. Tateyama Caldera Sabo Museum, 5, 1-8 (in Japanese).

Ochiai, S. and Kashiwaya, K. (2003) A conceptual model of sedimentation processes for a hydrogeomorphological study in Lake Baikal: *In* Kashiwaya, K. ed. *Long Continental Records from Lake Baikal*. Springer-Verlag, Tokyo, 297-312.

Ochiai, S., Nagao, S., Yamamoto, M., Itono, T., Kashiwaya, K., Fukui, K. and Iida, H. (2013) Deposition records in lake sediments in western Japan of radioactive Cs from

the Fukushima Dai-ichi nuclear power plant accident: Applied Radiation and Isotopes, **81**, 366-370.

Ormsby, J. F. A. (1961) Design of numerical filters with applications to missile data processing: Journal of the Association for Computing Machinery, **8**, 440-466.

Shiga Prefecture (1966) *Shigaken Saigaishi (History of Disaster in Shiga Prefecture)*, Shiga Prefecture, Otsu, 222p. (in Japanese).

Shimada, T., Kashiwaya, K., Hyodo, M. and Masuzawa, T. (2002) Hydro-environmental fluctuation in a lake-catchment system during the late Holocene inferred from Lake Yogo sediments: Transactions, Japanese Geomorphological Union, **23**, 415-431 (in Japanese with English abstract).

Somiya, I. (2000) Biwako no gaisetsu (Outline of Lake Biwa), *In* Somiya, I. ed. *Biwako -Sono Kankyou to Suishitsu Keisei (Lake Biwa -Its Environment and Water Quality).* Gihodo Shuppan Co., Ltd, Tokyo, 1-7 (in Japanese).

Støren, E. N., Dahl, S. O., Nesje, A. and Paasche, Ø. (2010) Identifying the sedimentary imprint of high-frequency Holocene river floods in lake sediments: development and application of a new method: Quaternary Science Reviews, **29**, 3021-3033.

Taishi, H. (1995) Recent sedimentation rates and sedimentary anomalies, *In* Okuda, S., Imberger, J. and Kumagai, M. eds. *Physical Processes in a Large Lake: Lake Biwa, Japan. Coastal and Estuarine Studies*. American Geophysical Union, Washington, DC, **48**, 141-152.

Taishi, H. and Kashiwaya, K. (1993) Biwako koteihyousou no taisekiijyou (Sedimentary anomalies detected in Lake Biwa surface sediments): Chikyu monthly symposium, **8**, 123-127 (in Japanese).

Takemura, K. (1990) Tectonic and climatic record of the Lake Biwa, Japan, region,

provided by the sediments deposited since Pliocene times: Palaeogeography, Palaeoclimatology, Palaeoecology, **78**, 185-193.

Tanaka, T. (2005) Water pollution factors of land use and river water quality in eutrophicated lake watersheds: Lake Oshima-Oonuma, Hokkaido, Japan: Journal of Human and Environmental Symbiosis, **11**, 13-22 (in Japanese with English abstract).

Tylmann, W., Turczyński, M. and Kinder, M. (2009) Sedimentation rates and erosion changes recorded in recent sediments of Lake Piaseczno, south-eastern Poland: GEOLOGIJA, **51**, 125-130.

Uemura, Y. (1987) *Nihon no chishitu 6 Kinki chihou (Geology of Japan 6 Kinki region)*, *In* Nihon no chishitu "Kinki chihou" editorial committee ed. Kyoritsu Shuppan Co., Ltd, Tokyo, 164-166 (in Japanese).

Xiao, J., Inouchi, Y., Kumai, H., Yoshikawa, S., Kondo, Y., Liu, T. and An, Z. (1997) Fluvial quartz flux to Lake Biwa of central Japan over the past 145,000 years: The Quaternary Research, **36**, 17-27.

Yamamoto, A. (1984) Grain size variation: *In* Horie, S. ed. *Lake Biwa*. Dr W. Junk Publishers, Dordrecht, 439-459.

Yamamoto, A., Kashiwaya, K. and Fukuyama, K. (1985) Periodic variations of grain size in Pleistocene sediments in Lake Biwa and earth-orbital cycles: Geophysical Research Letters, **12**, 585-588.

Yoshimoto, M., Takarada, S. and Takahashi, R. (2007) Eruptive history of Hokkaido-Komagatake volcano, northern Japan: Journal of the Geological Society of Japan, **113**, **Supplement**, 81-92 (in Japanese with English abstract).

Abstract

Lacustrine sediments and lake-catchment systems (Lake Biwa, Lake Onuma, and Takidani-ike) were checked to clarify the hydro-environmental fluctuation in the instrumental observation period.

The analysis of the Lake Biwa core sediments showed that disastrous flood events, the Isewan Typhoon (1959) and Meiji heavy rainfall (1896), are clearly recorded in the physical properties of the sediments; the density and mineral content of the sediments from the events were large. They are positively proportional to rainfall intensity (70-mm excess rainfall). The mineral grain size distribution in lakes may be a function of the rainfall intensity in the catchment and the transporting distance from the river mouth.

The physical properties of Lake Onuma core sediments indicate that the mineral grain size correlates with precipitation, especially in summer period. The earth-surface processes are different in summer period and winter (snow cover and snowmelt) period in snowfall area.

Instrumental observation with sediment traps in Takidani-ike, Kanazawa, suggests that the sedimentation rate could be expressed as a function of precipitation intensity (external factor) and decrease in water level (increase in erosible area) (system factor).

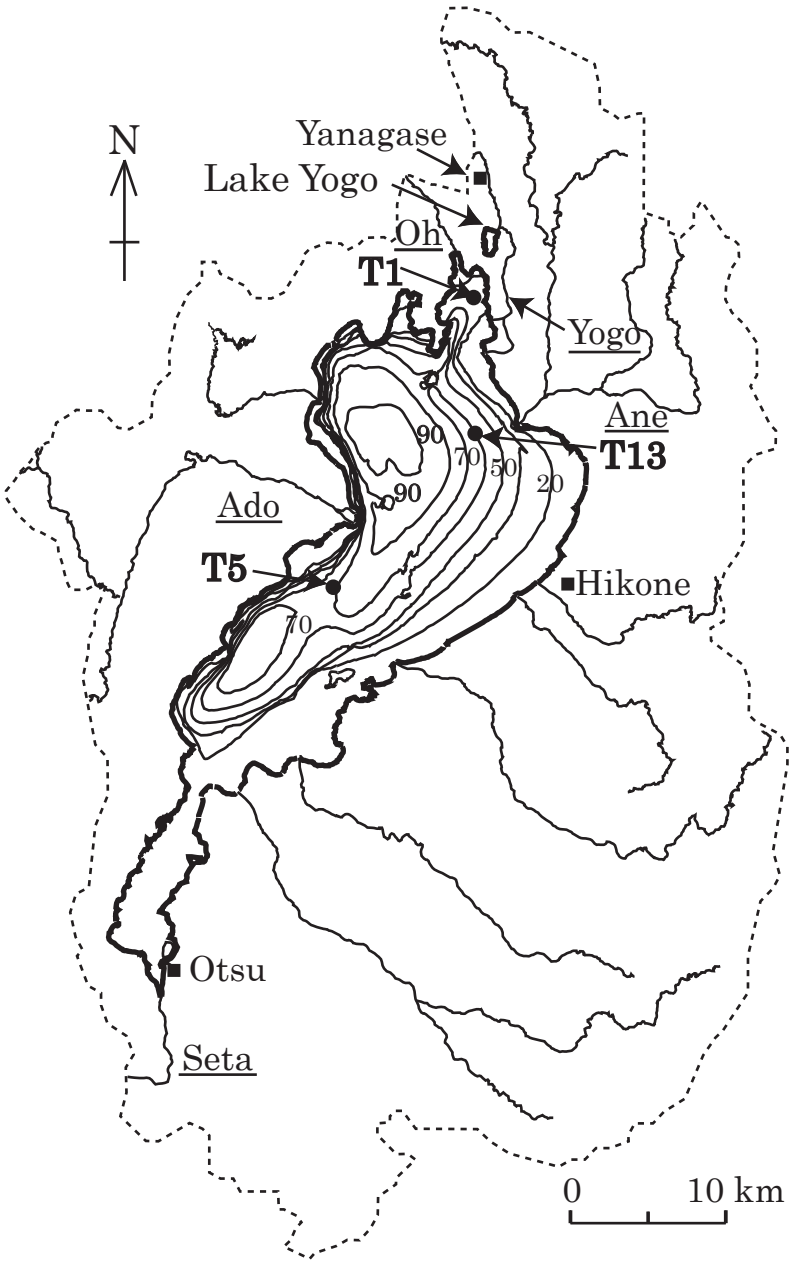

Fig. 2.1. Sampling points of core sediments in Lake Biwa. Underlining signifies a river.

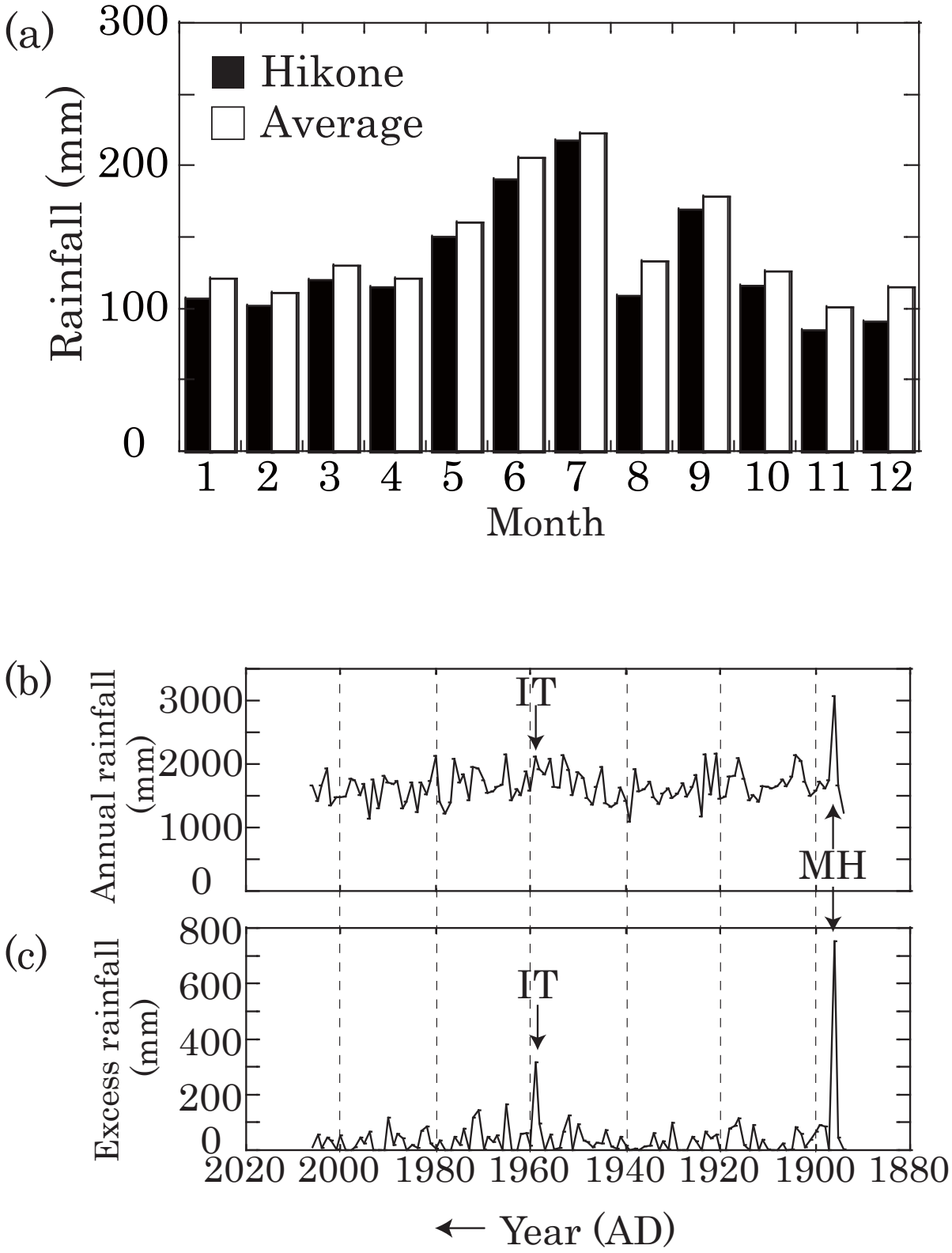

Fig. 2.2. Rainfall data observed in Hikone.
(a) Monthly rainfall. Hikone (black), average of 10 stations in catchment (white); (b) annual rainfall; (c) 70-mm excess rainfall in Hikone. IT; Isewan Typhoon (1959), MH; Meiji heavy rainfall (1896).

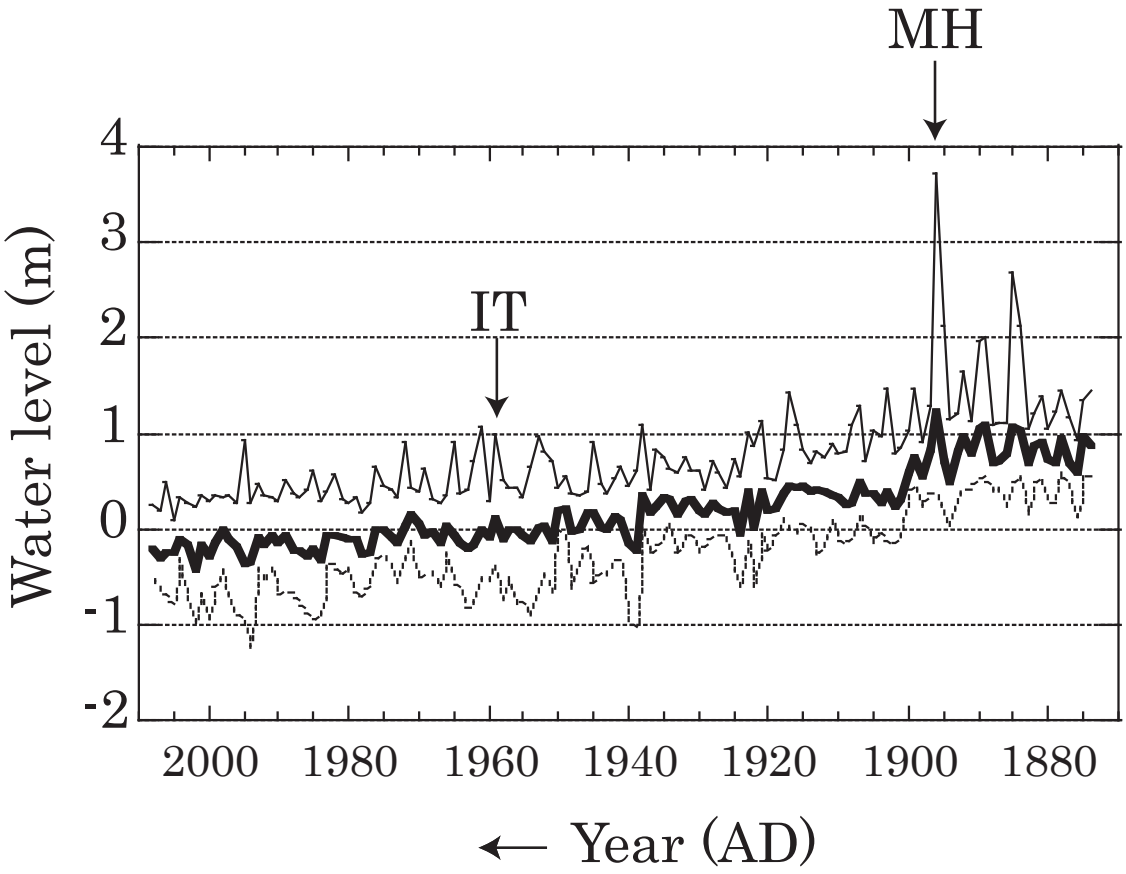

Fig. 2.3. Daily lake water level in Lake Biwa. Maximum (thin solid line), average (thick solid line), minimum (dashed line). IT; Isewan Typhoon (1959), MH; Meiji heavy rainfall (1896).

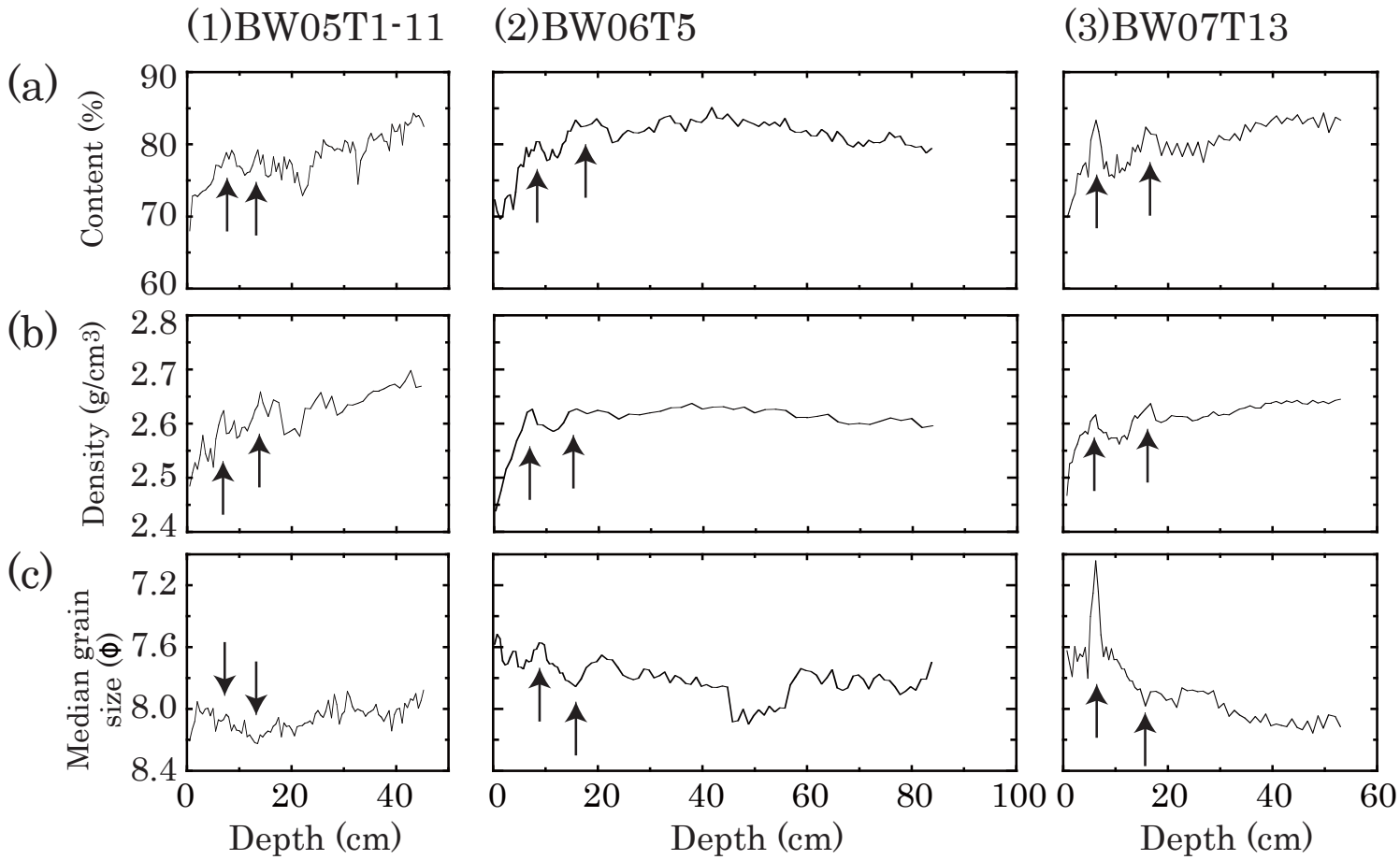

Fig. 2.4. Changes in physical properties of the three sediment cores:
(1) BW05T1-11, (2) BW06T5, and (3) BW07T13. (a) mineral content (%),
(b) grain density (g/cm3) and (c) mineral grain size (Φ). Arrows show the peaks.

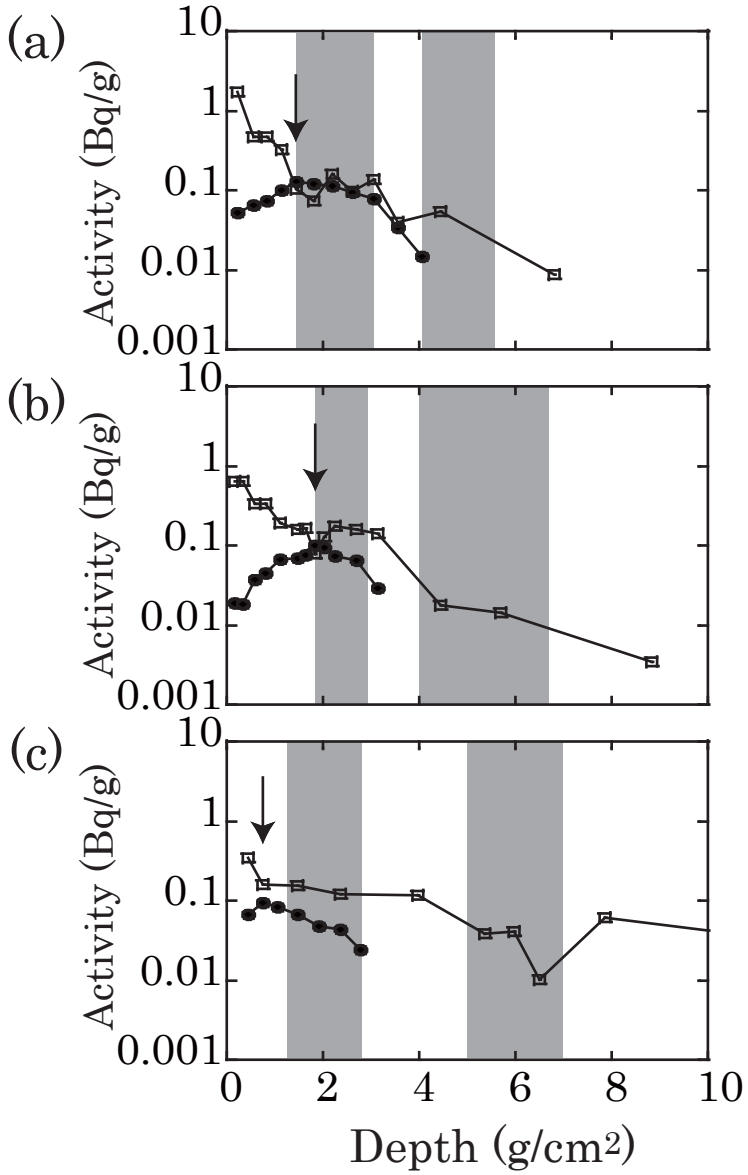

Fig. 2.5. Changes in excess Pb-210 concentration (squares) and Cs-137 concentration (solid circles). (a) BW05T1-11, (b) BW06T5 and (c) BW07T13. Maximum value in Cs-137 concentration (arrow) indicates the layer deposited around 1963. Shaded regions show the depth of two peaks in mineral content and density.

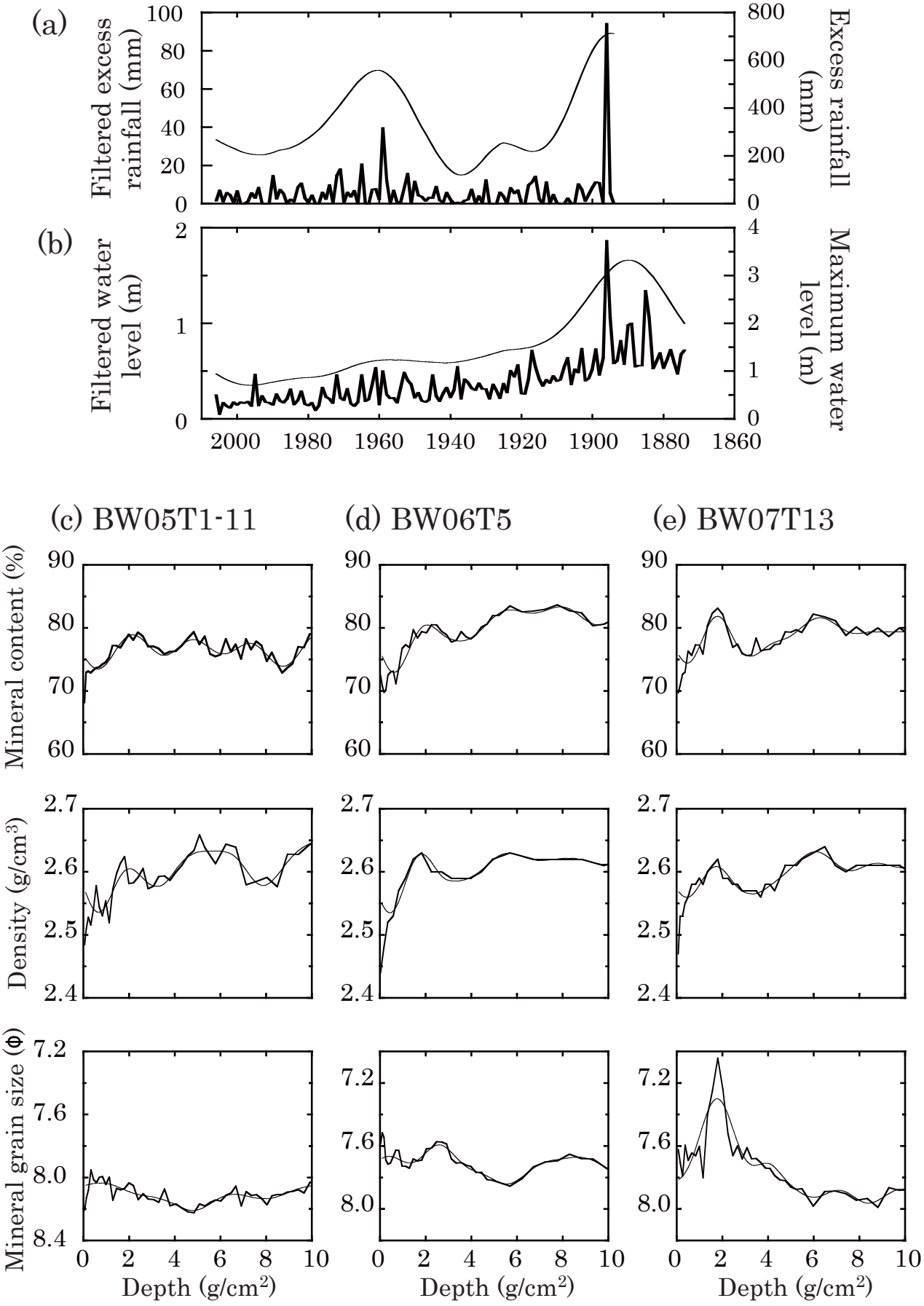

Fig. 2.6. Changes in 70-mm excess rainfall (a), water level (b) and physical properties (mineral content, grain density, and mineral grain size) of the three sediment cores; (c) BW05T1-11, (d) BW06T5 and (e) BW07T13. Arrows show the peaks of the physical properties. Row data (thick solid line), filtered ones (thin solid line).

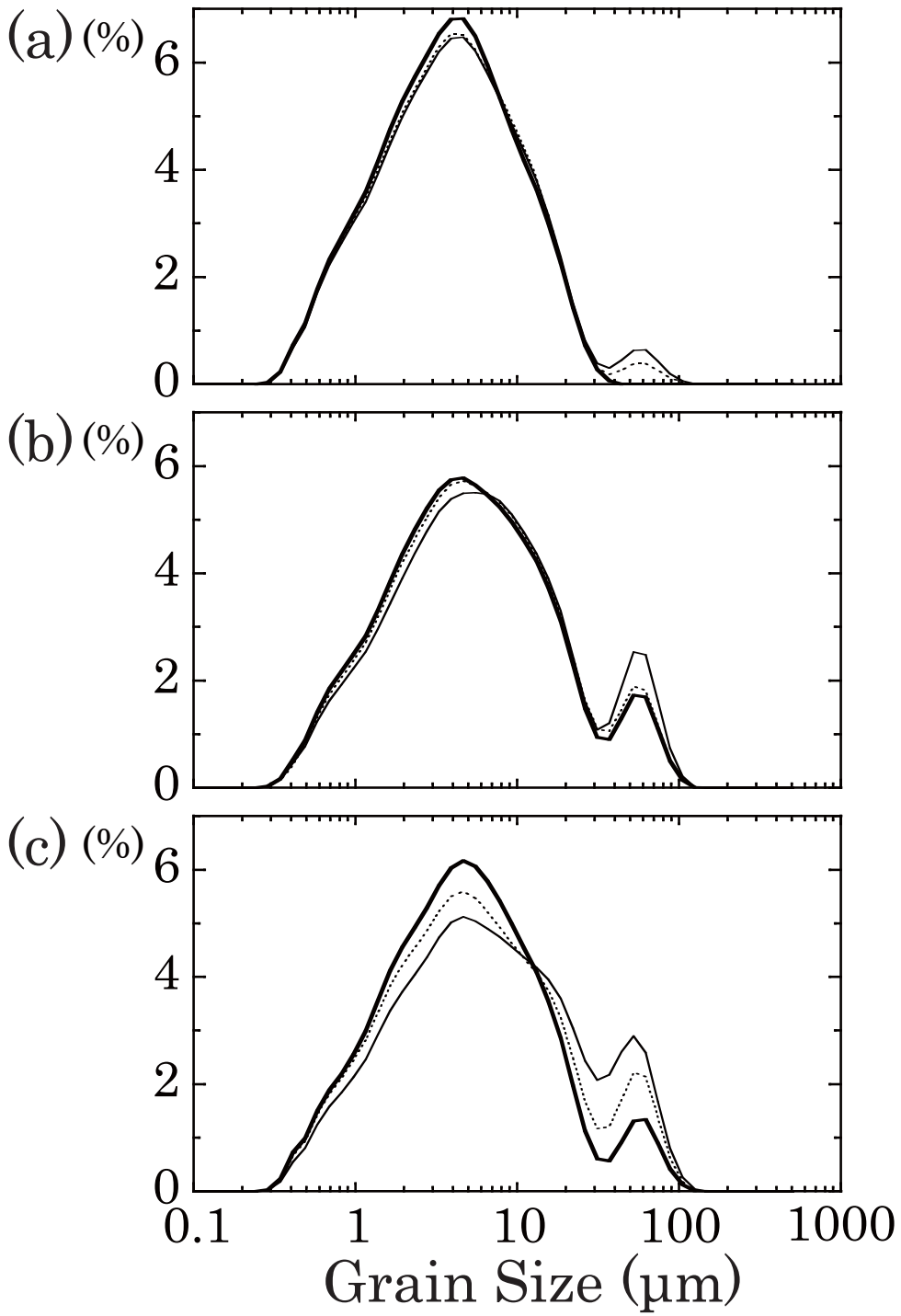

Fig. 2.7. Mineral grain size distribution. (a) BW05T1-11, (b) BW06T5 and(c) BW07T13. IT period (thin solid line), MH period (thick solid line) and IT-MH period (dashed line).

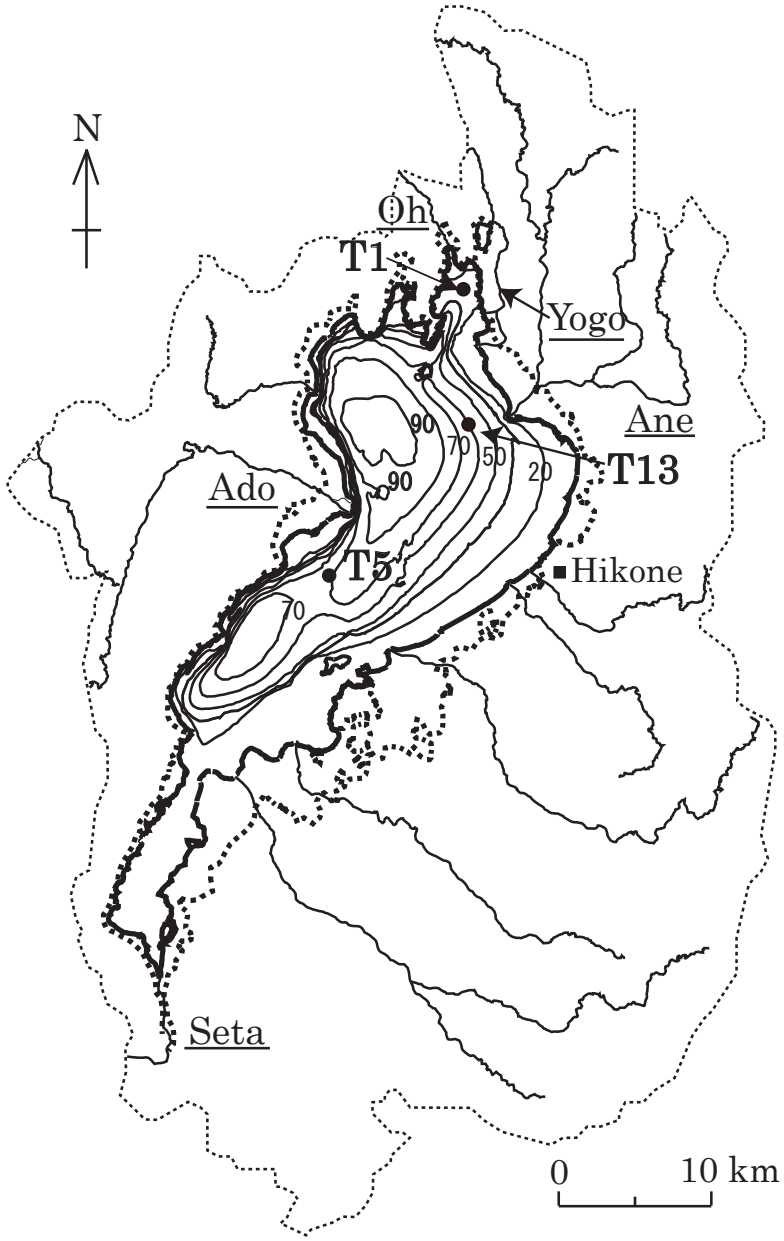

Fig. 2.8. Map of flood area in Meiji heavy rainfall. Border (dashed line), normal shore line at present (thick solid line). The underlined labels show the rivers.

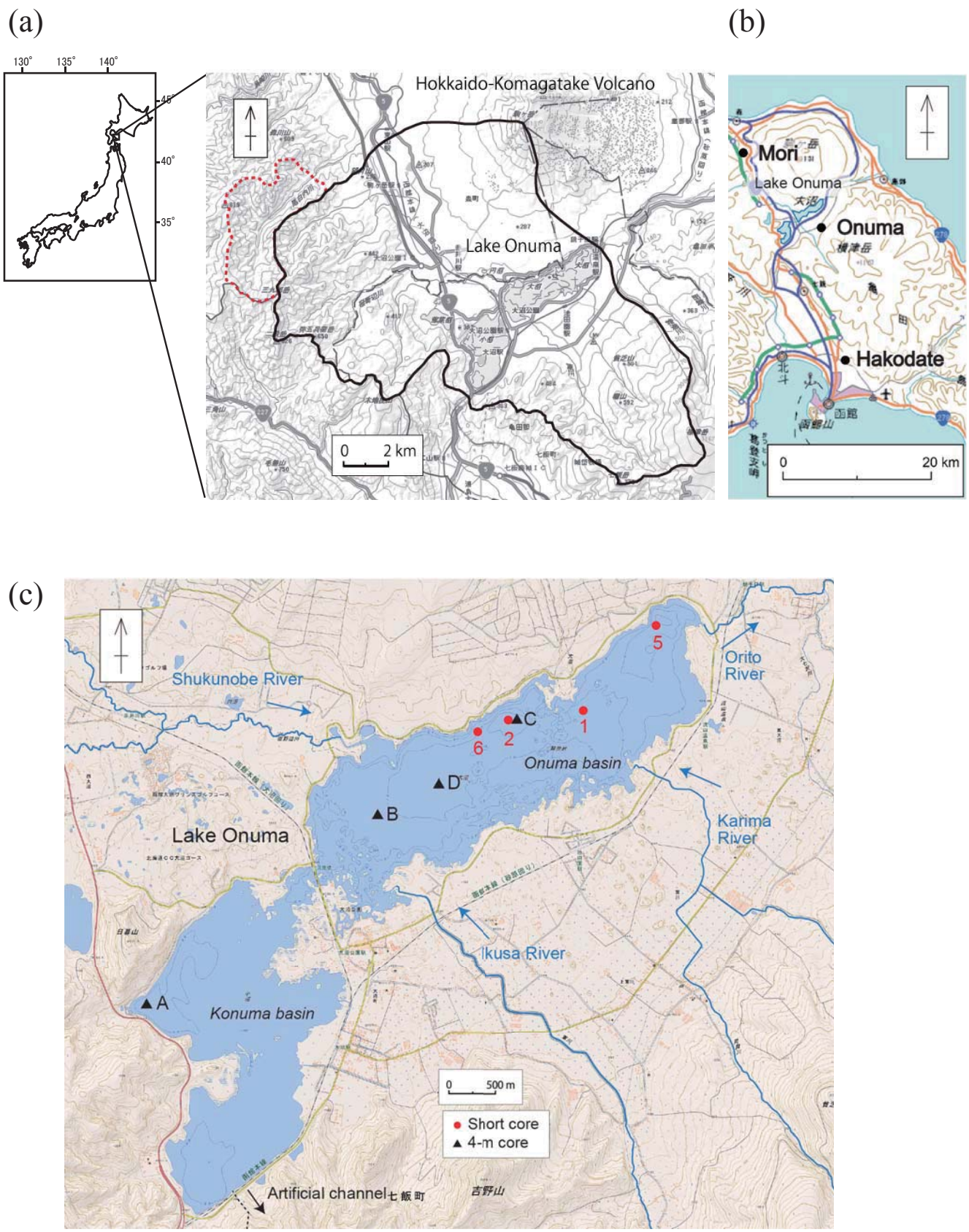

Fig. 3.1. Index map of Lake Onuma.
(a) catchment of Lake Onuma. Original catchment area (solid line) and enlarged catchment area in 1978 (red, dashed line), (b) map of meteorological observatories around the catchment and (c) sampling points in Lake Onuma; short sediment cores (closed circle) and 4-m sediment cores (closed triangle). These maps are modified after GSI Maps (Geospatial Information Authority of Japan).

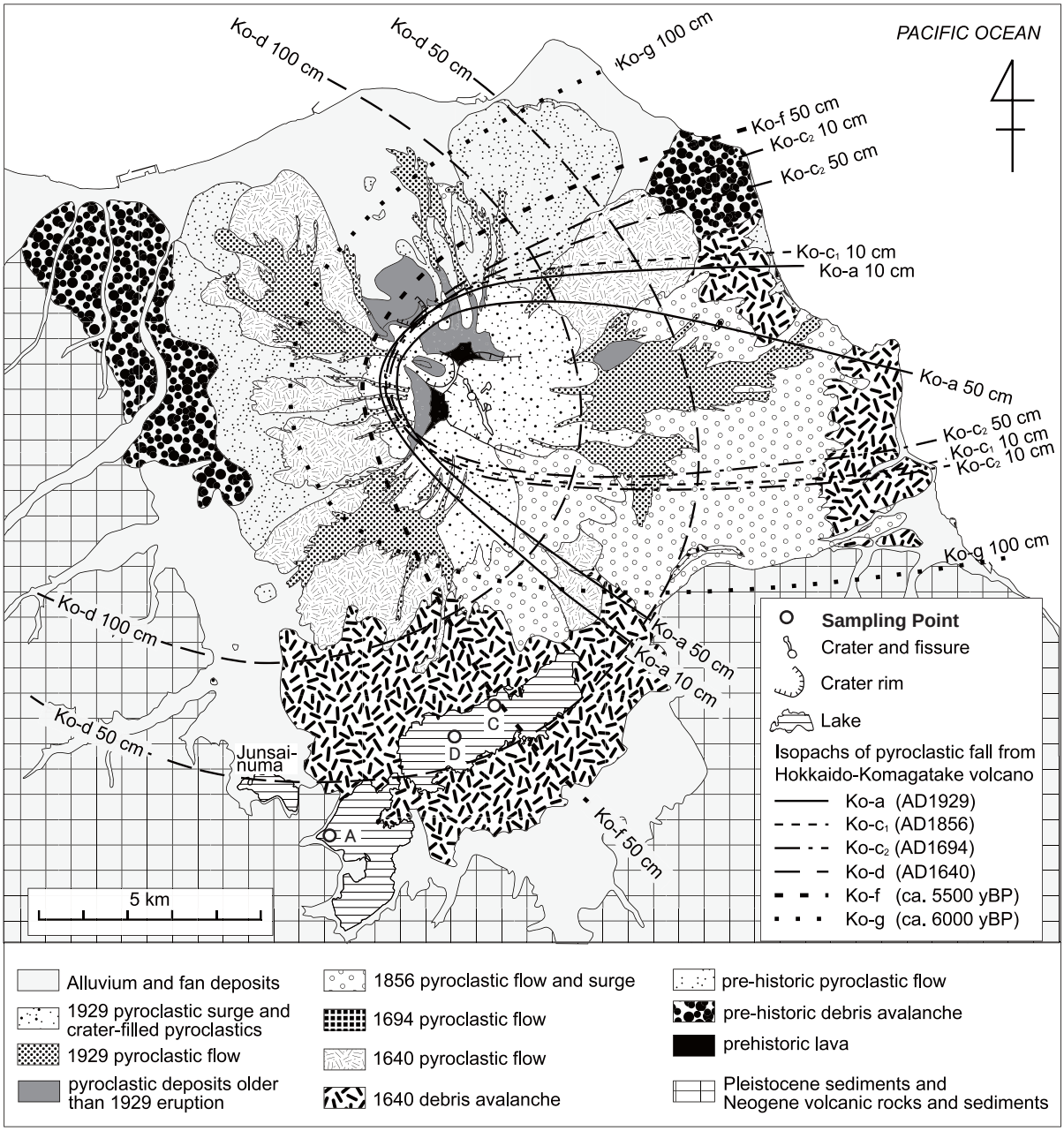

Fig. 3.2. Geological map around Lake Onuma.
This map is modified after Yoshimoto et al., 2007.
Sampling point of 4-m core sediments (circle).

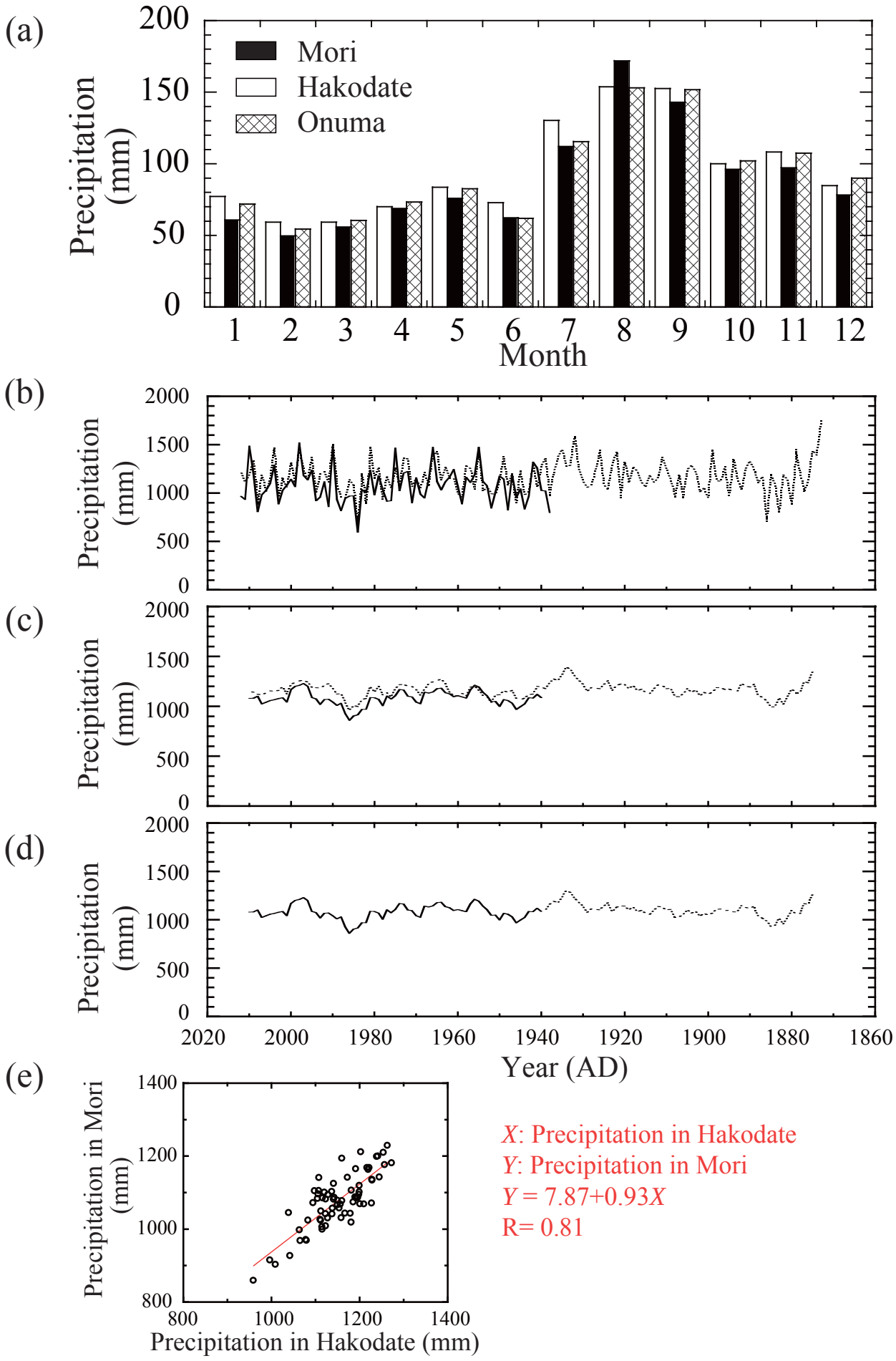

Fig. 3.3. Observational climatic data around Lake Onuma.
(a) average monthly precipitation (1981-2010). Mori (black), Hakodate (white) and Onuma (cross), (b) annual precipitation in Mori (solid line) and Hakodate (dashed line), (c) 5-year running average of annual precipitation in Mori (solid line) and Hakodate (dashed line), (d) estimated 5-year average precipitation in Mori (dashed line is estimated) and (e) relationship between 5-year running average of annual precipitation in Mori and Hakodate.

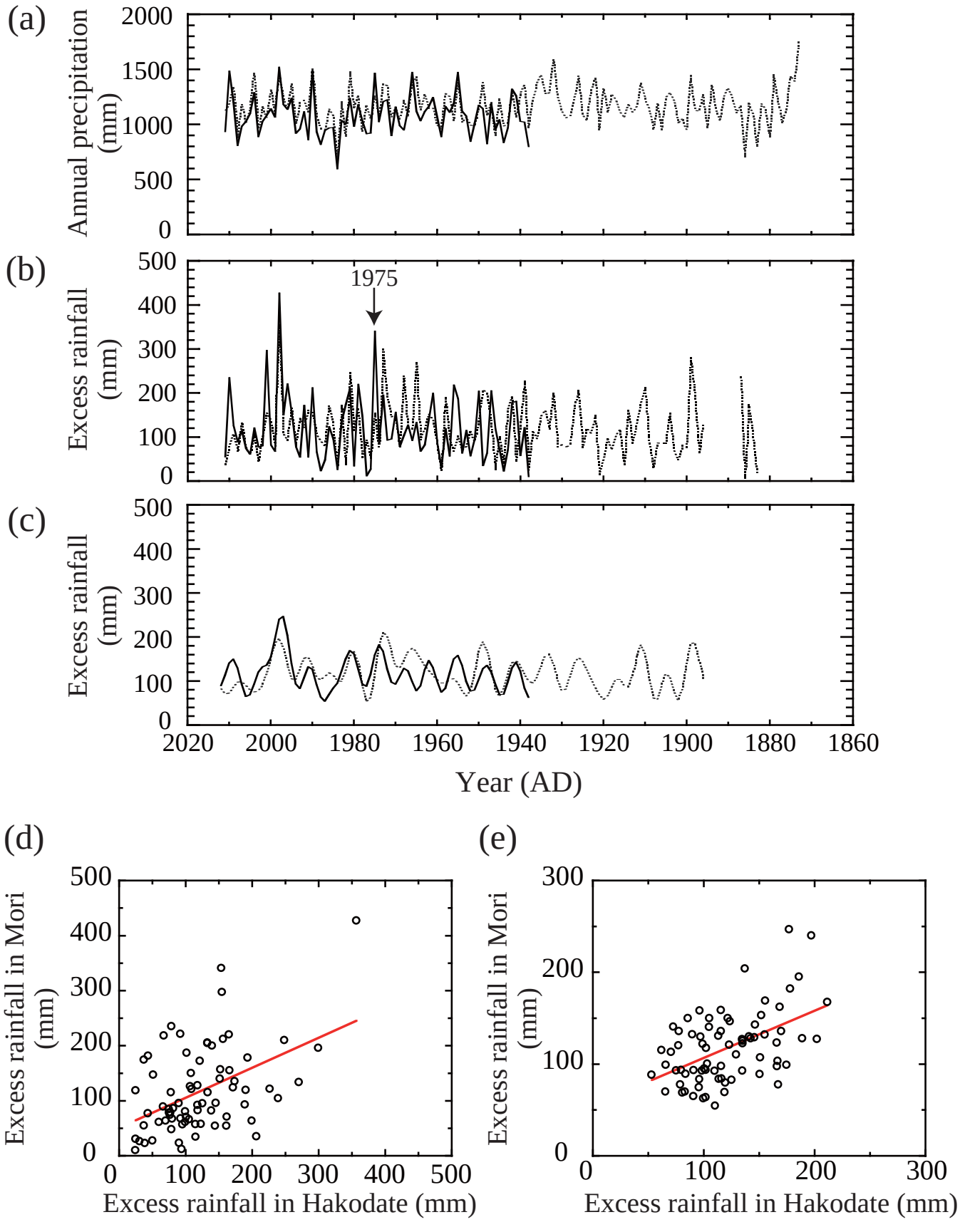

Fig. 3.4. Observational meteorological data around Lake Onuma.
Observational data in Mori (solid line) and in Hakodate (dashed line);
(a) annual precipitation, (b) 30mm excess rainfall. Arrow indicates 1975, and (c) filtered 30 mm excess rainfall. Relationship between 30 mm excess rainfall in Mori and in Hakodate. (d) row data and (e) filtered data. Regression curves are expressed as follows,
(Y: excess rainfall in Mori, X: excess rainfall in Hakodate and R: correlation coefficient)
$Y = 51 + 0.55X$, R = 0.46 for low data (d) and
$Y = 55 + 0.51X$, R = 0.50 for filtered data (e).

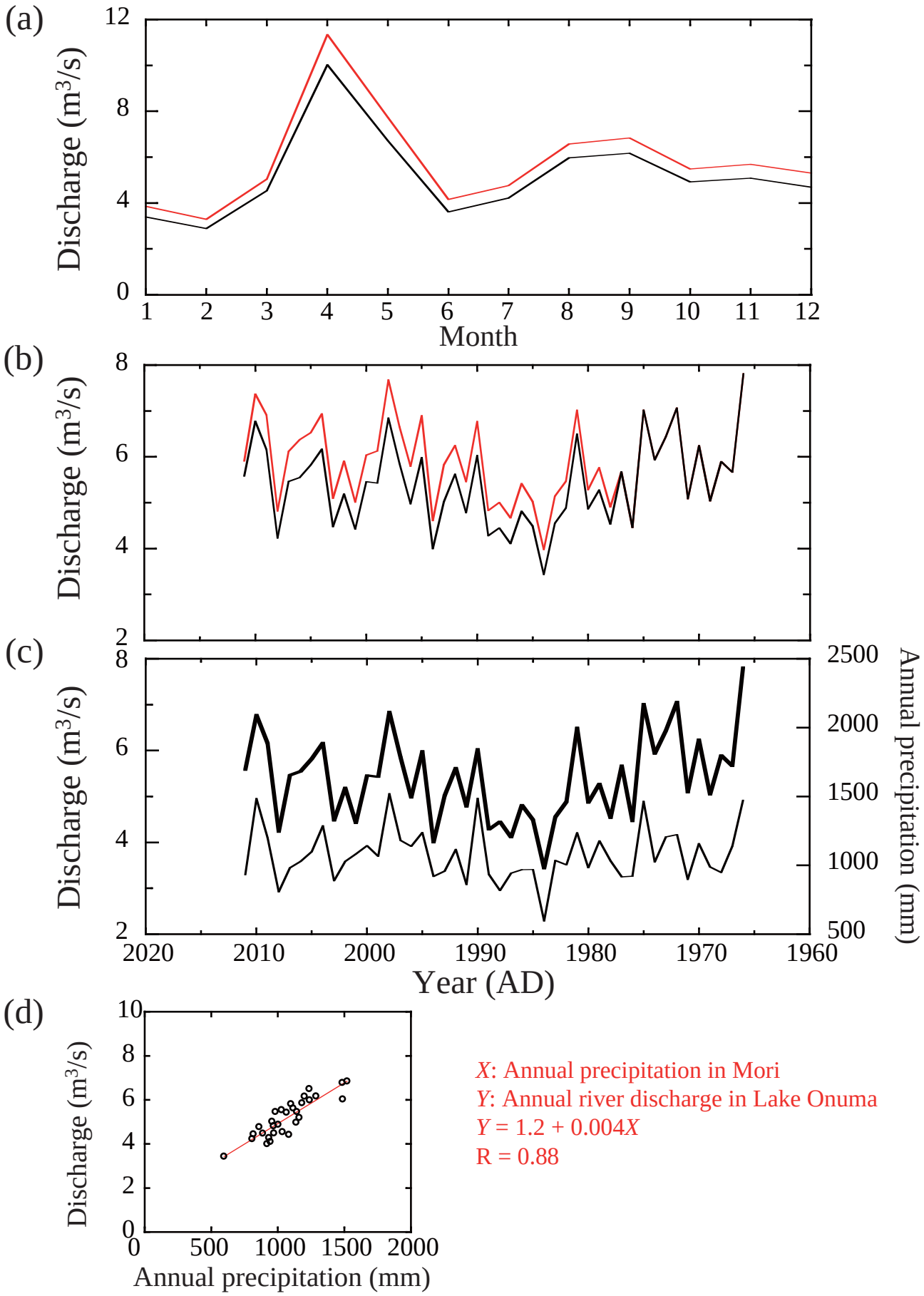

Fig. 3.5. River discharge in Lake Onuma.
Total river discharge (additional plus original; red) and original river discharge (black); (a) average monthly discharge (1981-2010), (b) annual discharge, (c) annual river discharge (thick solid line) and precipitation in Mori (thin solid line), and (d) relationship between annual river discharge and annual precipitation in Mori (1981-2010).

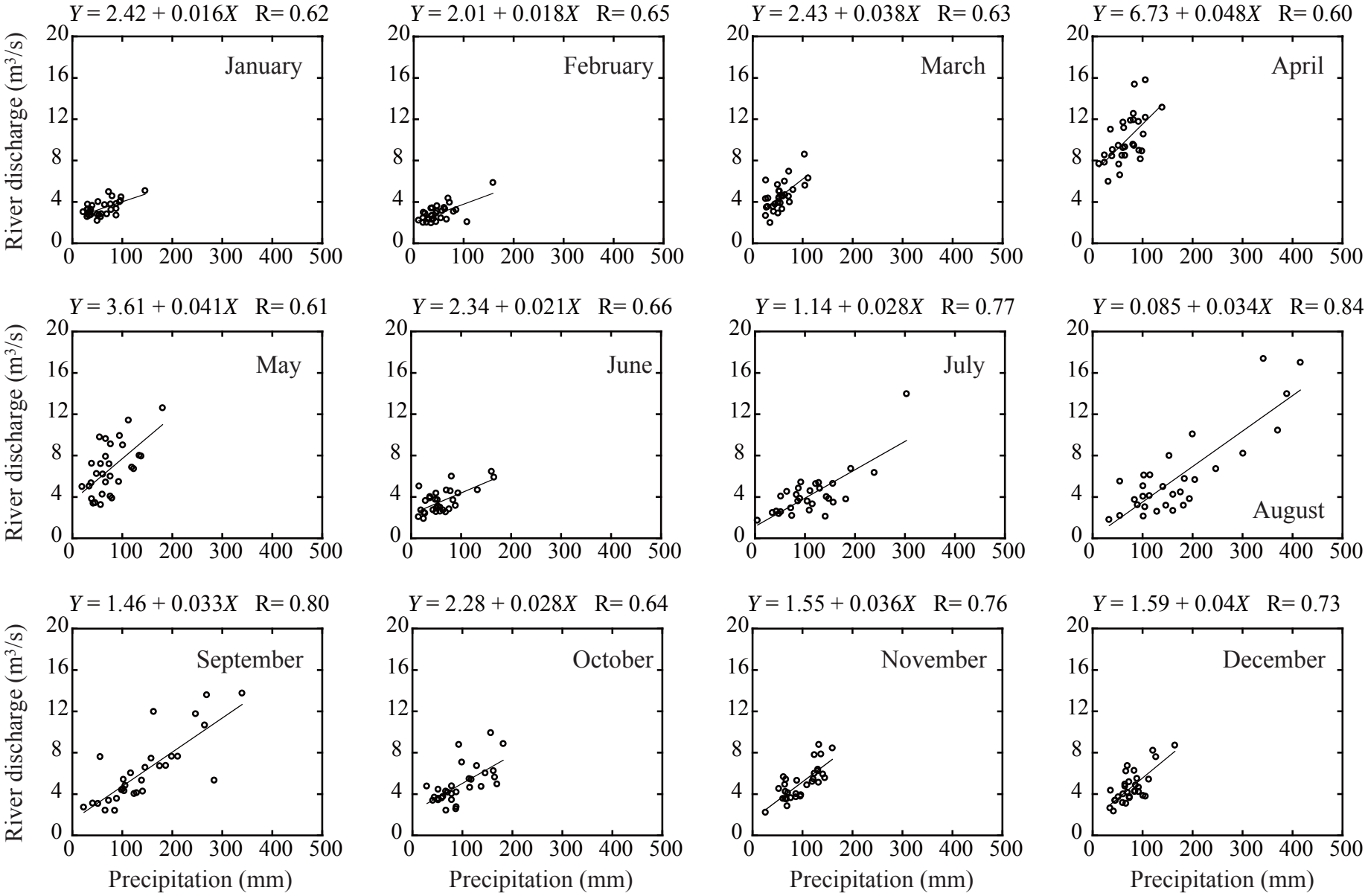

Fig. 3.6. Monthly relationship between river discharge in Lake Onuma and precipitation in Mori.

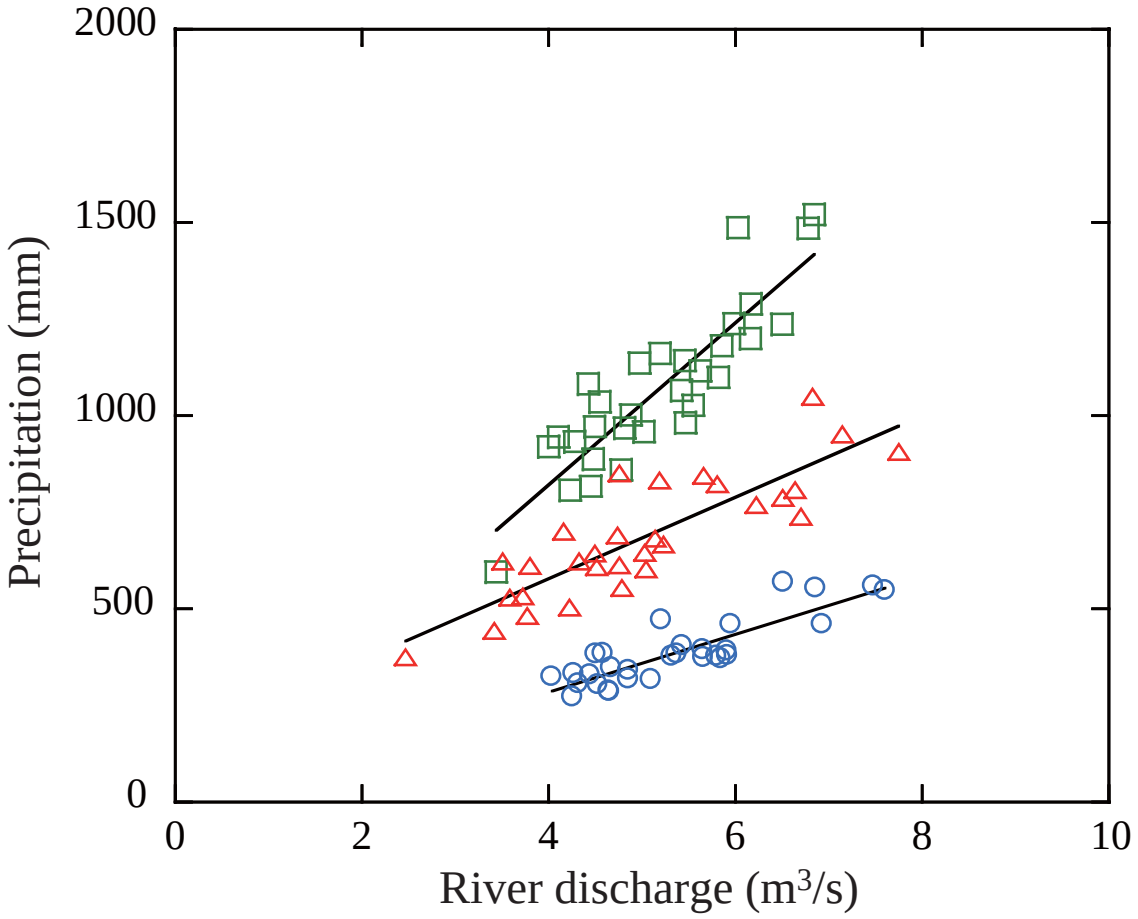

Fig. 3.7. Relationship between seasonal precipitation in Mori and river discharge in Lake Onuma during 1981-2010.
Annual precipitation and average river discharge (green, square), seasonal precipitation and average river discharge in summer period (June to November, red, triangle) and that in winter period (December to May, blue, circle).
Regression curves are expressed as follows;
(*Y*: precipitation, *X*: river discharge and R: correlation coefficient)
$Y = -16.0 + 209X$, R = 0.88 for annual,
$Y = 156 + 105X$, R = 0.85 for summer period,
and $Y = -15.1 + 74.8X$, R = 0.86 for winter period.

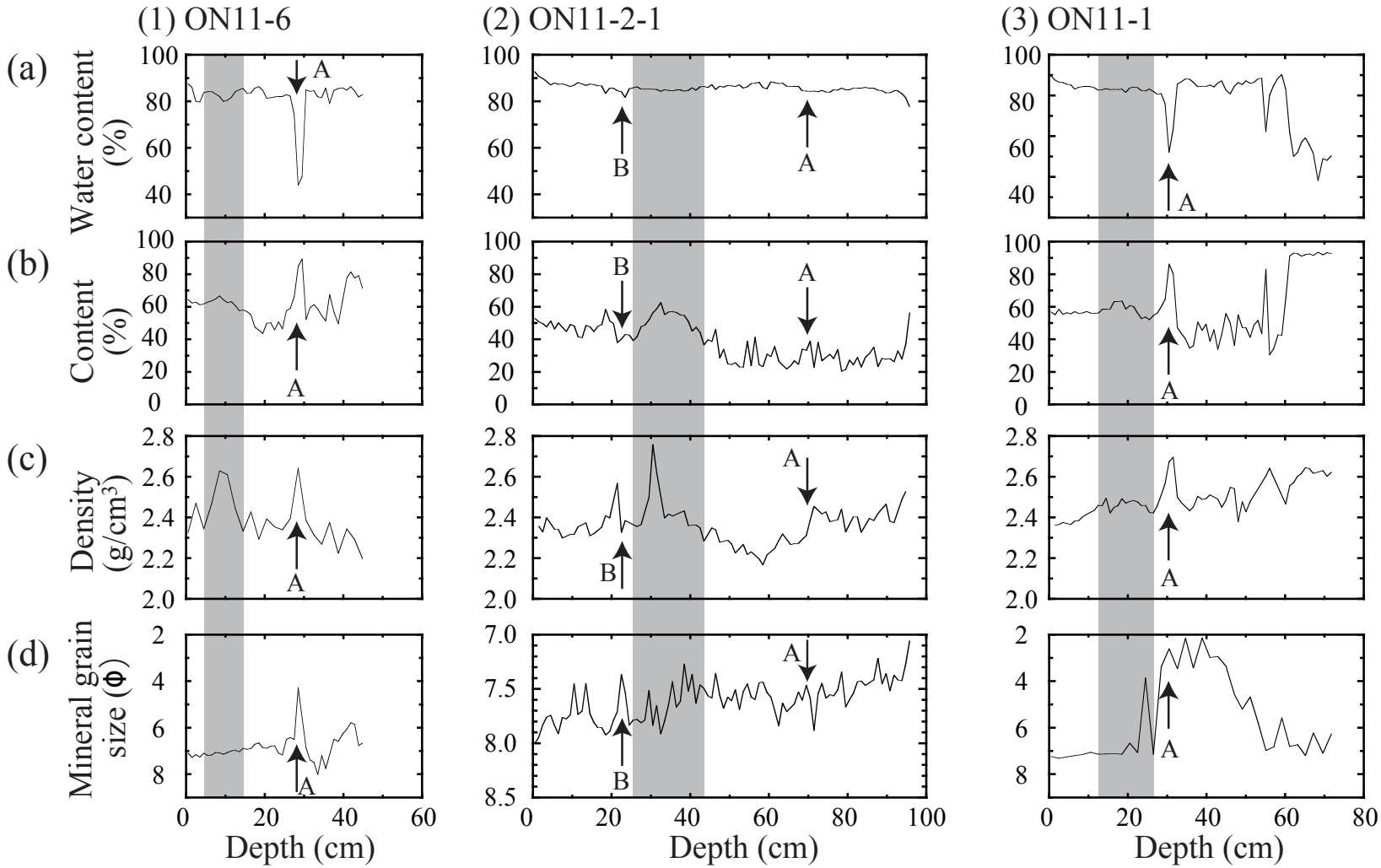

Fig. 3.8. Physical properties of short core sediments from Lake Onuma.
(1) ON11-6, (2) ON11-2-1 and (3) ON11-1.
(a) water content (%), (b) mineral content (%), (c) density (g/cm^3) and (d) mineral grain size (Φ).
Arrow-A shows estimated AD1929 eruption.
Arrow-B shows estimated typhoon in AD1975.
Shaded region shows the depth of peak in mineral content and density.

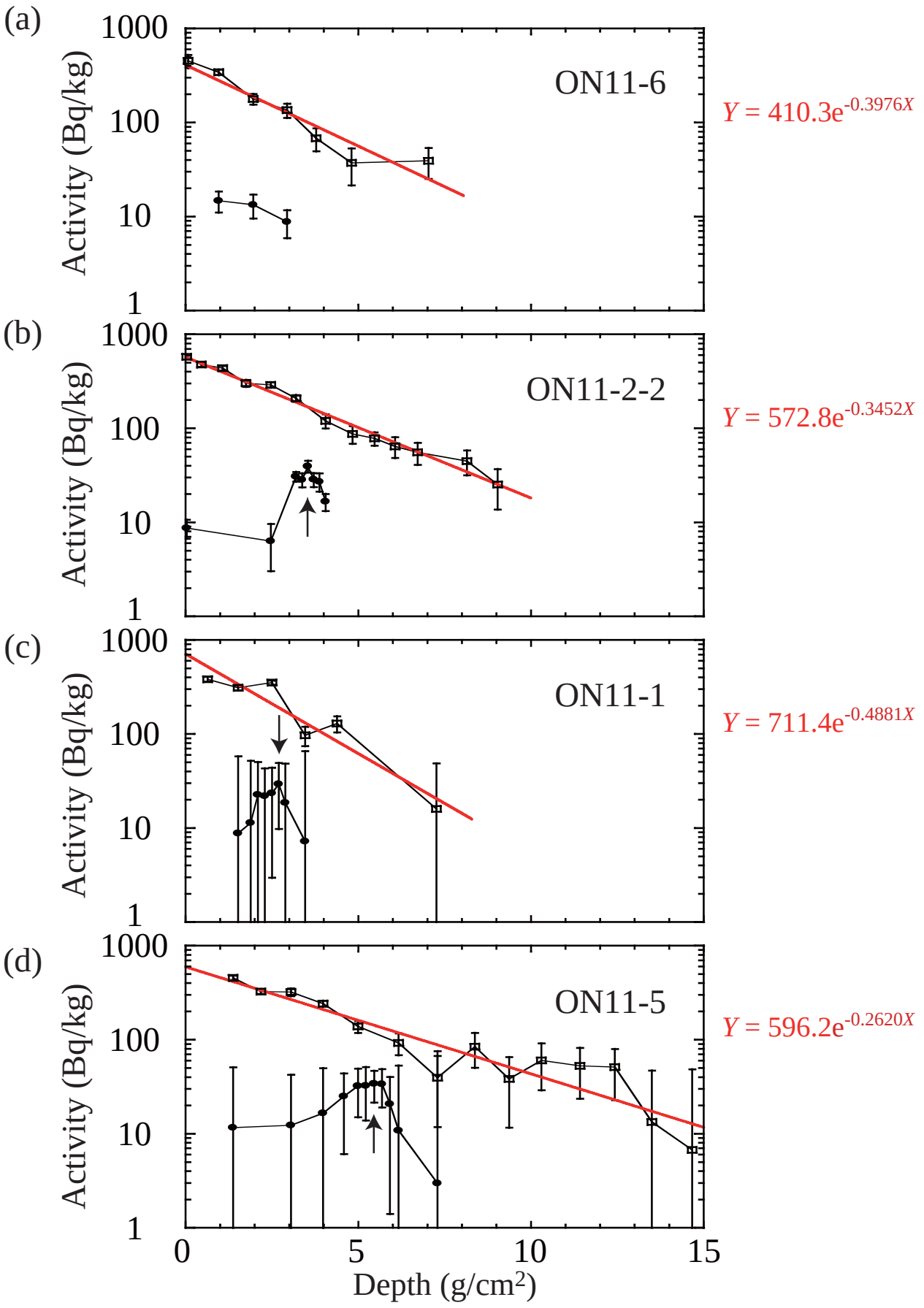

Fig. 3.9. Changes in excess Pb-210 concentration (square) and Cs-137 concentration (circle). The largest value in Cs-137 concentration (arrow) indicates the layer deposited around AD 1963. (a) ON11-6, (b) ON11-2-2, (c) ON11-1 and (d) ON11-5. Concentration of ON11-2-2 and ON11-6 are analyzed by Ochiai (personal com.).

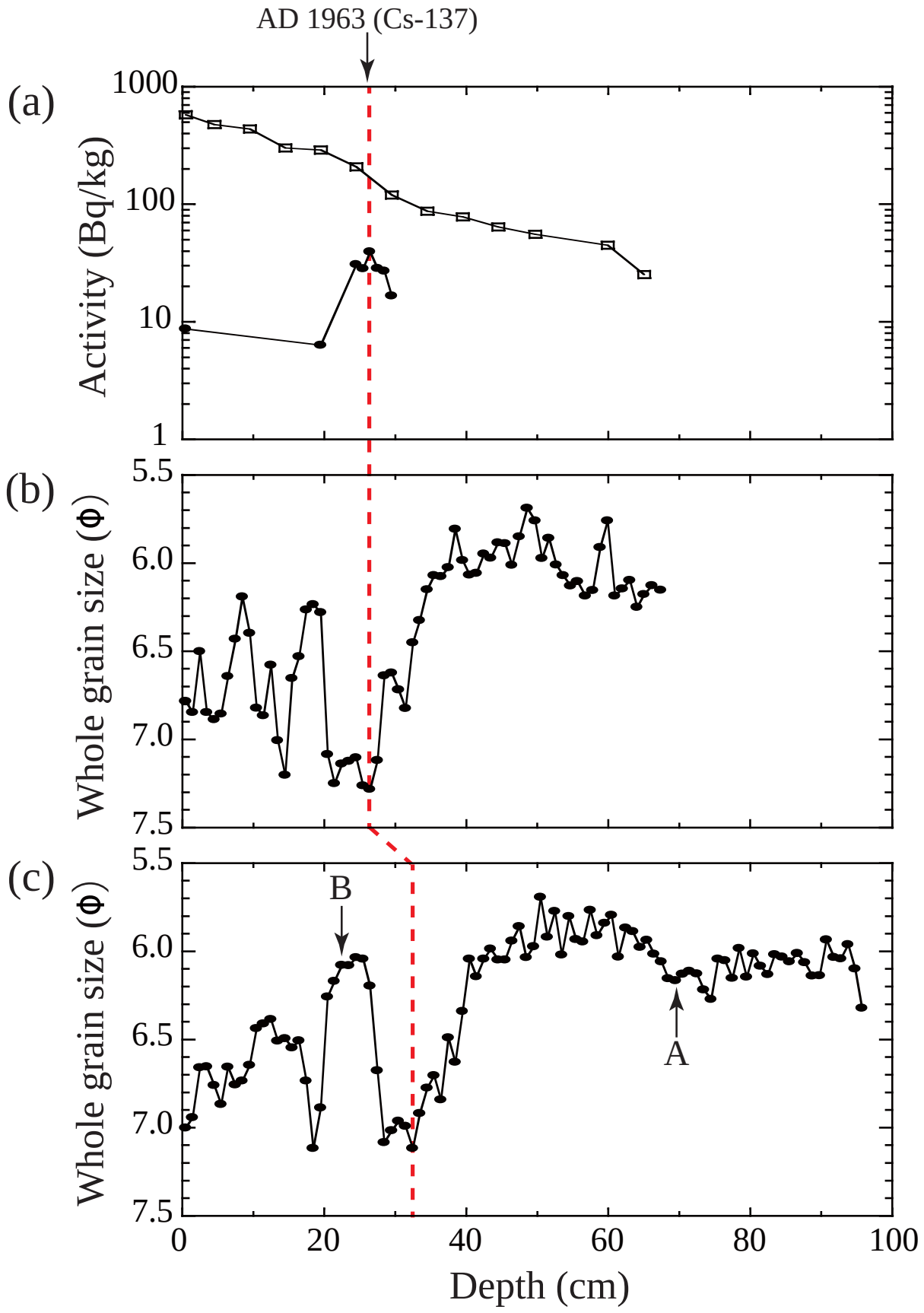

Fig. 3.10. Estimation of Cs-137 for ON11-2-1.
(a) Changes in excess Pb-210 (square) and Cs-137 (circle) concentration of ON11-2-2, (b) whole grain size of ON11-2-2 and (c) whole grain size of ON11-2-1.
Arrow-A shows estimated 1929 eruption.
Arrow-B shows estimated typhoon in 1975.

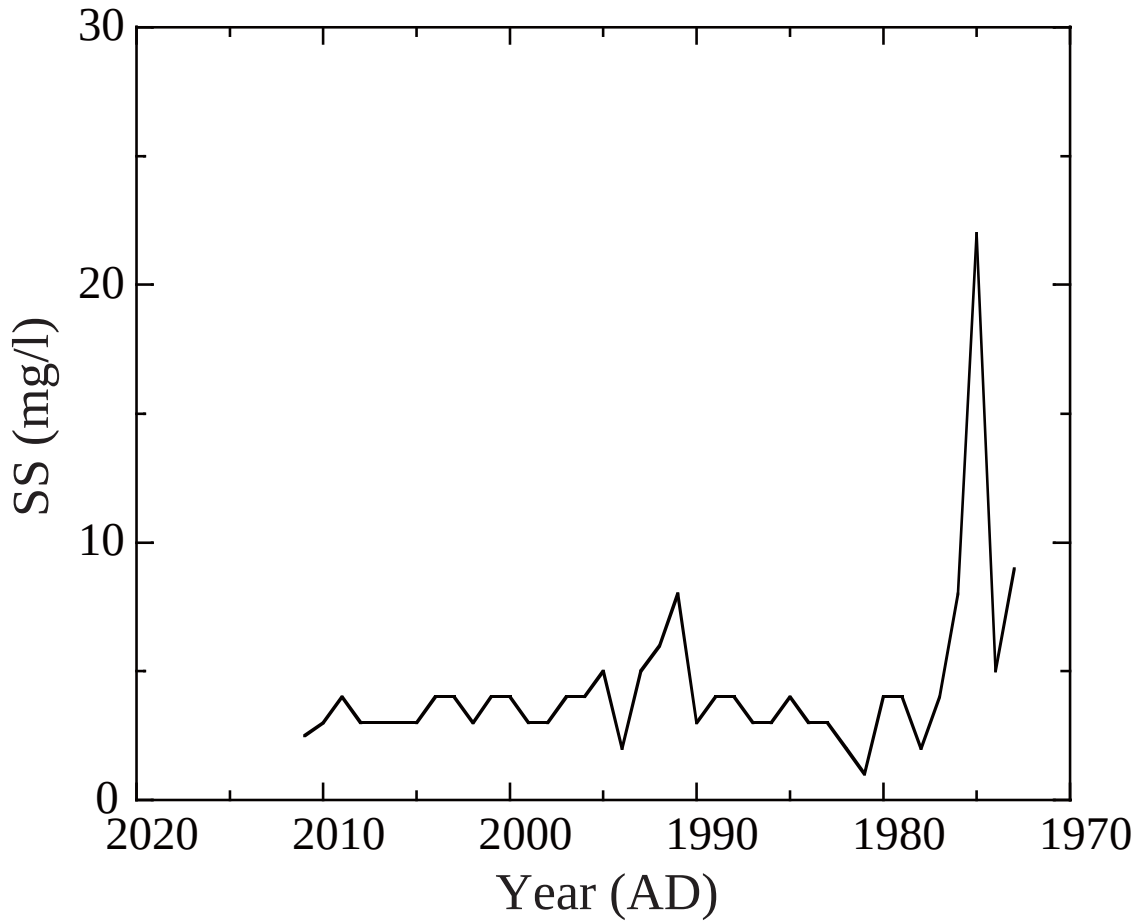

Fig. 3.11. Fluctuation in suspended sediment, in Lake Onuma (Hokkaido Government, 2012).

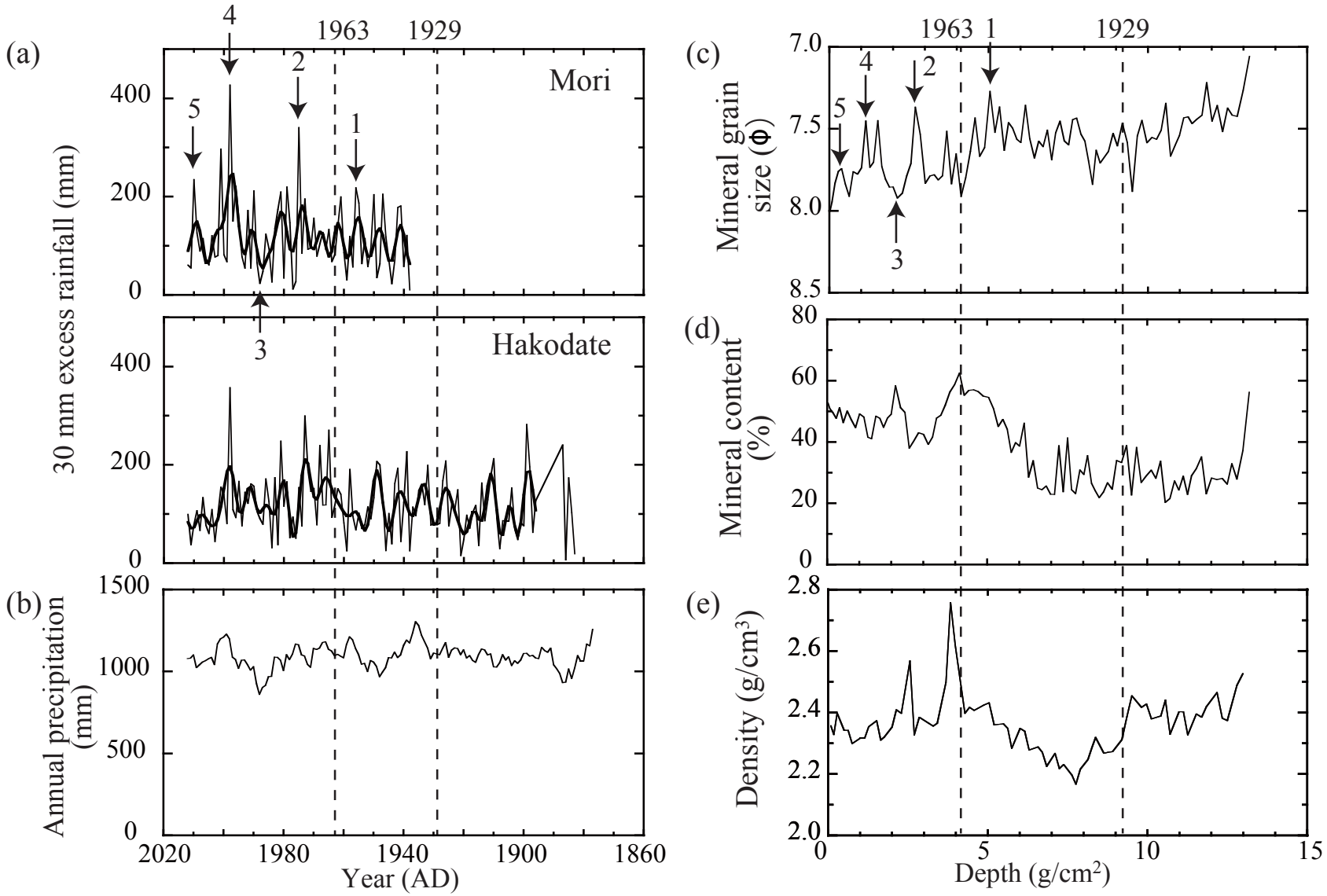

Fig. 3.12. Comparison observational climatic data with physical properties of sediment.
(a) 30 mm excess rainfall in Mori and Hakodate, (b) 5-year running average of annual precipitation in Mori, (c) mineral grain size (Φ), (d) mineral content (%) and (e) density (g/cm^3) of ON11-2-1.
Arrows show the corresponding peaks; 1 (1956), 2 (1975), 3(1988), 4 (1998) and 5 (2010).

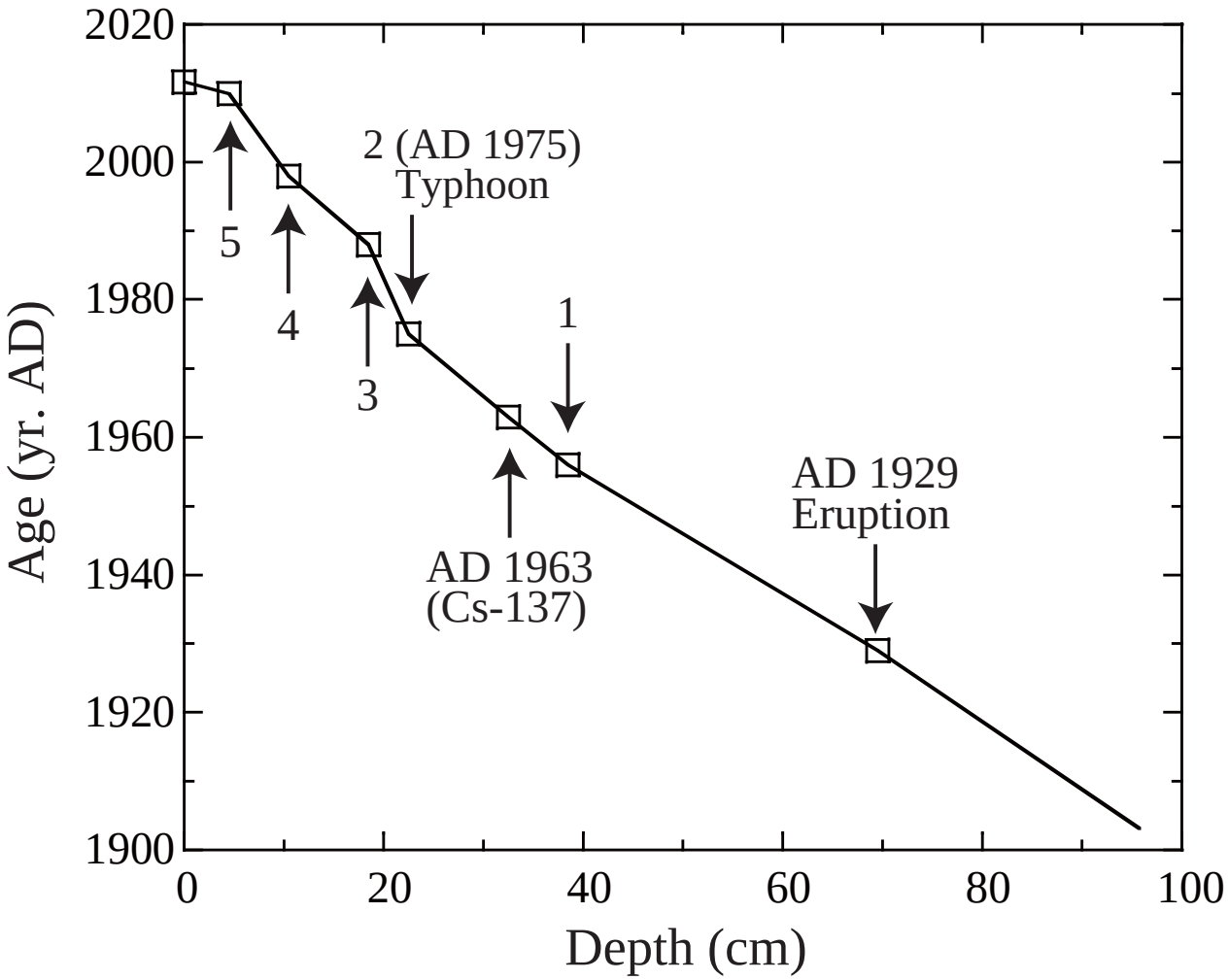

Fig. 3.13. Age model for ON11-2-1 core.
Squares are corresponded to the arrows in Fig. 3.12a, c.

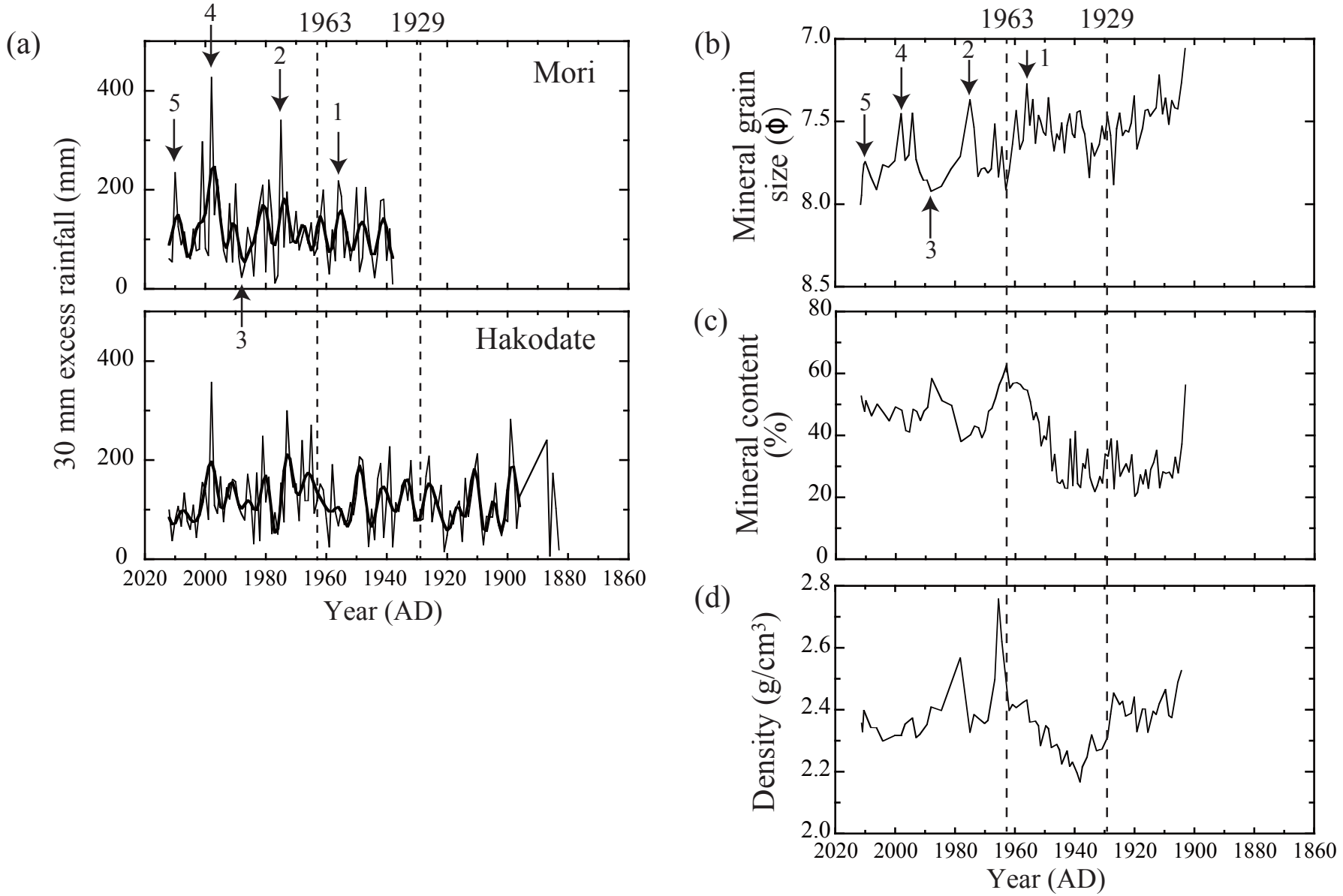

Fig. 3.14. Comparison excess rainfall with physical properties of sediment.
(a) 30 mm excess rainfall in Mori and Hakodate, (b) mineral grain size (Φ), (c) mineral content (%) and (d) density (g/cm^3) of ON11-2-1.
Arrows show the corresponding peaks; 1 (1956), 2 (1975), 3(1988), 4 (1998) and 5 (2010).

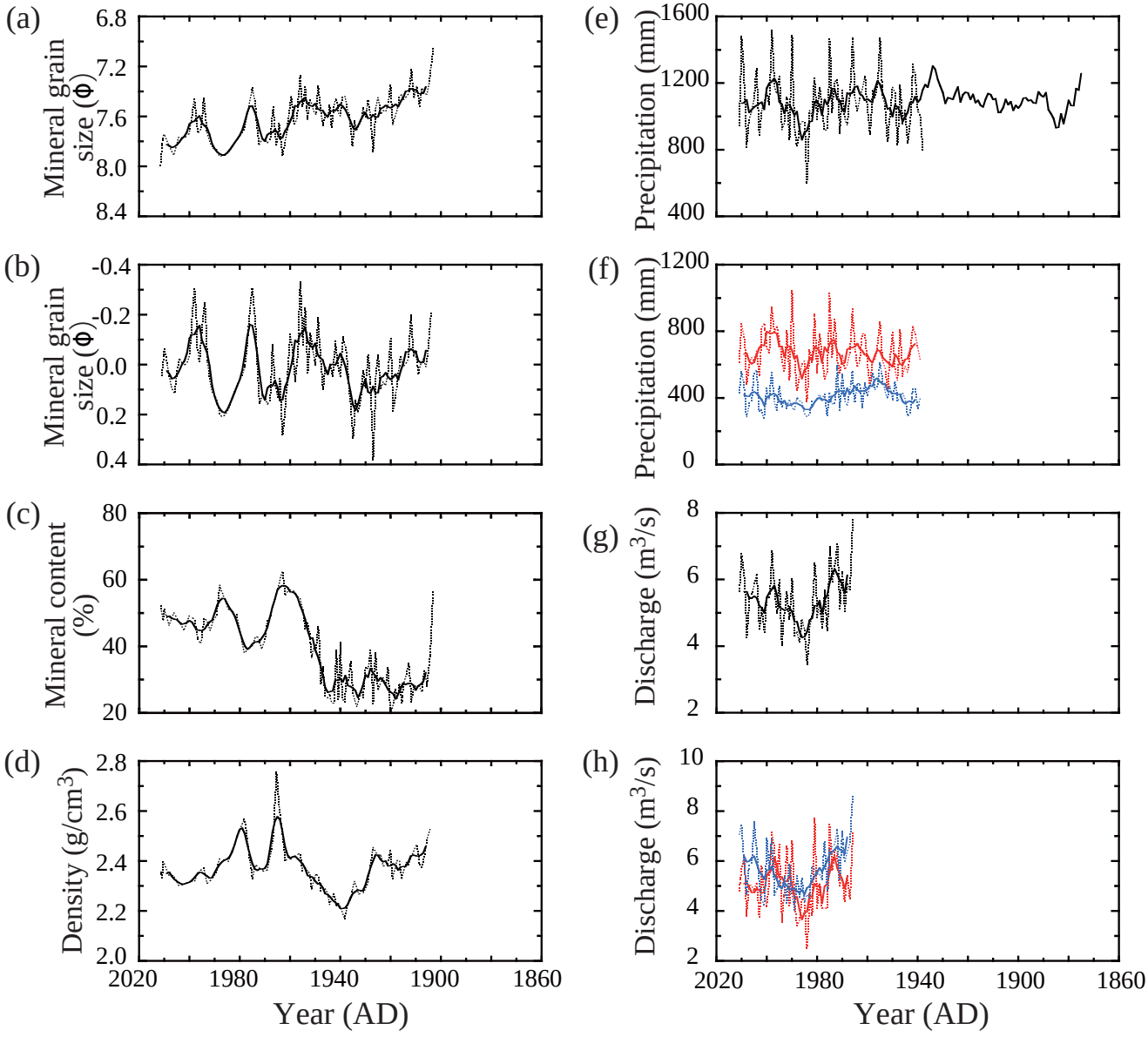

Fig. 3.15. Comparison physical properties of sediment with seasonal hydrological data. Row data (dashed line) and 5-year running average (thick solid line) ;
(a) mineral grain size (Φ), (b) detrended mineral grain size (Φ), (c) mineral content (%) and (d) density (g/cm^3) of ON11-2-1. Observed data (dashed line), 5-year running average (solid line), annual (black), summer period (red) and winter period (blue); (e) estimated annual precipitation in Mori, (f) seasonal precipitation in Mori, (g) annual river discharge and (h) seasonal river discharge in Lake Onuma.

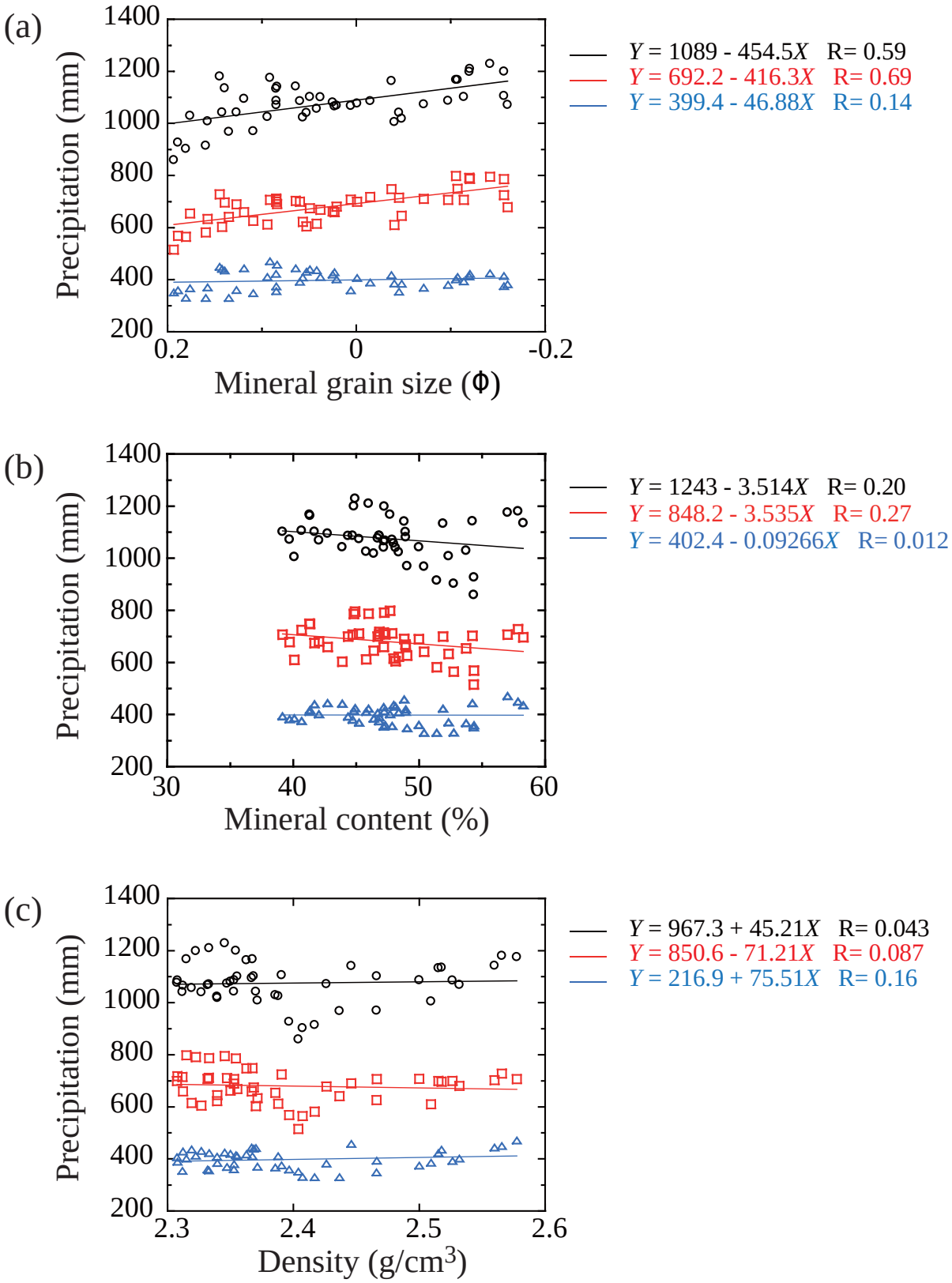

Fig. 3.16. Relationship between 5-year running average of precipitation in Mori and physical properties of ON11-2-1 during 1963-2009; (a) dertrended mineral grain size, (b) mineral content and (c) density of ON11-2-1. Annual precipitation (black, circle), seasonal precipitation; summer period (red, square) and winter period (blue, triangle).

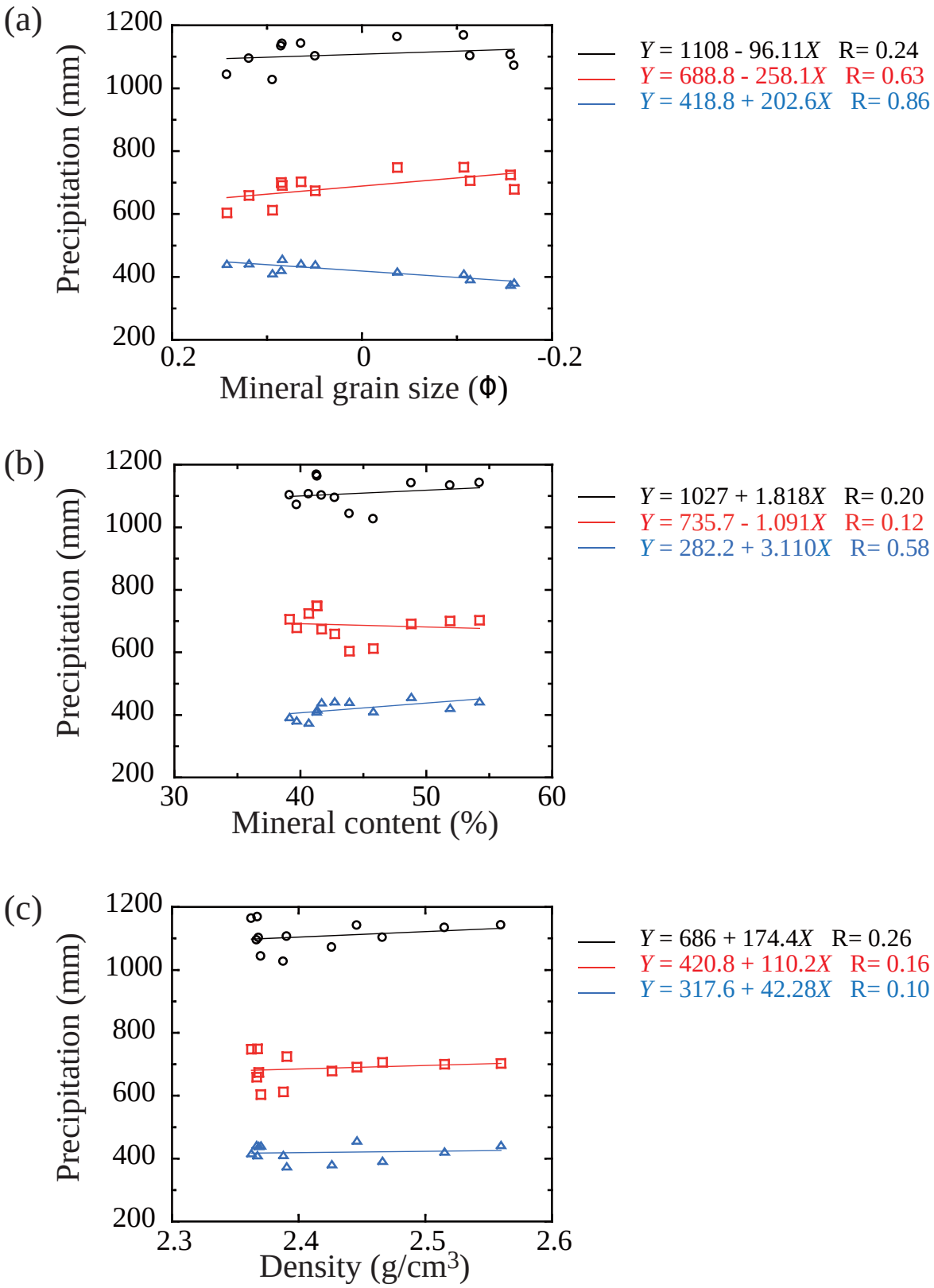

Fig. 3.17. Relationship between 5-year running average of precipitation in Mori and physical properties of ON11-2-1 during 1966-1977; (a) dertrended mineral grain size, (b) mineral content and (c) density of ON11-2-1. Annual precipitation (black, circle), seasonal precipitation; summer period (red, square) and winter period (blue, triangle).

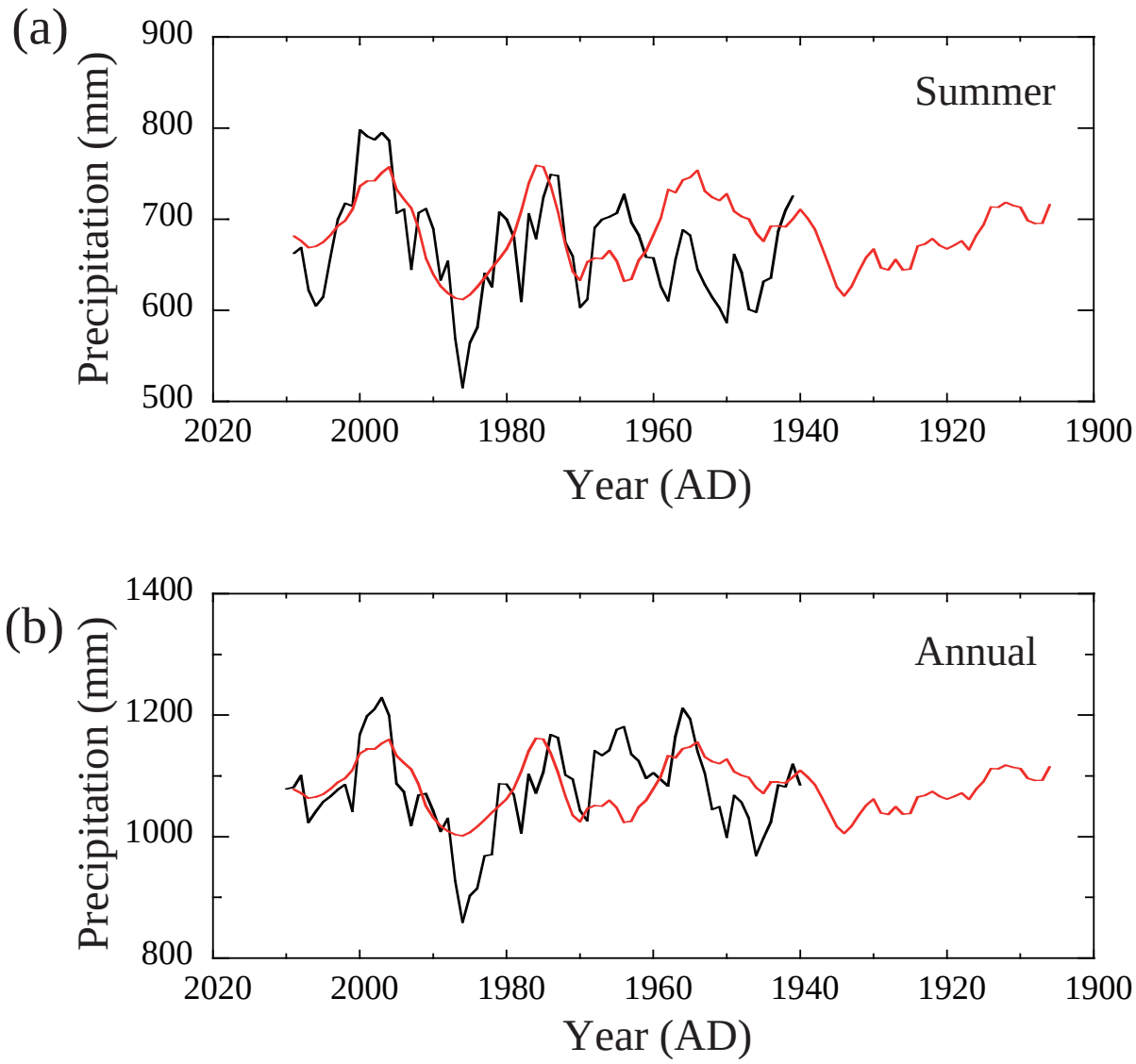

Fig. 3.18. Estimated 5-year running average of precipitation in Mori. Precipitation in (a) summer period and (b) annual. Observational precipitation in Mori (black) and estimated precipitation using regression curve in mineral grain size (red).

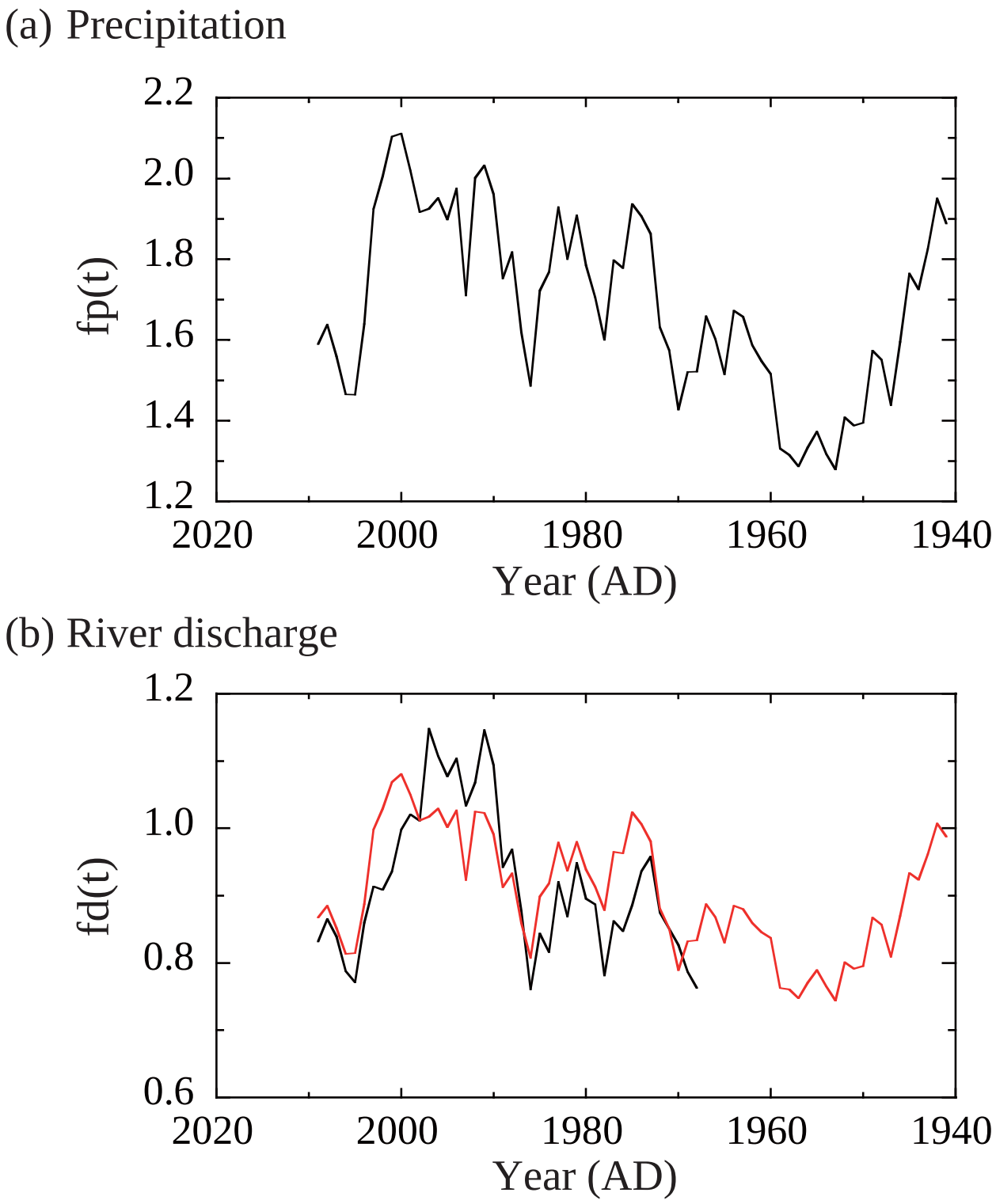

Fig. 3.19. The seasonal contribution of precipitation and river discharge in summer period to winter period (5-year running average). (a) fp(t); ratio of summer precipitation to winter precipitation and (b) fd(t); ratio of summer river discharge to winter river discharge. Observational data (black) and estimated data (red); based on estimated precipitation (mineral grain size).

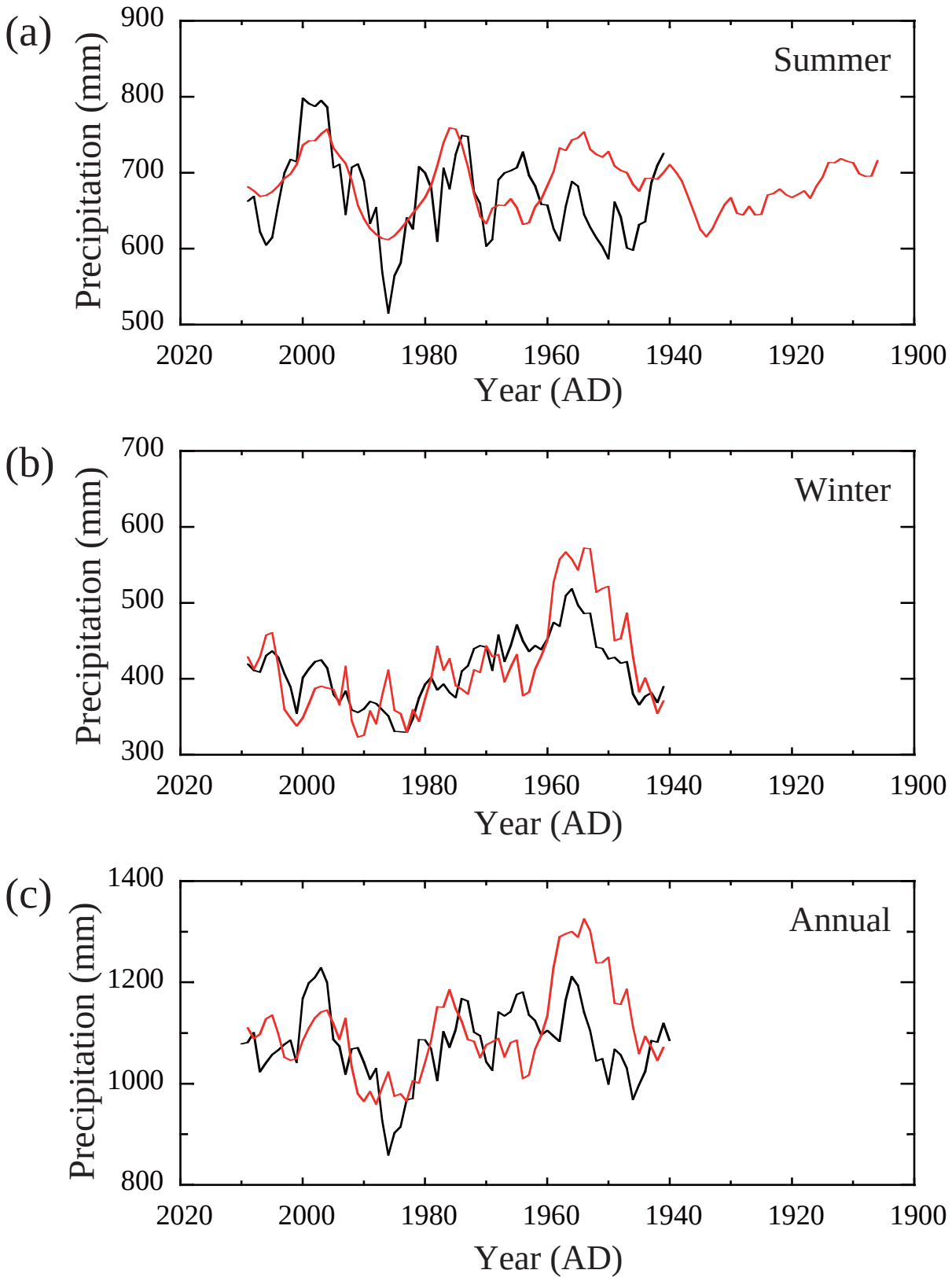

Fig. 3.20. Estimated 5-year running average of precipitation in Mori. Precipitation in (a) summer period, (b) winter period and (b) annual. Observational precipitation in Mori (black) and estimated precipitation by mineral grain size and observational precipitation; seasonal precipitation and ratio of summer precipitation to winter precipitation (red).

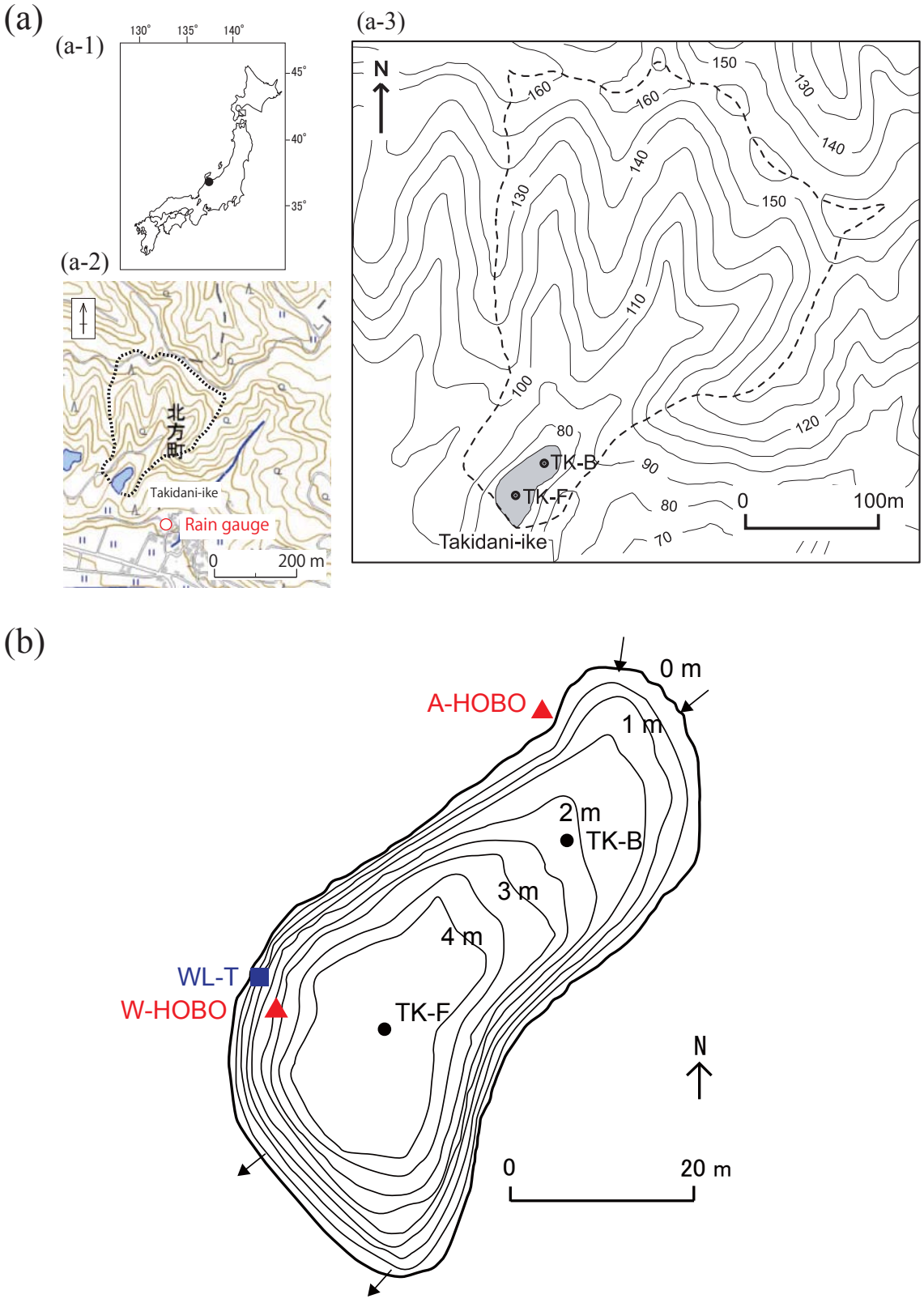

Fig. 4.1. Index map of Takidani-ike.
(a) Catchment and surrounding area of Takidani-ike (modified after GSI Maps, Geospatial Information Authority of Japan (a-2), and after Ochiai et al., 2013 (a-3)) and (b) contour map of water depth in Takidani-ike (modified after Fujie, 2005). Sediment trap; TK-B and TK-F, black circle, water level gauge; Trutrack (WL-T, blue square) and absolute pressure loggers (triangle) in the lake bottom (W-HOBO) and on shore (A-HOBO).

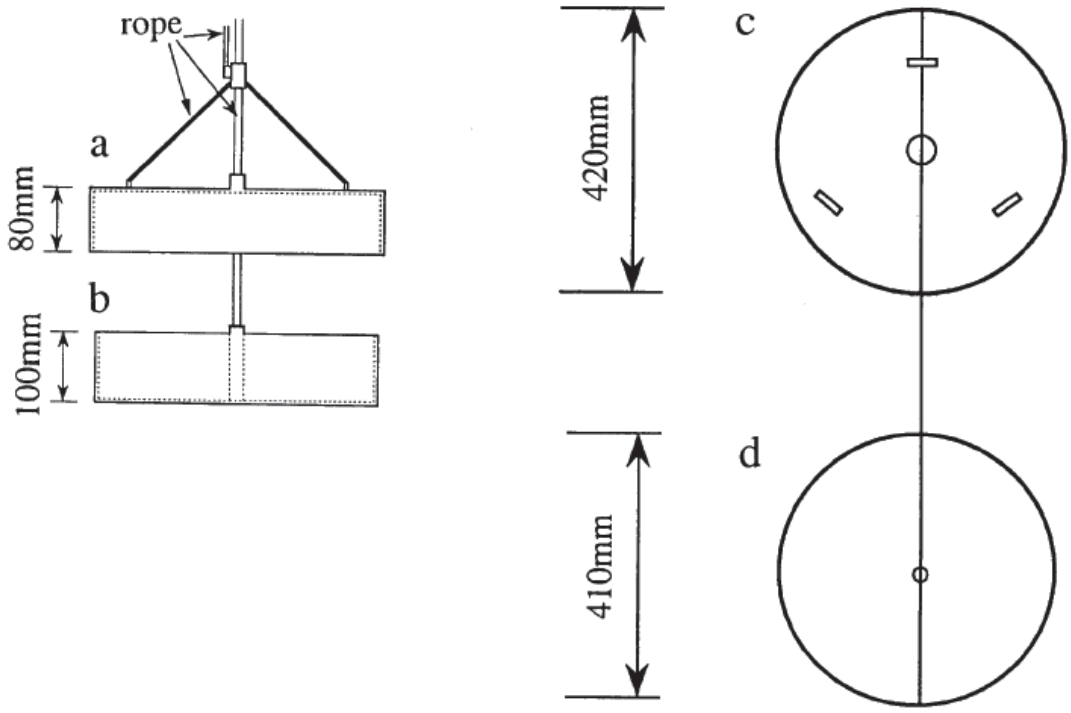

Fig. 4.2. Plan figures of sediment trap.
(a) sectional plan of cover, (b) sectional plan to trap, (c) plan figure of the cover and (d) plan figure of the trap (after Kashiwaya et al., 1995).

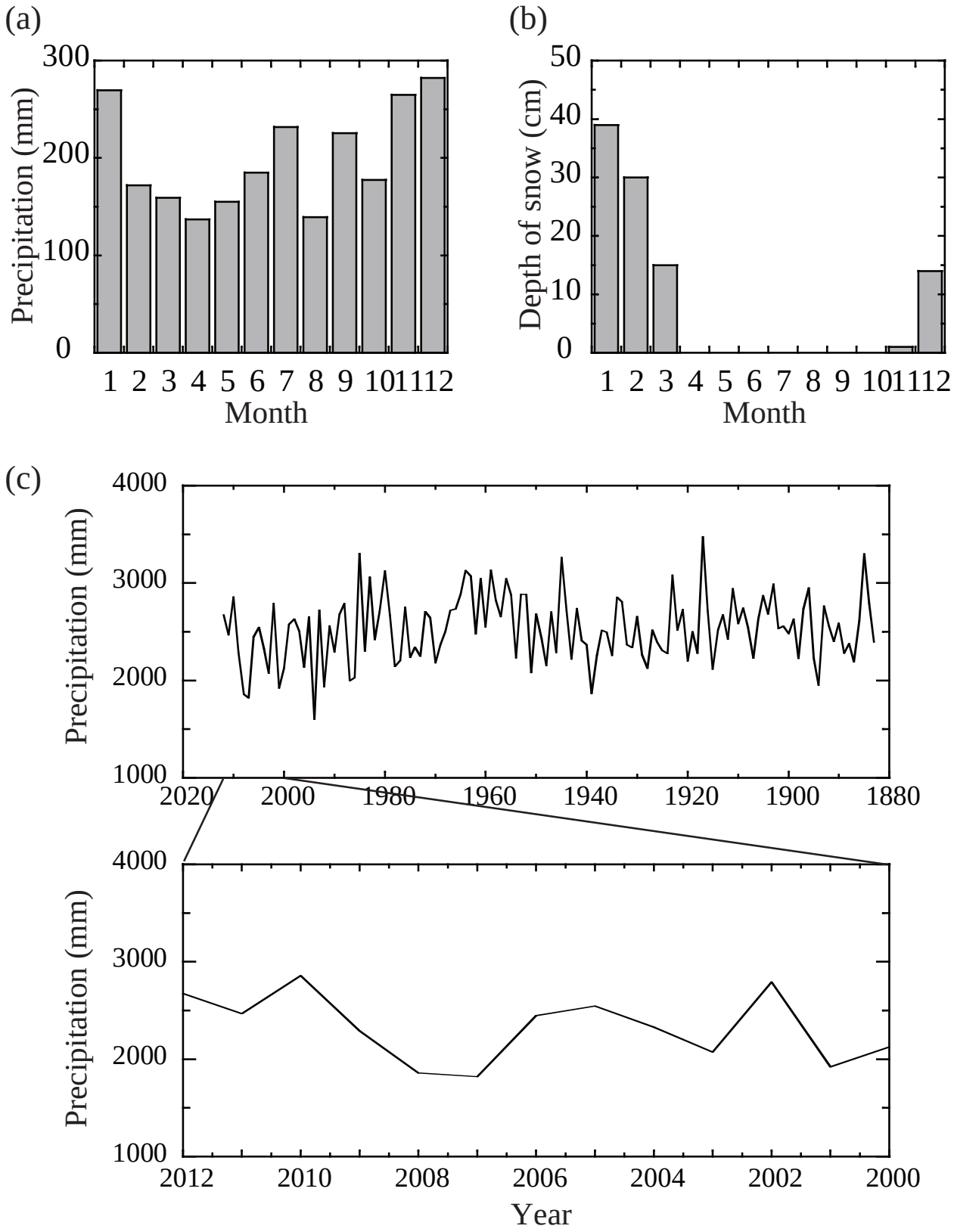

Fig. 4.3. Meteorological data observed in Kanazawa.
(a) Average monthly precipitation during 1981-2010, (b) average monthly changes on the maximum depth of snow during 1981-2010 and (c) annual precipitation.

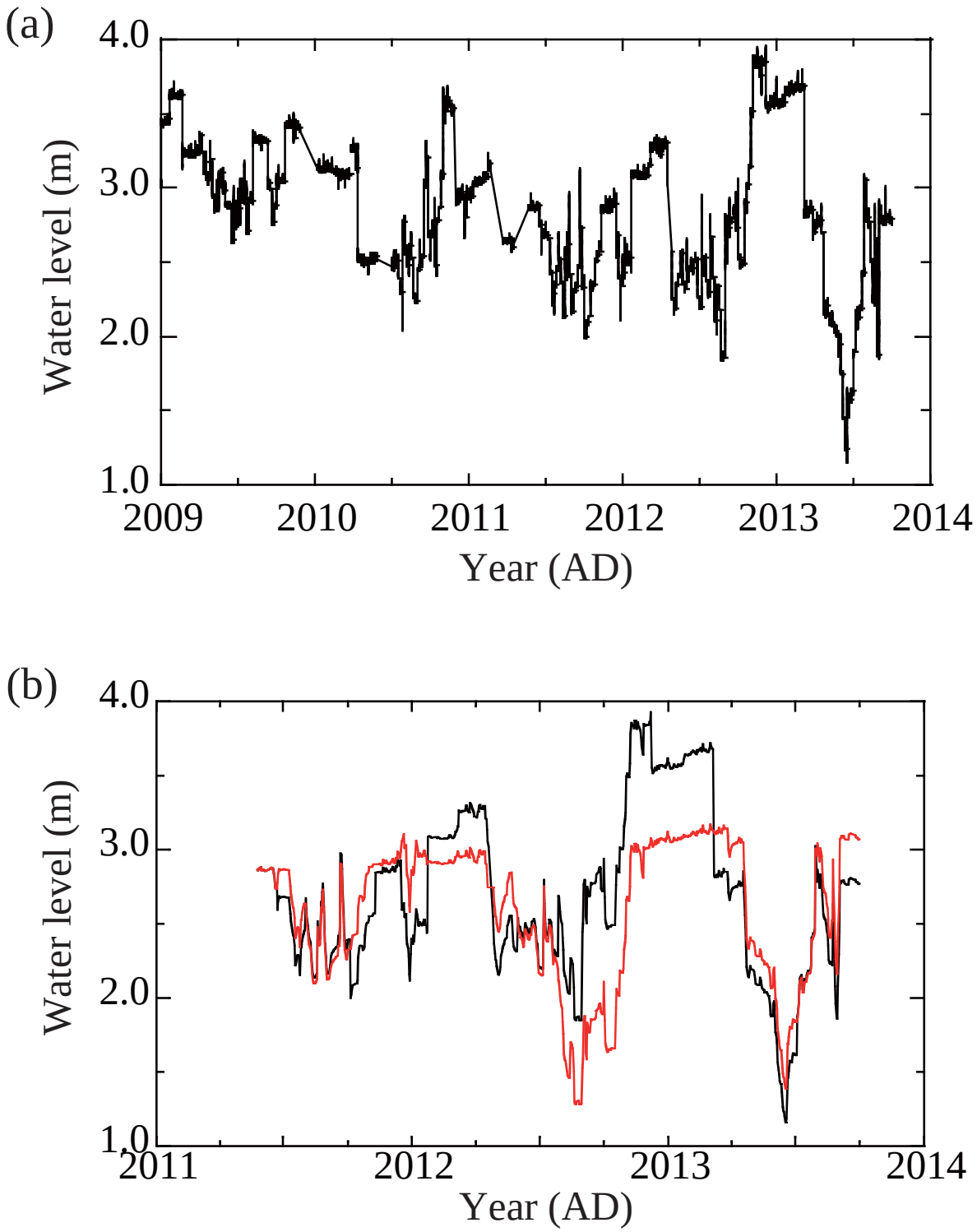

Fig. 4.4. Water level observed with absolute pressure logger (HOBO). (a) Water level and (b) daily minimum water level; row data (black) and calibrated level ($WL_C(t)$, red).

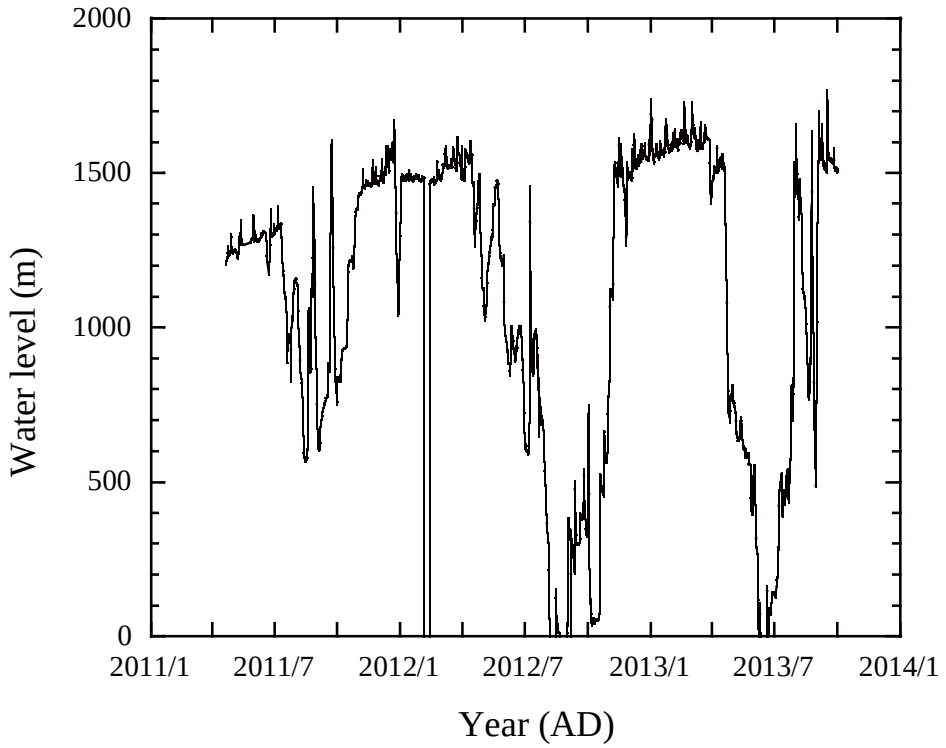

Fig. 4.5. Water level observed with a capacitance water level logger (Trutrack).

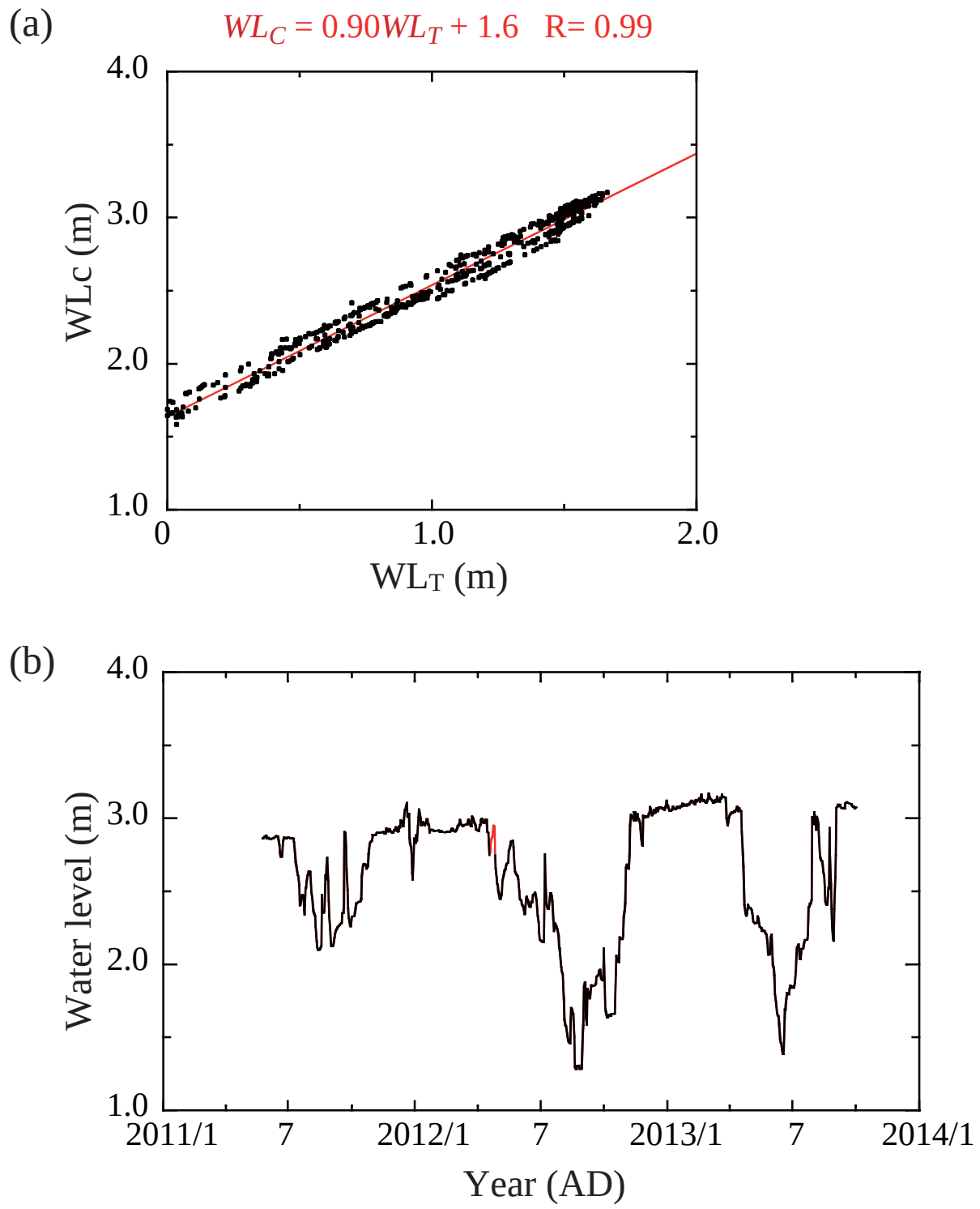

Fig. 4.6. Water level of Takidani-ike observed with HOBO, calibrated with data of Trutrack. (a) The relationship between water level observed with HOBO (WL_C) and one with Trutrack (WL_T) in the interval of May, 25, 2011 to October, 2, 2013 and (b) water level observed with HOBO; calibrated water level (WL_C, black) and interpolated water level in the missing interval using data observed with Trutrack (red).

(a) TK-F

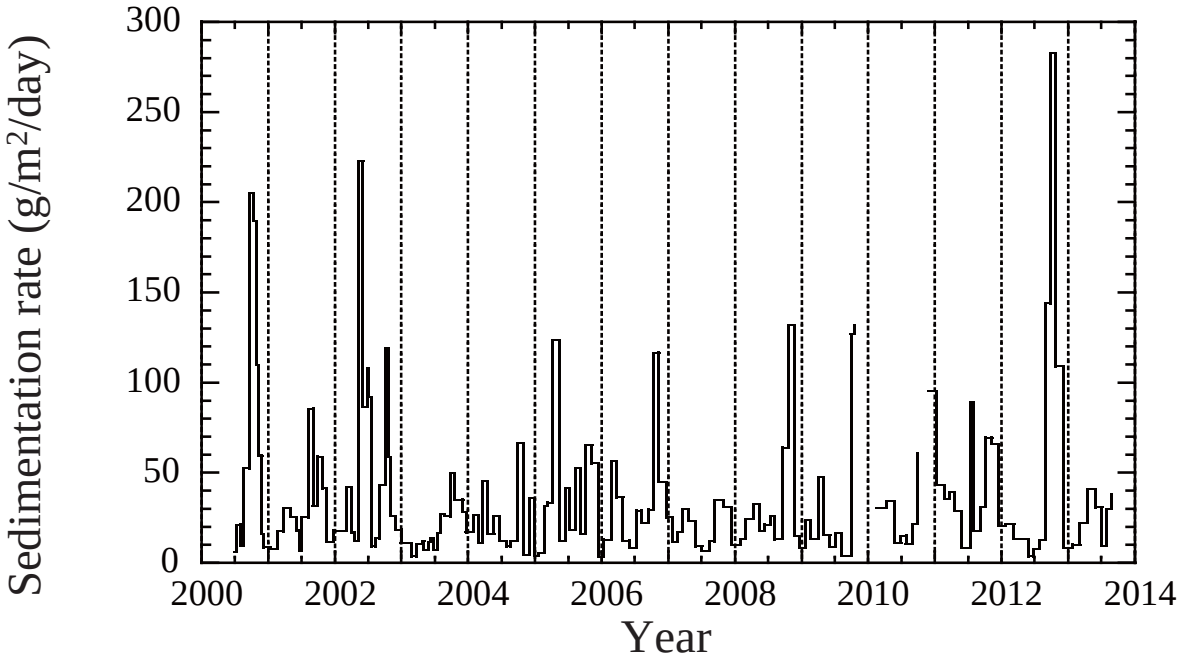

(b) TK-B

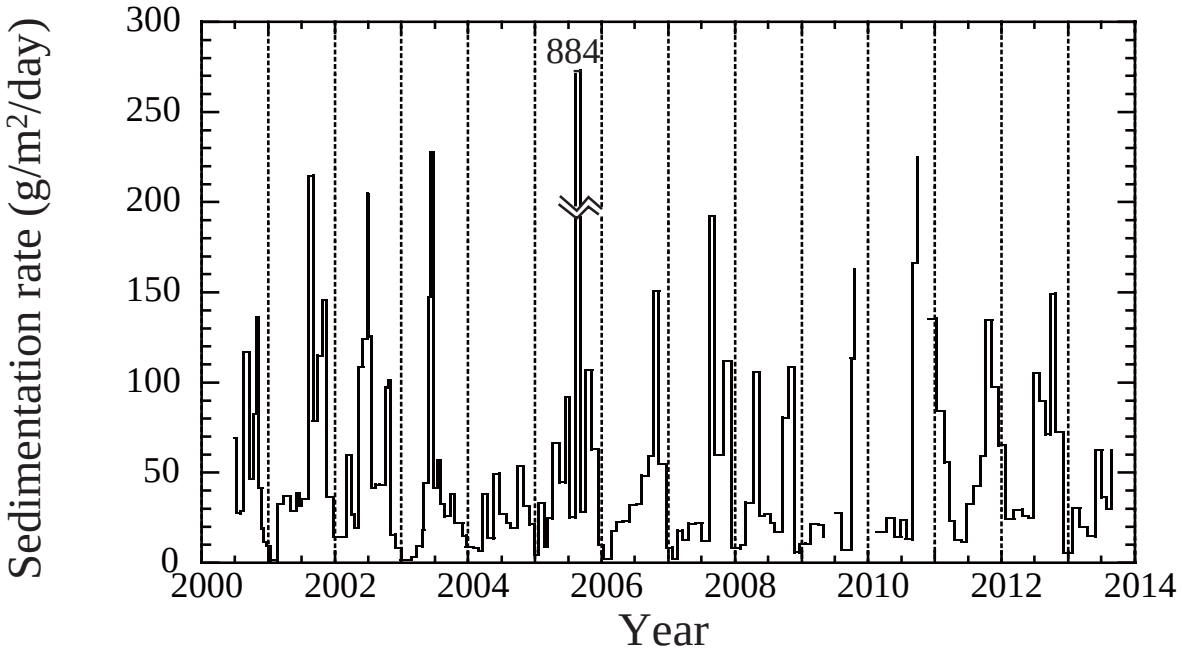

Fig. 4.7. Sedimentation rate in Takidani-ike;
(a) sediment trap TK-F and (b) sediment trap TK-B.

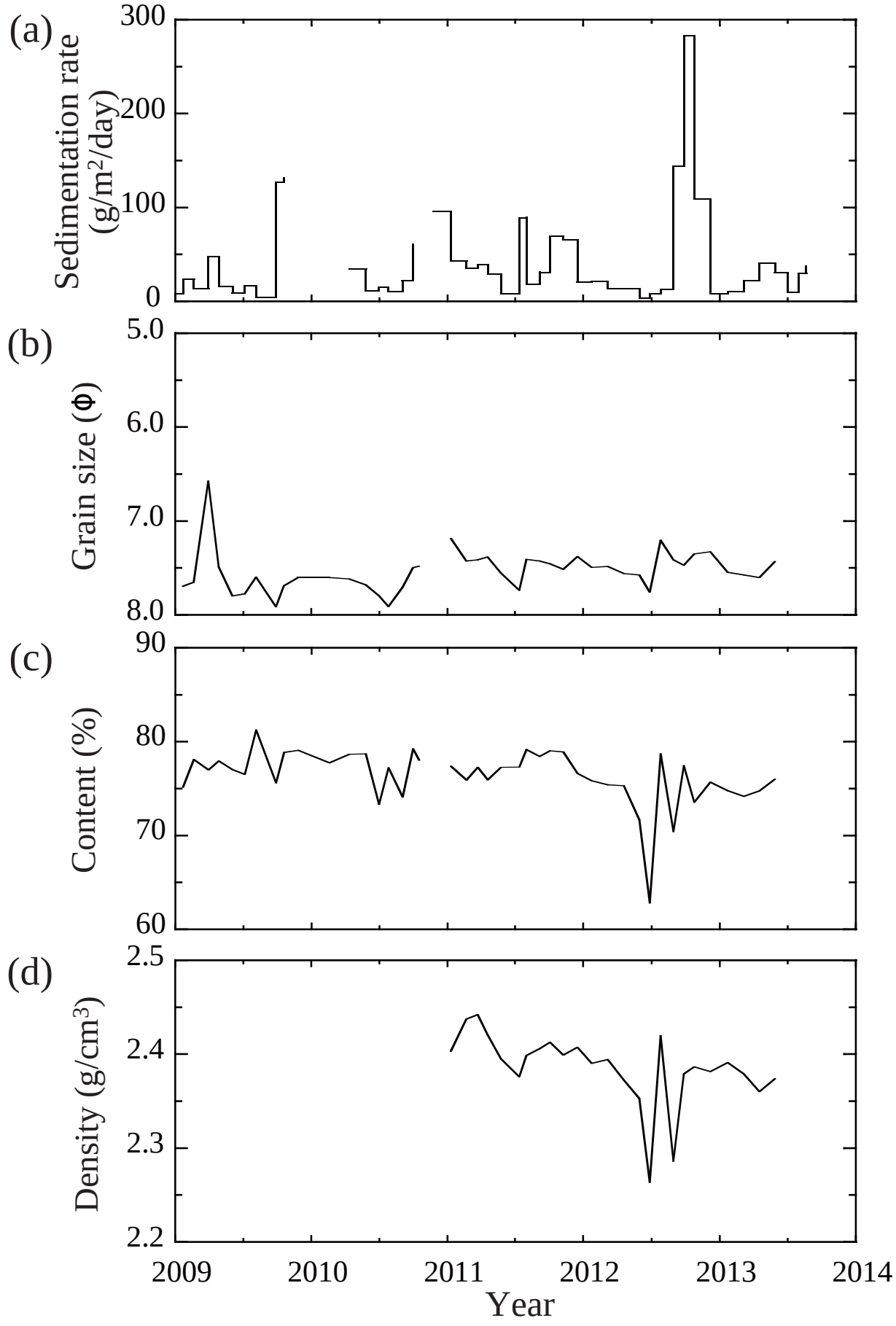

Fig. 4.8. Sedimentation rate and physical properties for sediment trap TK-F since 2009. (a) sedimentation rate, (b) mineral grain size, (c) mineral content and (d) density.

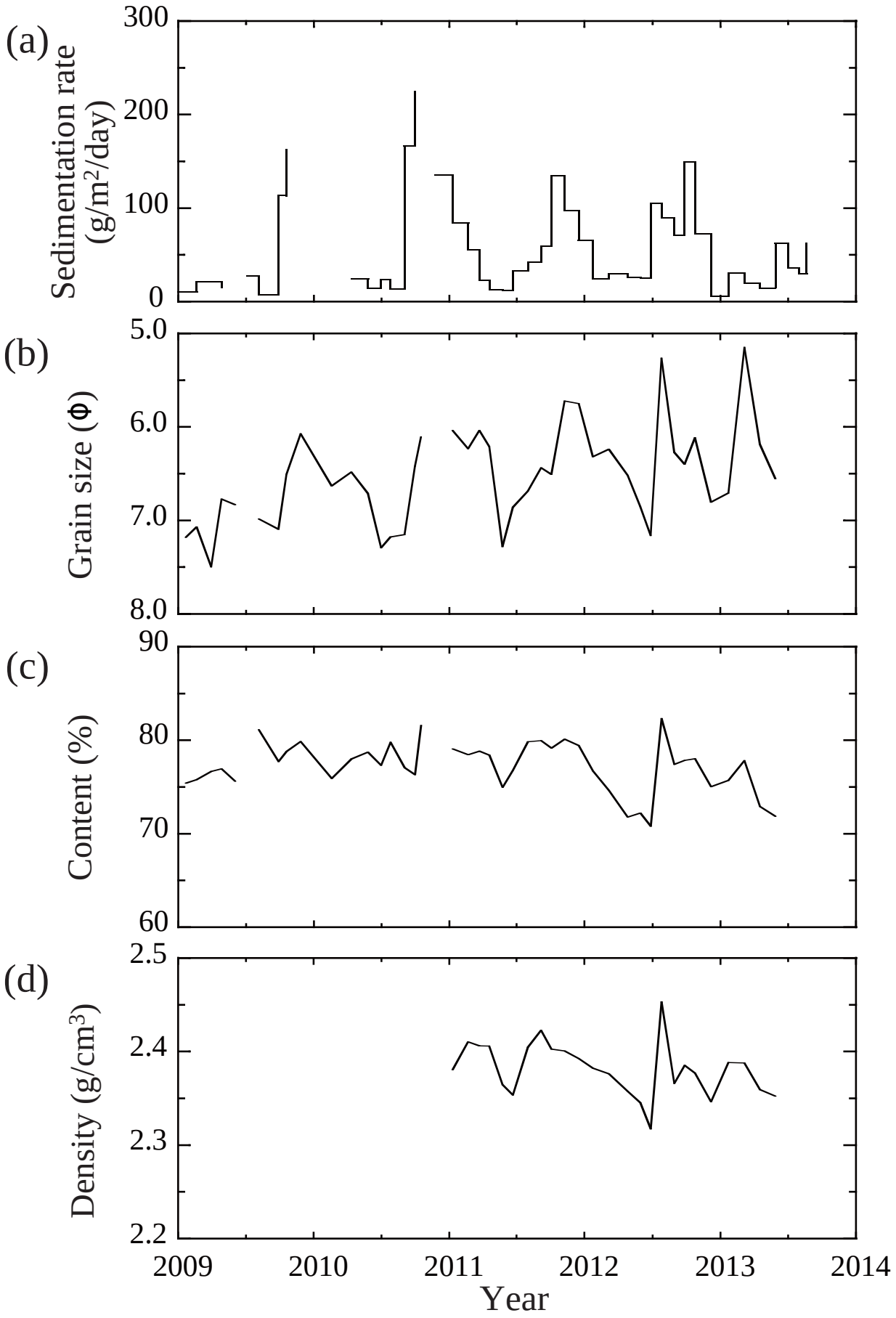

Fig. 4.9. Sedimentation rate and physical properties for sediment trap TK-B since 2009. (a) sedimentation rate, (b) mineral grain size, (c) mineral content and (d) density.

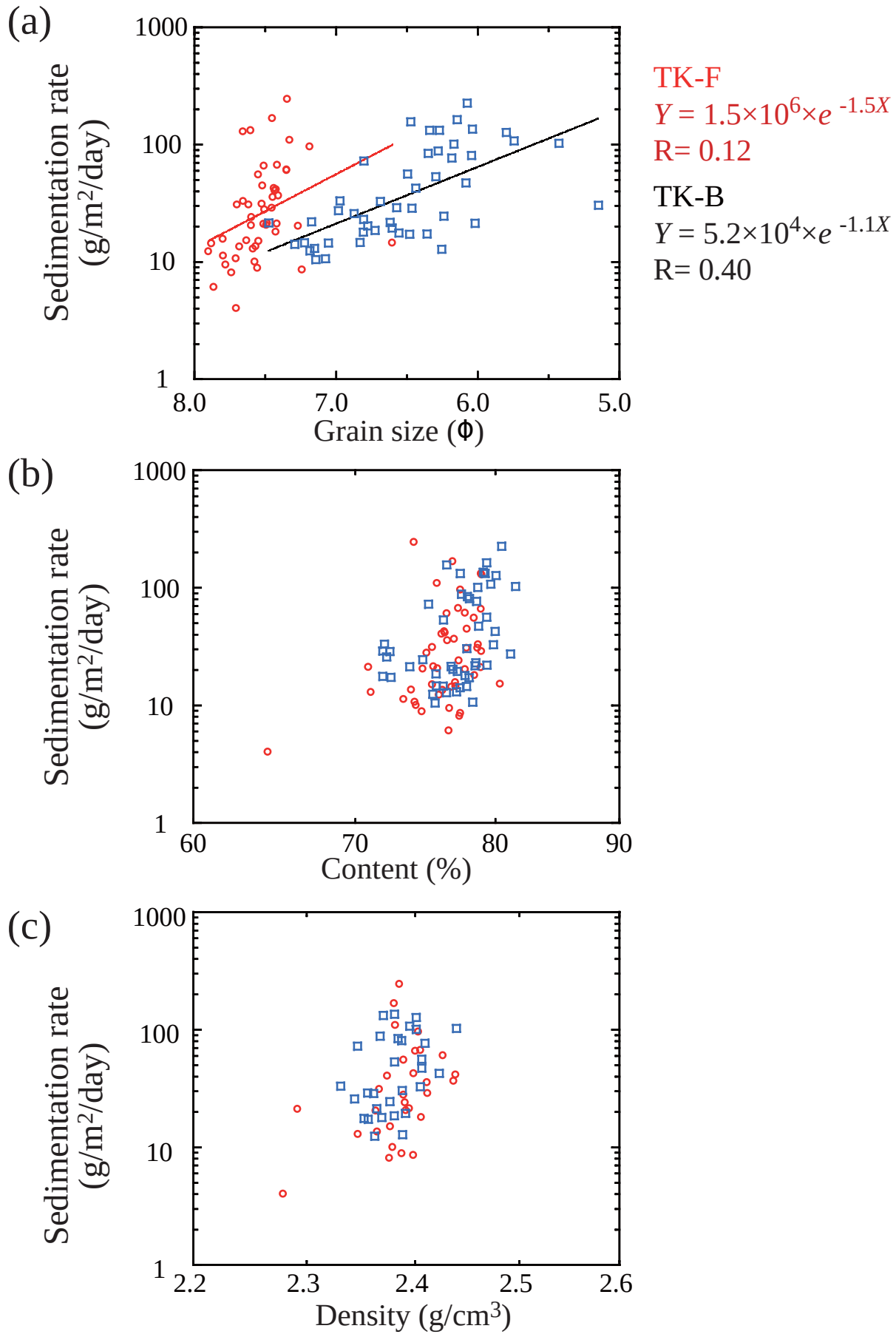

Fig. 4.10. The relationship between monthly sedimentation rate and physical properties of sediments with the traps during Jan., 2009-May, 2013; TK-F (red, circle) and TK-B (blue, square). Physical properties; (a) mineral grain size, (b) mineral content and (c) density.

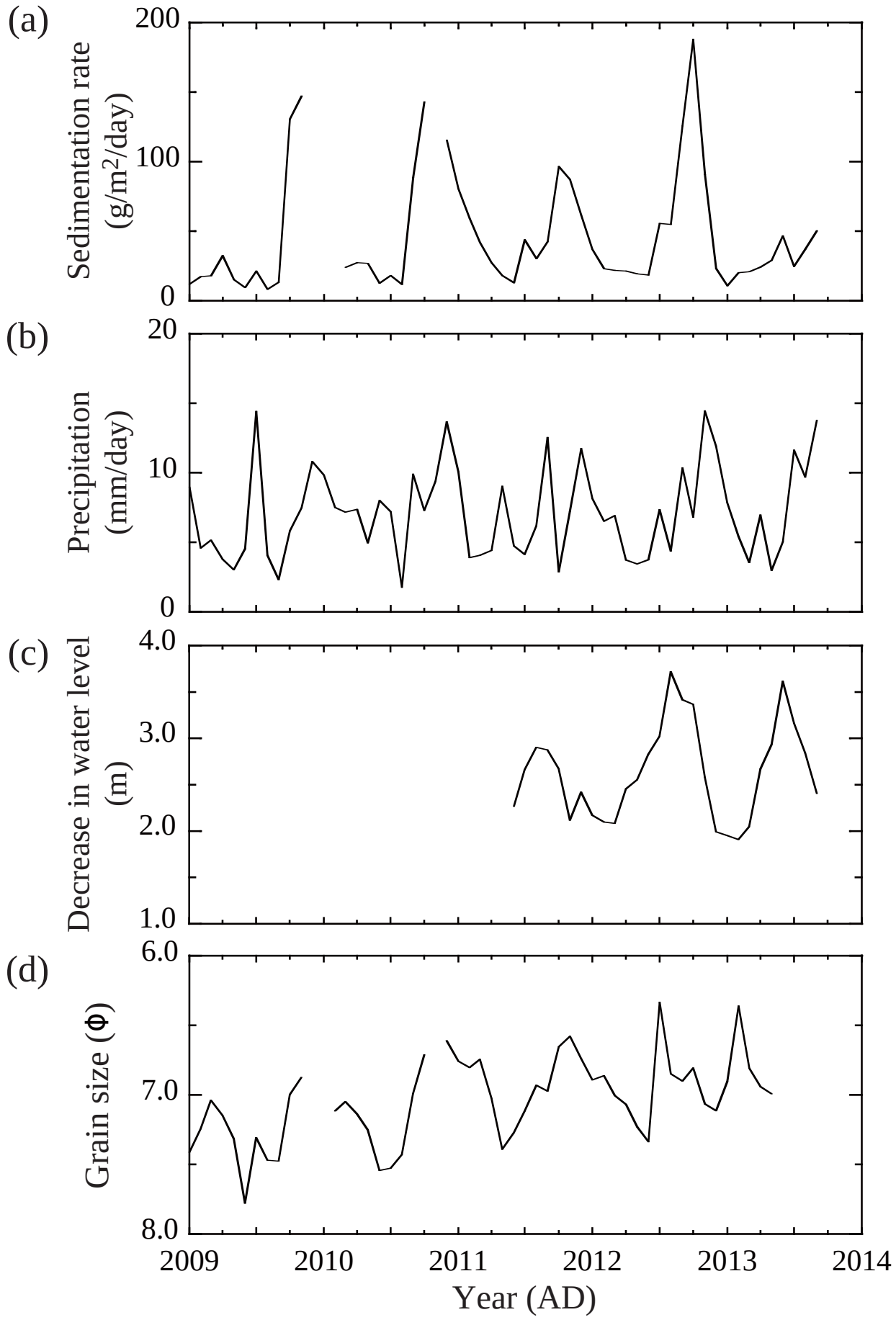

Fig. 4.11. Monthly changes in average sedimentation rate, hydrological data (precipitation and water level) and grain size. (a) sedimentation rate, (b) precipitation intensity and (c) WL_D; decrease in water level and (d) mineral grain size.

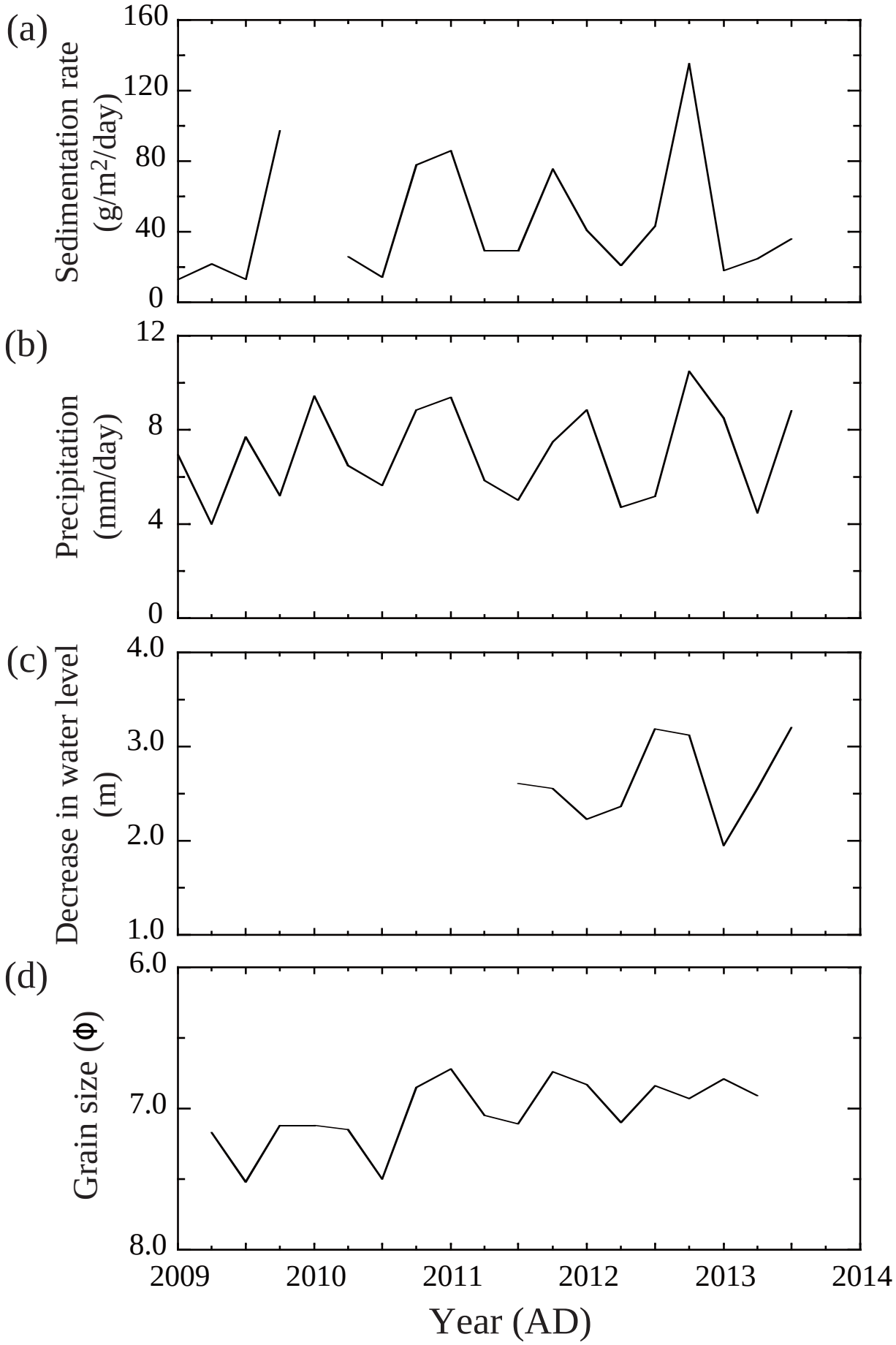

Fig. 4.12. Seasonal changes of average sedimentation rate, hydrological data (precipitation and water level) and grain size. (a) sedimentation rate, (b) precipitation intensity and (c) WL_D; decrease in water level and (d) mineral grain size.

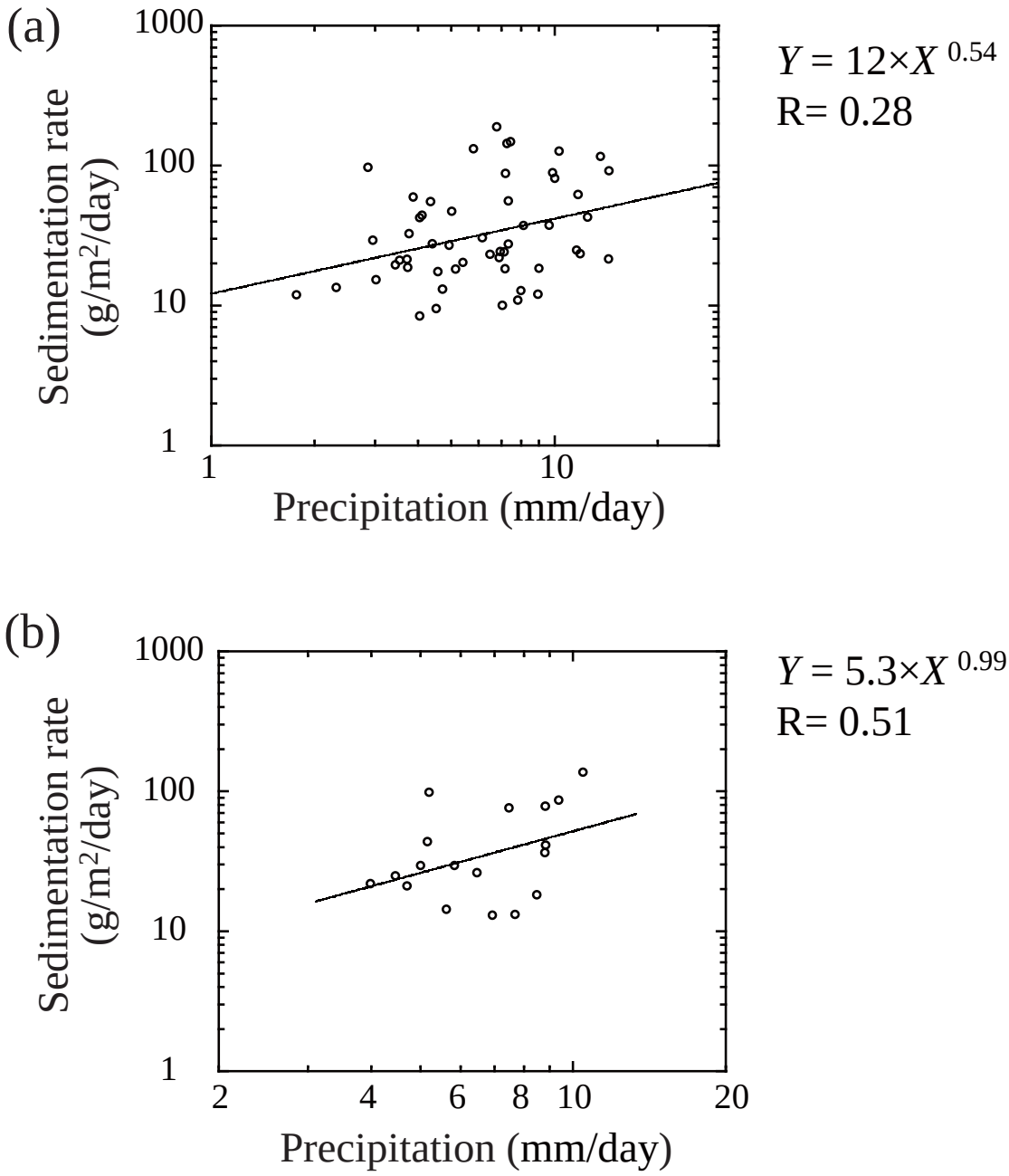

Fig. 4.13. The relationship between average sedimentation rate and precipitation intensity. (a) monthly relationship during Dec., 2008-Aug., 2013 and (b) seasonal relationship during winter period in 2009-summer period in 2013.

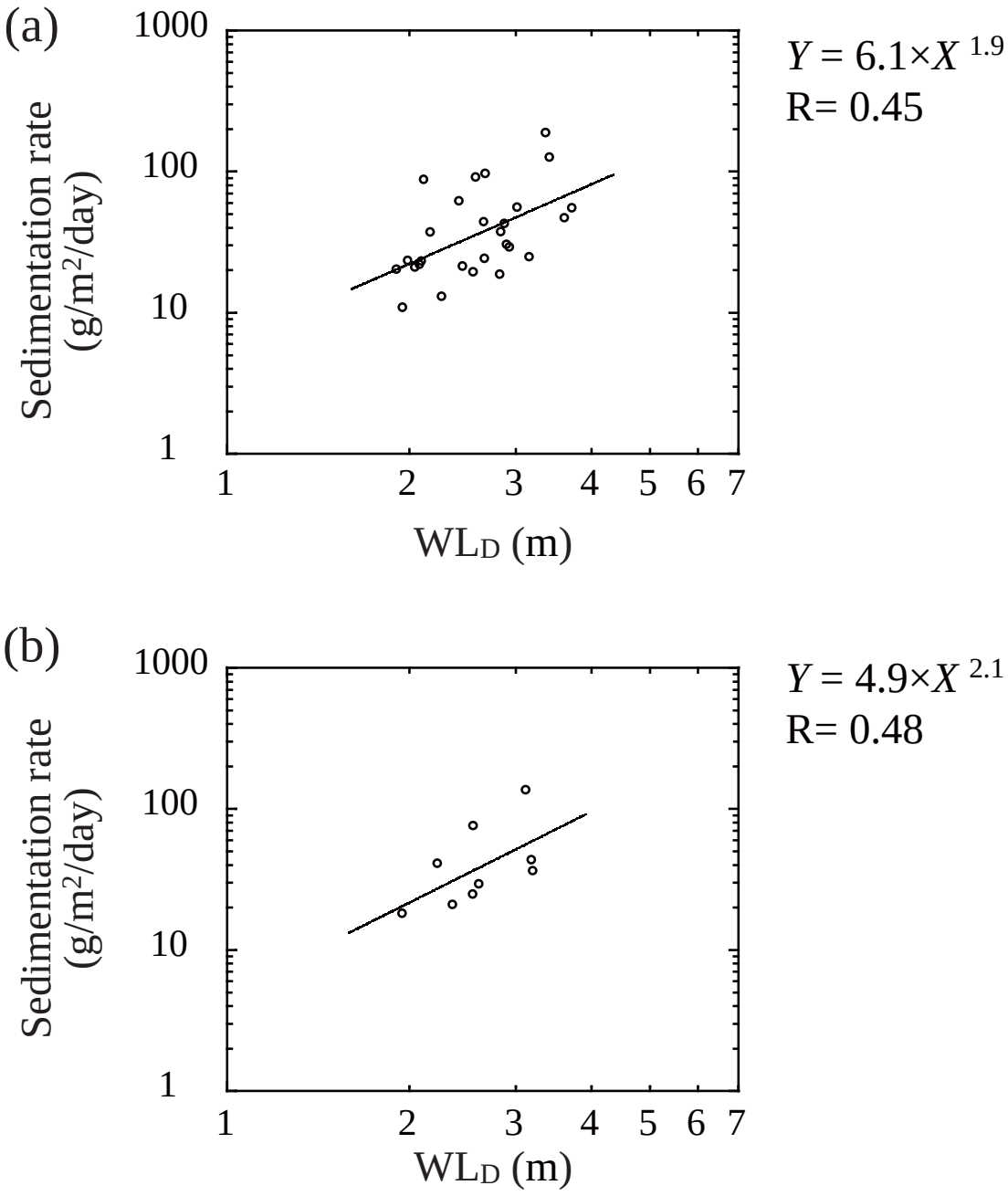

Fig. 4.14. The relationship between average sedimentation rate and decrease in water level (WL_D). (a) monthly relationship during Jun., 2011-Aug., 2013 and (b) seasonal relationship in the interval of summer period in 2011-summer period in 2013.

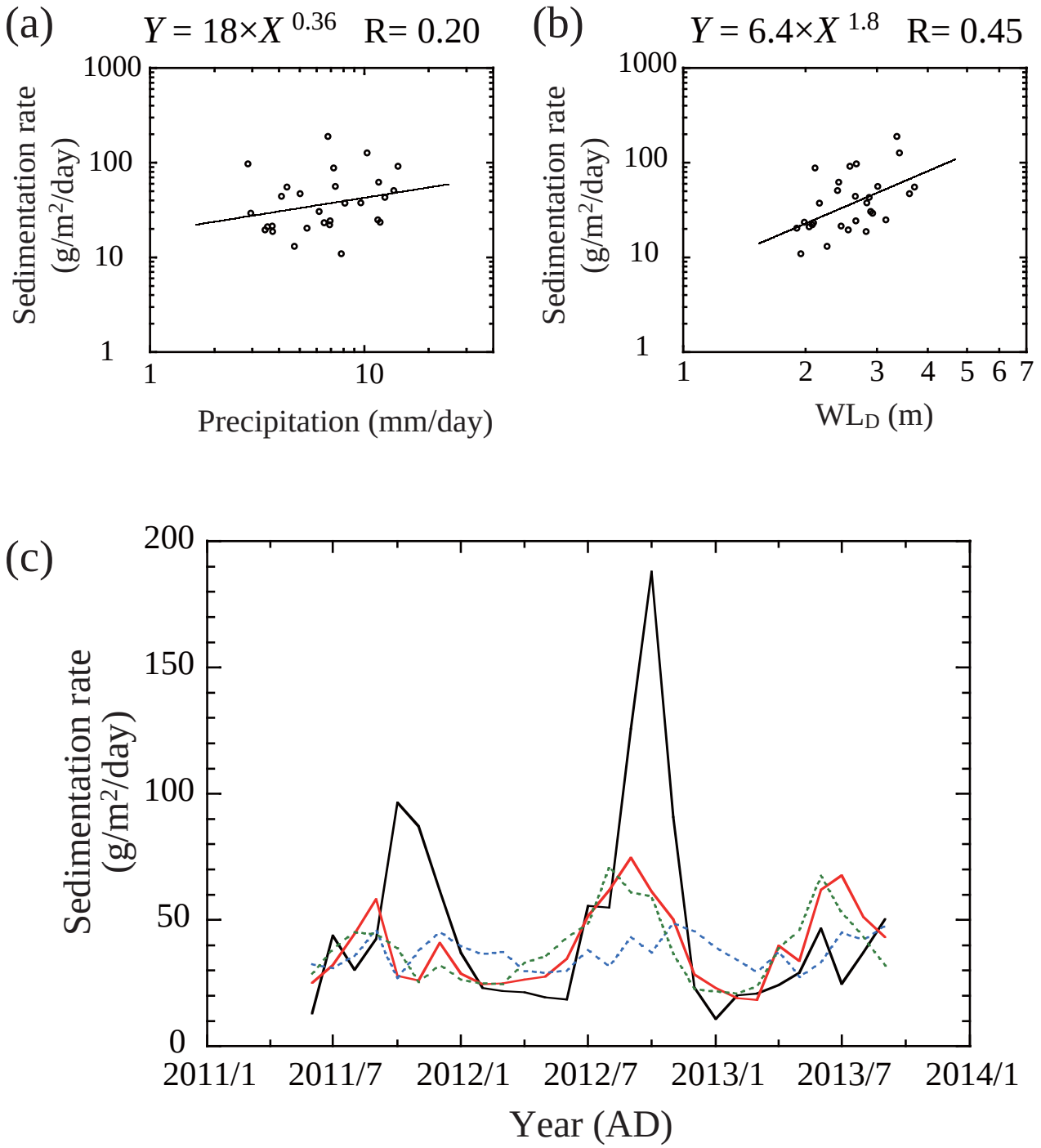

Fig. 4.15. Multiple regression analysis of monthly sedimentation rate during June, 2011 to September, 2013.
(a) The relationship between average sedimentation rate (g/m^2/day) and precipitation intensity (mm/day), (b) the relationship between average sedimentation rate and decrease in water level (WL_D; m) and (c) monthly average sedimentation rate; observational data (black) and estimated values; multiple regression analysis (red), precipitation (blue, dashed line) and decrease in water level (green, dashed line).

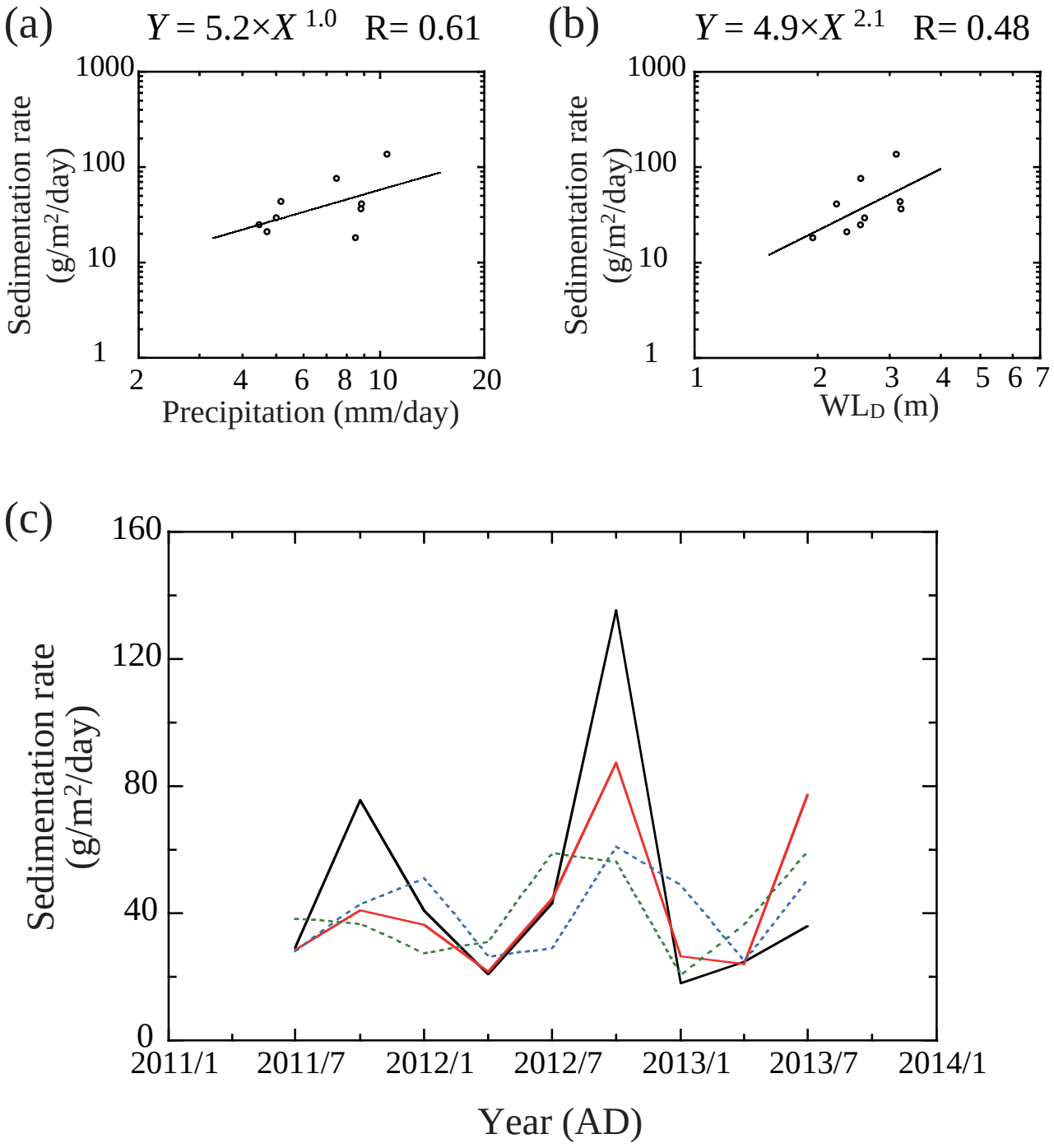

Fig. 4.16. Multiple regression analysis of seasonal sedimentation rate during summer period in 2011 to summer period in 2013.
(a) The relationship between average sedimentation rate (g/m^2/day) and precipitation intensity (mm/day), (b) the relationship between average sedimentation rate and decrease in water level (WL_D; m) and
(c) seasonal average sedimentation rate; observational data (black) and estimated values; multiple regression analysis (red), precipitation (blue, dashed line) and decrease in water level (green, dashed line).

Table 2.1. Information of sediment cores obtained from Lake Biwa.

Core number	Lengh (cm)	Depth (m)	Date	Sampling point	Latitude	Longitude	Analytical interval (cm)
BW05T1-11	45	32	22/6/2005	T1	N35°29'01.089"	E136°10'54.492"	0.5
BW05T1-4	399	32	22/6/2005	T1	N35°29'01.089"	E136°10'54.492"	2.0
BW06T5	84	70	18/5/2006	T5	N35°16.1805'	E136°03.8764'	0.5/1.0
BW07T13	53	60	14/2/2007	T13	N35°22.4533'	E136°11.1320'	0.5/1.0

Table 2.2. C-14 dates for three core samples.

Sample number	Depth (cm)	Material	C-14 Age (yr BP)	Calibrated Age (cal. yr BP)
BW05T1-4-139	282	Wood	1,230±30	1,129±30
BW05T1-4-197	398	Wood	1,730±40	1,632±47
BW06T5-86	71	Wood	390±40	468±23

Table. 2.3. Average physical properties for three periods (IT, IT-MH, MH) in the three cores. IT; Isewan Typhoon, IT-MH; Between IT and MH, MH; Meiji heavy rainfall.

Core number	Period	Density (g/cm^3)	Mineral content (%)	Mineral grain size (Φ)
BW05T1-11	IT	2.60	77.9	8.09
	Between IT and MH	2.59	76.4	8.12
	MH	2.62	77.3	8.19
BW06T5	IT	2.60	79.7	7.59
	Between IT and MH	2.59	78.3	7.71
	MH	2.62	81.6	7.79
BW07T13	IT	2.59	79.6	7.44
	Between IT and MH	2.58	76.9	7.73
	MH	2.62	80.5	7.89

Table 3.1. Eruptive history of Hokkaido-Komagatake Volcano in historical period. This table is modified after Yoshimoto et al., 2007.

Age (AD)	Tephra	Activity
1929	Ko-a	Plinian fall / pyroclastic flow
1856	Ko-c1	Plinian fall / pyroclastic flow / lava dome
1694	Ko-c2	Plinian fall / pyroclastic flow
1640	Ko-d	Plinian fall / pyroclastic flow, sector collapse

Table 3.2. Information on sediment cores obtained from Lake Onuma.

Sampling point	Latitude	Longitude	Depth (m)	Core number	Lengh (cm)	Sampling Date	Analytical interval (cm)
1	N42°00'12".0	E140°42'04".5	6.4	ON11-1	72	20/9/2011	1.0
2	N42°00'09".4	E140°41'28".7	11.2	ON11-2-1	96	20/9/2011	1.0
				ON11-2-2	68	20/9/2011	1.0
5	N42°00'41".6	E140°42'34".9	7.6	ON11-5	78	20/9/2011	1.0
6	N42°00'05".3	E140°41'13".7	8.3	ON11-6	45	20/9/2011	1.0 / 2.0
A	N41°58'34".5	E140°38'45".6	3.3	ON12A	223	6/6/2012	2.5
				ON12AS02	76	6/6/2012	1.0
B	N41°59'38".4	E140°40'33".5	7.6	ON12B	ca. 300	5/6/2012	-
				ON12BS01, BS02	-	5/6/2012	-
C	N42°00'09".3	E140°41'31".7	11.7	ON12C	392	5/6/2012	1.0 / 2.5
				ON12CS01	80	5/6/2012	1.0
D	N41°59'50".0	E140°40'57".5	9.5	ON12D	223	6/6/2012	1.0 / 2.5 / 3.0
				ON12DS01	66	6/6/2012	1.0

ON11-6; density (every 2.0 cm)
ON12C and ON12D ; water content (every 1.0 cm), other items (every 2.5 or 3.0 cm)
ON12D is sliced every 2.5 cm in sec 3-4, 3.0 cm in sec 1-2.
ON12B, ON12BS01and BS02 are not sliced.

Table 3.3. Average sedimentation rates of sediment cores.

Core number		ON11-6	ON11-2-2	ON11-2-1	ON11-1	ON11-5
Average sedimentation rate ($g/cm^2/yr$)	1963-2011		0.073	0.085	0.055	0.112
	Whole period	0.078	0.090	0.105	0.064	0.119

Table. 4.1. Summary of multiple regression analyses for sedimentation rate with precipitation and decrease in water level.

	Monthly relationship	Seasonally relationship
Correlation coefficient, R	0.58	0.77
Determination coefficient, R^2	0.34	0.60
Calibrated determination coefficient, R^2	0.29	0.47
Standard error	0.59	0.47
number of data	28	9

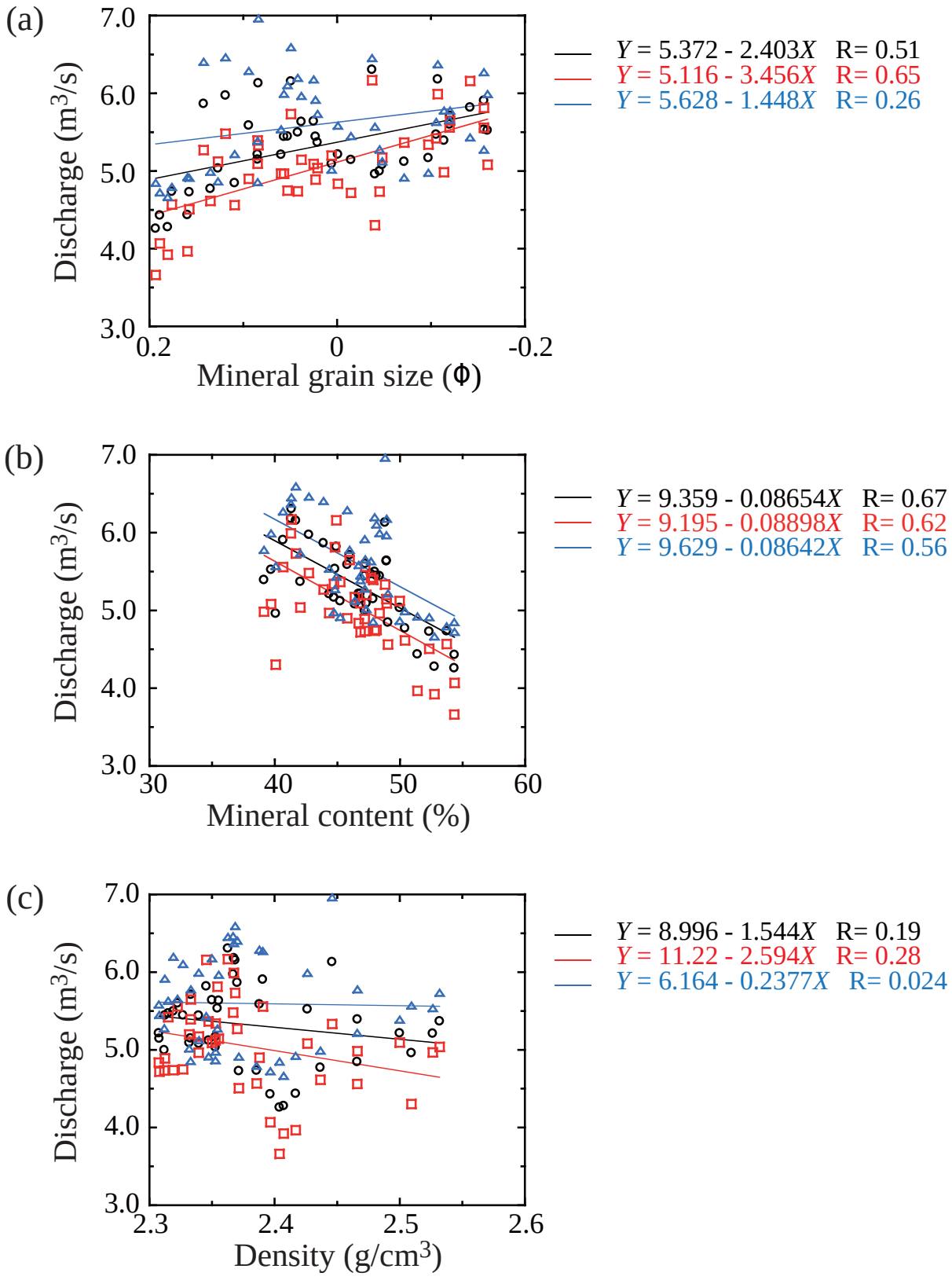

Appended Fig. 3.1. Relationship between 5-year running average of river discharge in Lake Onuma and physical properties of ON11-2-1 during 1963-2009. (a) dertrended mineral grain size, (b) mineral content and (c) density of ON11-2-1. Original river discharge; annual (black, circle), seasonal precipitation; summer period (red, square) and winter period (blue, triangle).

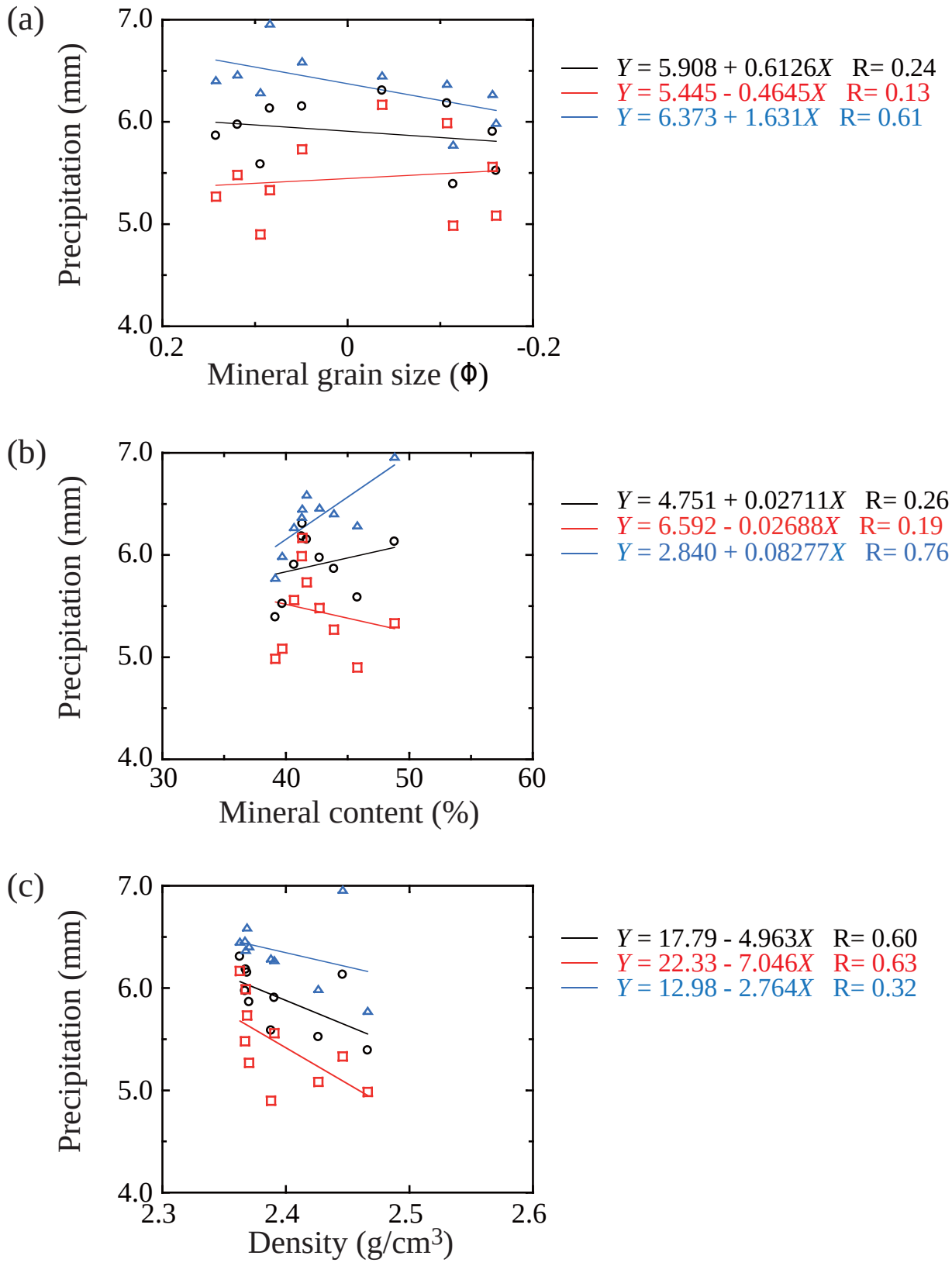

Appended Fig. 3.2. Relationship between 5-year running average of river discharge in Lake Onuma and physical properties of ON11-2-1 during 1968-1977. (a) dertrended mineral grain size, (b) mineral content and (c) density of ON11-2-1. Original river discharge; annual (black, circle), summer period (red, square) and winter period (blue, triangle).